The novel mitochondrial outer membrane protein Mcp3 follows a unique IMP-dependent import pathway

Dissertation

der Mathematisch-Naturwissenschaftlichen Fakultät

der Eberhard Karls Universität Tübingen

zur Erlangung des Grades eines

Doktors der Naturwissenschaften

(Dr. rer. nat.)

vorgelegt von

Monika Sonja Sinzel

aus Heidenheim an der Brenz

Tübingen

2017

Gedruckt mit Genehmigung der Mathematisch-Naturwissenschaftlichen Fakultät der Eberhard Karls Universität Tübingen.

Tag der mündlichen Qualifikation:	04.12.2017
Dekan:	Prof. Dr. Wolfgang Rosenstiel
1. Berichterstatter:	Prof. Dr. Doron Rapaport
2. Berichterstatter:	Prof. Dr. Ralf-Peter Jansen

Contents

1. List of abbreviations

ATP	adenosine triphosphate
BN-PAGE	blue native polyacrylamide gel electrophoresis
CCCP	carbonyl cyanide m-chlorophenyl hydrazone
CL	cardiolipin
DNA	deoxyribonucleic acid
EDTA	ethylenediaminetetraacetic acid
EMC	ER membrane protein complex
ER	endoplasmic reticulum
ERMES	ER-mitochondria encounter structure
GFP	green fluorescent protein
HA	hemagglutinin
IMP	inner membrane peptidase
IMS	intermembrane space
kDa	kilodalton
MAM	mitochondria-associated membrane
MBP	maltose binding protein
MDM	mitochondrial distribution and morphology
MICOS	mitochondrial inner membrane complex
MIM	mitochondrial inner membrane
MIM complex	mitochondrial import complex
MOM	mitochondrial outer membrane
MPP	matrix processing peptidase
mtDNA	mitochondrial DNA
MTS	mitochondrial targeting sequence
OXA	oxidase assembly
PA	phosphatidic acid
PC	phosphatidylcholine
PE	phosphatidylethanolamine
PI	phosphatidylinositol
PS	phosphatidylserine
ROS	reactive oxygen species
SAM	sorting and assembly machinery

SMP	synaptotagmin-like, mitochondrial and lipid-binding protein
TCC	tricarboxylic acid cycle
TIM	translocase of the inner membrane
TMD	transmembrane domain
TOB	topogenesis of outer-membrane β-barrel proteins
TOM	translocase of the outer membrane
vCLAMP	vacuole and mitochondria patch

2. Summary

Mitochondria are essential organelles of most eukaryotic cells and are involved in many important cellular activities. The viability of cells greatly depends on proper function of mitochondria, not only because mitochondria are 'the powerhouse of the cell', in fact they also play essential roles in metabolic processes and cellular signaling. Many neurological diseases are associated with mitochondrial disorders, illustrating the need to identify new components that participate in maintaining mitochondrial integrity. Mitochondria harbor two membranes, the mitochondrial outer membrane and inner membrane, which both have a characteristic phospholipid composition distinguishing them from all other cellular membranes. Maintenance of cellular and mitochondrial lipid homeostasis depends on membrane contact sites and the exchange of phospholipids between organelles. In yeast, connections between mitochondria and the endoplasmic reticulum (ER) are mediated by the ER-mitochondria encounter structure (ERMES) which has a crucial role in many cellular processes. Defects in ERMES lead to a multitude of phenotypes, but the precise molecular function of the ERMES complex and its subunit Mdm10 (mitochondrial distribution and morphology 10) is still not entirely understood. In order to shed light on this topic we searched for suppressors of the *mdm10*Δ growth defect and found a novel mitochondrial protein which we named Mcp3 for Mdm10 complementing protein 3.

Mcp3 follows a unique biogenesis pathway. It is initially recognized by the mitochondrial import receptor Tom70 and crosses the outer membrane via the translocase of the outer membrane. Mcp3 is then handed over to the translocase of the inner membrane (TIM23) and gets processed by the inner membrane peptidase. Subsequently, mature Mcp3 is released to the intermembrane space and integrates into the outer membrane in a process that possibly involves the mitochondrial import complex. Mcp3 is the first outer membrane protein that is reported to be processed by a peptidase of the inner membrane and therefore follows a novel biogenesis pathway.

3. Zusammenfassung

Mitochondrien sind essentielle Organellen der meisten eukaryotischen Zellen und an vielen wichtigen zellulären Prozessen beteiligt. Das Wachstum von Zellen hängt stark von der ordnungsgemäßen Funktion der Mitochondrien ab, nicht nur weil diese „die Kraftwerke der Zelle“ sind, sondern weil sie auch eine essentielle Rolle im Stoffwechsel oder in der zellulären Signaltransduktion spielen. Viele neurologische Erkrankungen stehen in Zusammenhang mit Funktionsstörungen der Mitochondrien. Dies macht die Notwendigkeit, neue Komponenten zu identifizieren die an der Aufrechterhaltung der mitochondrialen Integrität beteiligt sind, deutlich. Die äußere und innere Membran der Mitochondrien hat jeweils eine charakteristische Phospholipidzusammensetzung, wodurch sie sich von allen anderen zellulären Membranen unterscheiden. Membrankontakte und der Austausch von Lipiden zwischen Zellorganellen tragen dabei maßgeblich zur Aufrechterhaltung des zellulären und mitochondrialen Lipidhaushalts bei. Der ERMES (*Endoplasmic reticulum-mitochondria encounter structure*) Komplex bewerkstelligt Verbindungen zwischen dem endoplasmatischen Retikulum und Mitochondrien in Hefezellen und hat eine bedeutende Rolle für viele zelluläre Prozesse. ERMES Defekte führen zu einer Vielzahl von Anomalien, die genaue molekulare Funktion des ERMES Komplexes und seiner Untereinheit Mdm10 (*Mitochondrial distribution and morphology 10*) ist jedoch unklar. Um Einblick in die eigentliche Funktion von Mdm10 und des ERMES Komplexes zu erhalten haben wir nach Suppressoren des *mdm10*Δ Wachstumsphänotyps gesucht und ein neues mitochondriales Protein gefunden, welches wir *Mdm10 complementing protein 3* (Mcp3) genannt haben.

Mcp3 folgt einem einzigartigen Biogeneseweg. Es wird zunächst vom mitochondrialen Importrezeptor Tom70 erkannt und passiert dann die Außenmembran durch die *translocase of the outer membrane*. Mcp3 wird daraufhin zur *translocase of the inner membrane* (TIM23) überführt und durch die *inner membrane peptidase* prozessiert. Maturiertes Mcp3 wird in den Intermembranraum freigesetzt und integriert in die Außenmembran, in einem Prozess von dem angenommen wird, dass es den *mitochondrial import* Komplex involviert. Mcp3 ist das erste beschriebene Außenmembranprotein, welches von einer Peptidase aus der Innenmembran prozessiert wird und folgt demnach einem neuartigen Biogeneseweg.

4. List of publications contained in this thesis

1. M. Sinzel, T. Tan, P. Wendling, H. Kalbacher, C. Özbalci, X. Chelius, B. Westermann, B. Brügger, D. Rapaport, and K.S. Dimmer. 2016. Mcp3 is a novel mitochondrial outer membrane protein that follows a unique IMP-dependent biogenesis pathway. *EMBO Reports*. 17:965-981.

2. O. Hermesh, C. Genz, I. Yofe, M. Sinzel, D. Rapaport, M. Schuldiner, and R.P. Jansen. 2014. Yeast phospholipid biosynthesis is linked to mRNA localization. *Journal of Cell Science*. 127:3373-3381.

5. Personal contribution to the publications contained in this thesis

1. M. Sinzel, T. Tan, P. Wendling, H. Kalbacher, C. Özbalci, X. Chelius, B. Westermann, B. Brügger, D. Rapaport, and K.S. Dimmer. 2016. Mcp3 is a novel mitochondrial outer membrane protein that follows a unique IMP-dependent biogenesis pathway. *EMBO Reports*. 17:965-981.

I performed the majority of the experiments with the exception of experiments shown in figure 4K and 8C. For the experiments described in figures EV1 and EV2, I prepared the cells and send them to our collaborators X. Chelius and B. Westermann for microscopic analysis. Furthermore, I prepared the mitochondria for experiments shown in figures 2C and 3C and provided them to our cooperation partners C. Özbalci and B. Brügger for mass spectrometric analysis. I participated in writing the manuscript.

For experiments described in figures 1A, 1B, 2C, 3A, 3B, 3E and 7E similar experiments or parts of the experiments as biological or technical repeats are already included in my diploma thesis 'Characterization of the yeast mitochondrial protein Fun14'.

2. O. Hermesh, C. Genz, I. Yofe, M. Sinzel, D. Rapaport, M. Schuldiner, and R.P. Jansen. 2014. Yeast phospholipid biosynthesis is linked to mRNA localization. *Journal of Cell Science*. 127:3373-3381.

I performed the experiment described in figure 4B in order to analyse phosphatidylethanolamine levels in cells that contain altered levels of enzymes involved in phospholipid biosynthesis.

6. Introduction

6.1 Origin, structure, and function of mitochondria

Mitochondria are essential organelles of most eukaryotic cells and play significant roles in metabolism, energy homeostasis and other important cellular processes. According to the endosymbiotic theory, mitochondria derive from aerobic bacteria that were incorporated by an anaerobic ancestor. This process is considered to have increased the chances of survival for the eukaryotic cell due to the symbionts ability to produce ATP by oxidative phosphorylation (Cavalier-Smith, 1987). Many mitochondrial features reminiscent of Gram-negative bacteria support the endosymbiotic theory. Mitochondria harbor two membranes that have a characteristic phospholipid composition differing greatly from all other eukaryotic membranes. Both membranes contain only low levels of sterols and sphingolipids, while the mitochondrial inner membrane (MIM) stands out for its high protein content and the presence of cardiolipin (CL). Additionally, the mitochondrial outer membrane (MOM) contains integral β-barrel proteins that are also found only in the outer membrane of Gram-negative bacteria and chloroplasts (Comte *et al.*, 1976; Zinser and Daum, 1995; Imai *et al.*, 2011).

The intermembrane space (IMS) of mitochondria lies between the MOM and MIM, whereas the lumen of mitochondria is referred to as matrix. Each mitochondrial compartment has specialized functions and therefore contains a distinct set of proteins. Some of these functions include catabolic reactions such as the tricarboxylic acid cycle (TCC) and oxidation of fatty acids, but also anabolic pathways like lipid biosynthesis and synthesis of several amino acids and nucleotides. Furthermore, mitochondria participate in the biosynthesis of heme and iron-sulfur clusters (Lill *et al.*, 1999). Moreover, mitochondria are involved in cell signaling, cell cycle progression, autophagy and apoptosis (Pizzo and Pozzan, 2007; Hailey *et al.*, 2010). As a consequence, mitochondria are linked to ageing, carcinogenesis, neurodegenerative diseases, and other disorders that arise from mutations in mitochondrial proteins (Chan, 2006).

Mitochondria establish intimate contact sites with the endoplasmic reticulum (ER), known as mitochondria associated ER membrane (MAM), which are required for lipid exchange and Ca^{2+} homeostasis. In yeast, these contact sites are mediated by the ERMES (ER-mitochondria encounter structure) complex (Kornmann *et al.*, 2009). Although mitochondria are tightly integrated into the cellular physiology they retained

some of their autonomy, which further supports the endosymbiotic theory. Similar to a typical bacterial genome, mitochondria harbor circular DNA, which can be transcribed and translated inside mitochondria. Unlike the cytosolic 80S species, mitochondrial 70S ribosomes are similar to bacterial ribosomes (Kitakawa and Isono, 1991; Graack and Wittmann-Liebold, 1998). However, the mitochondrial DNA (mtDNA) encodes only few proteins and most mitochondrial proteins are translated in the cytosol and need to be imported via dedicated protein complexes within the outer and the inner membrane of mitochondria (Gray *et al.*, 1999; Wallace, 2005).

6.2 Protein import into mitochondria

In the course of the endosymbiotic process most genes of the mitochondrial progenitor were transferred to the nucleus, probably to allow the cell a better regulation of many important processes that take place in mitochondria. As a result, the nucleus encodes about 1000-1500 mitochondrial proteins in humans and approximately 800 proteins in more simple organisms, like yeast, while the mtDNA encodes only 1% of the mitochondrial proteome (8 in yeast and 13 in humans) (Gray *et al.*, 1999; Sickmann *et al.*, 2003; Westermann and Neupert, 2003; Wallace, 2005). Hence, mitochondrial precursor proteins are translated on cytosolic ribosomes and have to be correctly targeted to their appropriate location.

Usually components of the translocase of the outer membrane (TOM complex), namely the primary mitochondrial import receptors Tom20 and Tom70 establish the initial contact of newly translated proteins with the mitochondria. Tom20 recognizes mainly precursor proteins with an N-terminal extension which serves as a classical targeting signal. These mitochondrial presequences typically consist of 15-55 amino acids and bear similar structural and electrochemical properties (Vogtle *et al.*, 2009). Tom20 was also shown to recognize β-barrel proteins which consist of antiparallel β-sheets that are arranged in a cylindrical shape (Jores and Rapaport, 2017). Tom70 predominantly recognizes precursors of carrier proteins with multiple internal targeting signals (Brix *et al.*, 2000). As a result of overlapping specificities, Tom20 and Tom70 can partially complement the absence of each other (Steger *et al.*, 1990).

Depending on their location within mitochondria, precursor proteins are further distributed to different import machineries within the outer and inner mitochondrial membrane. Most mitochondrial preproteins are handed over from the primary import receptors to the secondary receptor and TOM core subunit Tom22, before being inserted into the protein conducting pore that is formed by the β-barrel protein Tom40 (Chacinska *et al.*, 2009). Similar substrate recognition profiles of Tom20 and Tom22 lead to a partial functional overlap (Yamano *et al.*, 2008).

Following the recognition by Tom70, few outer membrane proteins containing one transmembrane spanning helix and all known helical multispan proteins of the MOM are, without the involvement of the Tom40 pore, further relayed to the mitochondrial import (MIM) complex, which contains the proteins Mim1 and Mim2 (Becker *et al.*, 2011; Papic *et al.*, 2011; Dimmer *et al.*, 2012) (Fig. 1, pathway 1).

Some mitochondrial proteins are integrated into the MOM independently of the known proteinaceous factors for mitochondrial import, as it is the case for tail anchored proteins in the MOM like Fis1 (Kemper *et al.*, 2008; Meineke *et al.*, 2008; Merklinger *et al.*, 2012).

The TOM complex mediates the transfer of β-barrel proteins across the MOM, from where they are further relayed to the topogenesis of outer membrane β-barrel proteins (TOB) complex, also termed the sorting and assembly machinery (SAM). The soluble Tim9-Tim10 (translocase of the inner membrane) and Tim8-Tim13 chaperone complexes (small TIMs; sTIMs) assist by shielding the hydrophobic precursor from the aqueous environment in the IMS (Paschen *et al.*, 2005) (Fig. 1, pathway 5).

The import of the small Tim proteins, as well as the biogenesis of other cysteine-containing proteins of the IMS is dependent on the Mia40-Erv1 (Mitochondrial intermembrane space Import and Assembly; Essential for Respiration and Viability) system (Ceh-Pavia *et al.*, 2013) (Fig. 1, pathway 2).

Carrier-like proteins with six hydrophobic transmembrane domains (TMDs) that are inserted into the inner membrane are also escorted through the IMS by sTIMs, although from the TOM to the TIM22 (translocase of the inner mitochondrial membrane) complex (Gebert *et al.*, 2008) (Fig. 1, pathway 4).

Presequence-containing proteins are transferred from the TOM complex further to the TIM23 complex (Neupert and Herrmann, 2007). The driving force for translocation of preproteins across the MIM is provided by ATP and the membrane potential ($\Delta\psi$), whilst the presequence is cleaved off by the matrix processing peptidase (MPP) (Fig. 1, pathway 3a). Preproteins destined for insertion into the MIM additionally contain hydrophobic stop-transfer sequences. These hydrophobic sequences act as secondary sorting signals, which arrest translocation across the MIM and induce the lateral release of the protein into the membrane (Glick *et al.*, 1992; Chacinska *et al.*, 2009) (Fig. 1, pathway 3b). Similar bipartite signals act in conservative sorting, wherein the protein is first targeted to the matrix. Upon cleavage by MPP, the hydrophobic sorting signal is exposed and the protein is inserted into the MIM via OXA1 (oxidase assembly 1) complex, alike proteins that are synthesized on mitochondrial ribosomes (Hartl *et al.*, 1986; Hell *et al.*, 1998; Neupert and Herrmann, 2007) (Fig. 1, pathway 6).

A subset of proteins is processed by the heterotrimeric protease complex inner membrane peptidase (IMP), which consists of the two catalytically active subunits Imp1 and Imp2 and the auxiliary protein Som1 (Nunnari *et al.*, 1993; Jan *et al.*, 2000). IMP functions subsequential of MPP and removes the hydrophobic sorting signal (Gakh *et al.*, 2002; Neupert and Herrmann, 2007) resulting in either a soluble IMS protein like Mcr1 or a MIM anchored protein like Mgr2 (Hahne *et al.*, 1994; Ieva *et al.*, 2013). Up to now only MIM or IMS proteins were identified to be processed by IMP (Fig. 1, pathway 3c).

A number of proteins follow routes diverging from the classical import pathways, such as the signal anchor protein Om45, which makes use of the presequence pathway involving the TOM and TIM23 complex but is ultimately assembled into the MOM by the MIM complex (Song 2014; Wenz 2014). Furthermore, the presequence containing proteins Mgr2 and Hmi1 are processed not from their N-, but C- termini (Lee *et al.*, 1999; Ieva *et al.*, 2013), whereas the matrix targeted protein Hsp10 is not processed by MPP (Rospert *et al.*, 1993).

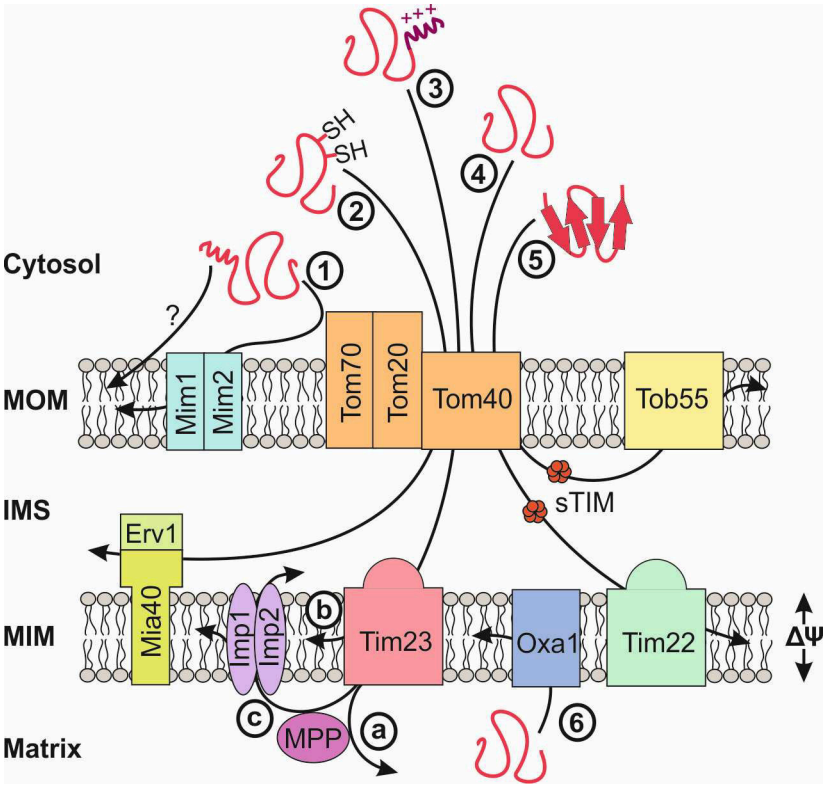

Figure 1. Protein sorting in mitochondria. Mitochondrial preproteins are synthesized in the cytosol where they are kept in an import competent state by cytosolic chaperones. Some α-helical proteins are inserted into the outer membrane in a process that involves the MIM complex, whereas for other signal- and tail-anchored proteins the import factors are unknown (1). Cysteine rich proteins of the intermembrane space cross the outer membrane via the TOM complex and obtain their native structure in a process that involves the Mia40/Erv1 complex (2). Proper positioning of proteins that take the presequence pathway depends on the membrane potential ($\Delta\psi$) and the TIM23 complex. Proteins processed by signal peptidases like MPP or IMP find their destination in the IMS, the MIM, or the matrix (3a-c). Carrier proteins of the inner membrane are handed over from TOM to the TIM22 complex with the help of small TIM chaperones in the IMS (4). The small TIMs are also involved in targeting β-barrel proteins to the TOB complex (5). Proteins that are synthesized on mitochondrial ribosomes in the matrix and some proteins with bipartite signals follow the conservative sorting pathway and are inserted to the MIM via Oxa1 (6).

6.3 Mitochondrial morphology at a glance

Mitochondria form highly dynamic, interconnected tubular structures beneath the cell cortex that undergo constant fusion and fission events (Nunnari *et al.*, 1997). It can be speculated that one advantage of such a large mitochondrial network is to allow the transmission of the mitochondrial membrane potential, thereby facilitating the energy transfer within cells from oxygen rich to oxygen poor regions (Westermann, 2008).

Several human diseases are connected to disorders in mitochondrial integrity, therefore understanding the processes and identifying novel components that determine mitochondrial morphology is of main interest. A suitable model organism for studying mitochondrial morphology is the baker's yeast *S. cerevisiae*, since many processes are conserved between yeast and higher eukaryotes. Furthermore, yeast can tolerate mitochondrial defects or the loss of mtDNA on fermentable carbon sources, whereas abolished mitochondrial respiration leads to inability of the cells to grow on non-fermentable carbon sources like lactate or glycerol. These mutants form smaller colonies during anaerobic growth and display the so called petite (pet^-) phenotype (Tzagoloff and Dieckmann, 1990). Since defects in mitochondrial morphology often lead to hampered respiration, yeast cells established in the search for novel morphology components.

Four major processes influence mitochondrial morphology and distribution, namely fusion, fission, tubulation, and transport along the cytoskeleton (Okamoto and Shaw, 2005). Fusion of mitochondria is a prerequisite for the interchange of mitochondrial membranes and matrix components, such as mtDNA. Considering that the mtDNA is potentially damaged by reactive oxygen species (ROS) during ATP production by oxidative phosphorylation, recombination of the mitochondrial genome is essential for repair. As a result, somatic mutations might be prevented and cellular aging could be delayed.

In yeast, the large GTPase Fzo1 in the MOM plays an important role in mitochondrial fusion. Cells lacking Fzo1 display fragmented mitochondria and are characterized by the loss of mtDNA (Rapaport *et al.*, 1998). Another essential factor for mitochondrial fusion is the MOM protein Ugo1. Ugo1 forms a complex with Mgm1, a dynamin-like GTPase in the MIM, therefore making it a prominent candidate for a fusogen of the inner membrane (Merz *et al.*, 2007).

Mitochondrial fission is an important process for the inheritance of mitochondria, since mitochondria cannot be created *de novo*, but rather have to be replicated and distributed inside the cell. Dnm1, which belongs to the dynamin subfamily of GTP-binding proteins is an essential component that is recruited to mitochondria at fission sites. Hence, deletion of *DNM1* in yeast cells leads to an aberrant mitochondrial morphology. Impaired fission and progressing fusion results in a highly branched, netlike mitochondrial system, which locates to only one side of the cell (Otsuga *et al.*, 1998). Furthermore, mitochondrial fission is regulated by the proteins Fis1, an integral outer membrane protein, as well as Mdv1 and its paralog Caf4. Mdv1 and Caf4 are soluble proteins that engage with Dnm1 and Fis1 at specific sites to induce fission (Fekkes *et al.*, 2000; Mozdy *et al.*, 2000; Tieu *et al.*, 2002; Okamoto and Shaw, 2005). Components of the fusion and fission machinery are often conserved among yeast and higher eukaryotes. The significance of mitochondrial morphology for cellular function is unquestionable, considering that disorders in mitochondrial integrity are connected to several human diseases. Disorders in the peripheral nervous system of higher eukaryotes are frequently connected to mutations in morphology components like DRP1 (Dnm1), MFN2 (Fzo1) and OPA1 (Mgm1) which are involved in mitochondrial fusion and fission. Since fragmented mitochondria constitute a step in programmed cell death, components of the fission machinery also participate in the initiation of apoptosis (Youle and Karbowski, 2005; Chan, 2006).

Mitochondria in yeast maintain their tubular shape and ensure distribution and inheritance by the ability of the organelle to move along the actin cytoskeleton (Merz *et al.*, 2007), a process for which Mdm10 and the ER-protein Mmm1 were shown to be required (Sogo and Yaffe, 1994; Boldogh *et al.*, 1998). Additionally, ERMES components were identified to function as tubulation mediators, because mutation or deletion of their encoding genes gives rise to condensed, giant organelles (Sogo and Yaffe, 1994). However, in higher eukaryotes the factors necessary for tubulation of mitochondria are unknown.

6.4 Relevance of ERMES in yeast

As mentioned before, tubulation, as well as distribution and inheritance of mitochondria is dependent on the ERMES complex (Sogo and Yaffe, 1994), a complex which is unique to fungi. Interestingly, the deletion of either ERMES gene leads to similar phenotypes regarding growth, mitochondrial inheritance and morphology, mitophagy, and phospholipid composition (Burgess *et al.*, 1994; Berger *et al.*, 1997; Youngman *et al.*, 2004; Kornmann *et al.*, 2009; Osman *et al.*, 2009; Nguyen *et al.*, 2012).

ERMES is a high molecular weight complex consisting of the integral MOM β-barrel protein Mdm10 (Mitochondrial distribution and morphology), the integral MOM protein Mmm2 (Maintenance of mitochondrial morphology 2) known also as Mdm34, the cytosolic protein Mdm12, and the integral ER protein Mmm1. The more loosely attached subunit Gem1 was suggested to regulate the size and number of ERMES complexes and to affect mitochondrial shape in a process that is independent of fusion and fission.

The mammalian orthologs of Gem1, Miro1 and Miro2 have been shown to influence the connection between mitochondria and the cytoskeleton (Frederick *et al.*, 2004; Frazier *et al.*, 2006; Kornmann *et al.*, 2011). Besides Miro1 and Miro2, ERMES complex was reported to be involved in this process by linking mtDNA and mitochondrial membranes to the actin cytoskeleton. As a consequence, deletion of genes encoding ERMES results in condensed and giant organelles that tend to lose mtDNA (Burgess *et al.*, 1994; Sogo and Yaffe, 1994; Berger *et al.*, 1997). ERMES complex not only contributes to the maintenance and inheritance of mitochondria, but is also implied in the biogenesis of the outer membrane. Several studies provide evidence that ERMES components function in the assembly of β-barrel proteins into the MOM (Meisinger *et al.*, 2004; Meisinger *et al.*, 2007; Yamano *et al.*, 2010). Other studies demonstrate that yeast cells require the ERMES complex in order to maintain a correct mitochondrial lipid composition. The complex establishes sites of close contact between ER and mitochondria, thereby probably facilitating or actively influencing the exchange of lipids between the two organelles (Kornmann *et al.*, 2009; Osman *et al.*, 2009; Yamano *et al.*, 2010; Nguyen *et al.*, 2012; Tamura *et al.*, 2012).

Collectively, it is evident that the ERMES complex is implicated in many important cellular processes, although the most prominent function is thought to be its involvement in lipid homeostasis.

6.5 ERMES complex and mitochondrial lipid homeostasis

The three types of lipids constituting biological membranes are phospholipids, sphingolipids and sterols, with phospholipids being most abundant. Phospholipids are amphipathic molecules with a polar head group and a hydrophobic part, where different combinations of the polar residue with acyl chains lead to a large variety of phospholipids. Each endogenous membrane system has a unique phospholipid profile, while the structural and functional characteristics of membranes are important for their interactions with proteins. For instance, the presence of negatively charged phosphatidylserine (PS) helps in directing positively charged proteins to the endocytic pathway (Yeung *et al.*, 2008). The mitochondrial phospholipid composition varies little among different cell types, indicating that grand alterations cannot be tolerated (Osman *et al.*, 2009). Indeed, changes in phospholipid levels or composition, as well as phospholipid damage can be linked to several human diseases such as ischemia, hypothyroidism, Barth syndrome and heart failure (Chicco and Sparagna, 2007; Gebert *et al.*, 2009; Joshi *et al.*, 2009).

The four major glycerophospolipid classes in yeast mitochondria are phosphatidylcholine (PC, 40%), phosphatidylethanolamine (PE, 26%), phosphatidylinositol (PI, 15%) and cardiolipin (CL, 13%), whereas PS (3%) and phosphatidic acid (PA, 2%) are less abundant (Zinser and Daum, 1995). The maintenance of a defined lipid composition depends on the ability of mitochondria to synthesize phospholipids such as CL, PE, and phosphatidylgylcerol (PG) from phospholipid precursors, whereas PA, PI, PS, PC and sterols need to be imported into mitochondria from other organelles (Osman *et al.*, 2010; Flis and Daum, 2013; Tamura *et al.*, 2013; Mejia and Hatch, 2016) (Fig. 2).

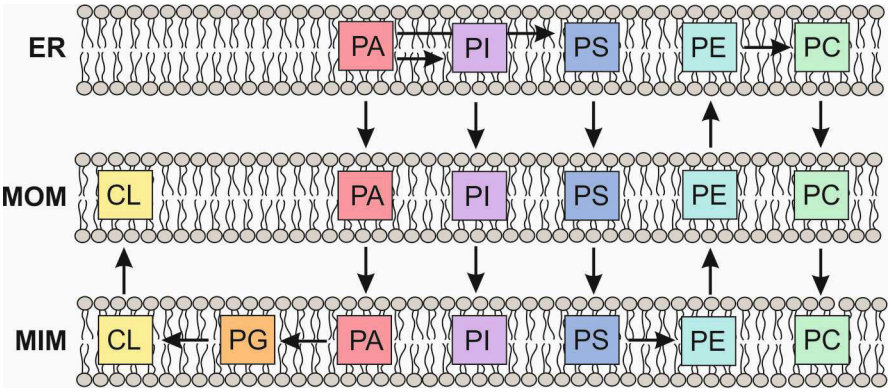

Figure 2. Phospholipid synthesis and lipid transport between ER and mitochondria. The phospholipid PA serves as a precursor for PI and PS synthesis in the ER, wherein PS is transported to mitochondria for the conversion to PE. PC synthesis in the ER requires the export of PE from mitochondria. Furthermore, PA is necessary for the production of PG and CL in mitochondria.

CL is a phospholipid with a special composition, since it contains four acyl chains. It is found solely in bacterial membranes or in mitochondria, particularly in the MIM where it has an important role for mitochondrial biogenesis and function. CL is important for respiration and oxidative phosphorylation (Hoch, 1992), as well as the biogenesis of certain mitochondrial proteins (Ou *et al.*, 1988; Gebert *et al.*, 2009; Sauerwald *et al.*, 2015). Furthermore, it was reported that CL is involved in orientation of receptors, channels and enzymes on the outer face of the MOM (Schug and Gottlieb, 2009). A lack of CL leads to destabilization of respiratory chain supercomplexes and the TIM23 translocase, a reduced activity of cytochrome *c* oxidase, and a reduced inner membrane potential $\Delta\psi$ (Jiang *et al.*, 2000; Lange *et al.*, 2001; Zhang *et al.*, 2002; Pfeiffer *et al.*, 2003; Zhang *et al.*, 2005). CL, as PE, is a cone-shaped lipid and has a preference for nonbilayer structures with a negative curvature (van den Brink-van der Laan *et al.*, 2004). The loss of either CL or PE can be tolerated by yeast cells, whereas cells lacking both phospholipids are non-viable, indicating overlapping functions (Gohil *et al.*, 2005). Consistently, several studies suggest a role for CL and mitochondrial PE in maintaining mitochondrial integrity (Osman *et al.*, 2009; Kuroda *et al.*, 2011; Tamura *et al.*, 2012). Moreover, cells lacking mitochondrial PE depleted of CL display reduced levels of Mgm1, which leads to defects in mitochondrial fusion with excessive fragmentation and loss of mtDNA. However, a lack of PE also favors the formation of respiratory chain supercomplexes (Bottinger *et al.*, 2012; Joshi *et al.*, 2012).

Considering that mitochondria are not part of the endomembrane system, mechanisms that allow non-vesicular lipid exchange between the organelles are necessary. Specialized sections of the ER, the so-called MAMs (Mitochondria-associated membranes) were reported to co-purify with enzymes involved in phospholipid biosynthesis and are implicated in lipid transport between the two organelles (Vance, 1990; Voelker, 1990; Ardail *et al.*, 1993; Gaigg *et al.*, 1995; Shiao *et al.*, 1995).

The ERMES complex in yeast was the first system described to participate in lipid exchange between mitochondria and the ER. Cells lacking individual subunits of the ERMES complex show reduced levels of mitochondrial PE and CL, suggesting that the ERMES structure is required for the exchange of phospholipids at ER–mitochondria contact sites. Additionally, the conversion of PS to PE and PC was decreased in cells depleted of ERMES components, emphasizing a role of ERMES in phospholipid exchange between ER and mitochondria (Kornmann *et al.*, 2009; Osman *et al.*, 2009; Nguyen *et al.*, 2012). Recent data indicate that the formation of respiratory chain supercomplexes in mitochondria lacking Mdm10 is altered. Furthermore, cells lacking Mdm10 display elevated mitochondrial ergosterol levels (Tan *et al.*, 2013). Until recently it remained unclear whether components of the ERMES complex actively contribute to the transport of phospholipids, or if the ERMES complex simply functions as a membrane tether ensuring the close proximity of ER and mitochondria. The prediction of synaptotagmin-like, mitochondrial and lipid-binding protein (SMP) domains in ERMES components sparked further investigations in this matter, leading to the finding that the SMP domains of Mmm1 and Mdm12 can indeed interact with lipids and form a hydrophobic channel that preferentially binds PC (Lee and Hong, 2006; Kopec *et al.*, 2010; AhYoung *et al.*, 2015).

Since the deletion of ERMES genes is not lethal, parallel processes for the lipid exchange between mitochondria and the ER, or with other organelles must exist. Furthermore, cellular PE levels remain largely unaffected in ERMES mutants, reinforcing the idea of alternate routes for lipid trafficking between the organelles (Kornmann *et al.*, 2009; Nguyen *et al.*, 2012; Voss *et al.*, 2012). Indeed, two recent studies provide evidence for alternative ways of mitochondria to exchange lipids with the remainder of the cell. The ER membrane protein complex (EMC) is suggested to function as an additional tether between mitochondria and ER and was shown to play a role in the transport of PS from the ER to mitochondria (Lahiri *et al.*, 2014). Additionally, contact sites between

mitochondria and the vacuole are mediated by the vacuole and mitochondria patch (vCLAMP), a tether which is marked by the vacuolar protein Vps39 and is implicated in PS to PC conversion. Interestingly, the elimination of both ERMES and vCLAMP contact sites is lethal, suggesting that the systems are partially redundant in providing phospholipids to mitochondria (Elbaz-Alon *et al.*, 2014; Honscher *et al.*, 2014). It was also shown that the lack of one contact site leads to the expansion of the other, wherein the extent of contact sites between mitochondria and either the ER or vacuole is regulated by the sterol transporter Lam6. Lam6 has two mammalian homologs, GRAMD1a and GRAMD1c, a circumstance which might help to identify contact site tethers in higher eukaryotes (Elbaz-Alon *et al.*, 2014; Elbaz-Alon *et al.*, 2015; Gatta *et al.*, 2015; Murley *et al.*, 2015).

Genetic manipulations of yeast are relatively easy to accomplish and are powerful tools to identify new components involved in lipid metabolism. For instance, Mcp1 (Mdm10 complementing protein), and Mcp2 were found in a screen for multicopy suppressors of the Mdm10 growth phenotype. A role for the two suppressors in a lipid transport pathway independent of ERMES was suggested already upon the identification of the two proteins (Tan *et al.*, 2013). The mode of action of this alternative pathway remains unclear, however only recently a physical interaction of Mcp1 with Vps13 was reported (John Peter *et al.*, 2017). Vps13 was previously described as a possible regulator of contact sites between mitochondria and the ER or vacuole, because point mutations in Vps13 led to cellular effects bypassing ERMES related defects (Lang *et al.*, 2015; John Peter *et al.*, 2017). Mcp1 is suggested to recruit Vps13 to mitochondria, thereby increasing the extent of contact sites between mitochondria and the vacuole, while tethering is mediated by the vacuolar fusion factor Vps39 and the vacuolar Rab GTPase Ypt7 (Elbaz-Alon *et al.*, 2014; John Peter *et al.*, 2017).

Additionally, it was reported that components of the mitochondrial contact site and cristae organizing system (MICOS) display a strong negative genetic interaction with *CRD1* and *GEP4*, enzymes of the CL synthesis pathway (Hoppins *et al.*, 2011). MICOS is involved in cristae formation and establishing sites of close contact between the MIM and MOM, thereby contributing to intramitochondrial lipid homeostasis (van der Laan *et al.*, 2016). MICOS was not only shown to play a role in CL metabolism, but was also reported to be involved in the decarboxylation of PS by bringing the MOM and the MIM in close contact. The proximity of the two membranes allows conversion of PS to PE by

the MIM enzyme phosphatidylserine decarboxylase 1 (Psd1) in the outer membrane (Aaltonen *et al.*, 2016). In MICOS deficient cells, the PS transporter Ups2-Mdm35 limits transport of PS to the MIM, thereby preventing PE accumulation in the mitochondria and in turn ensuring cristae formation and mitochondrial respiration (Tamura *et al.*, 2012; Aaltonen *et al.*, 2016). Mdm35 was additionally reported to form a complex with Ups1 involved in the transport of PA across the IMS, therefore playing an important role in CL biosynthesis (Connerth *et al.*, 2012; Tamura *et al.*, 2012). The loss of Ups1 can be compensated by overexpression of Mdm31, a protein which was also reported to restore altered mitochondrial CL levels in cells lacking ERMES (Tamura *et al.*, 2012).

The progress made in deciphering the complex relation of organellar contacts and lipid homeostasis demonstrates that the search for suppressors of ERMES phenotypes can provide valuable information to help unraveling the many interconnected activities of ERMES. The presence of the ERMES complex in common ancestors of metazoans and fungi leads to the assumption that alternative routes rendered the ERMES complex dispensable in the course of evolution (Flinner *et al.*, 2013; Wideman *et al.*, 2013). The identification of pathways that can bypass ERMES thereby might contribute to understand lipid transport in higher eukaryotes, which is largely unsolved.

7. Aim of the study

A multitude of different functions are proposed for ERMES, such as the involvement in processes like mitophagy, protein biogenesis of the outer membrane, maintenance of mitochondrial morphology, inheritance of the mitochondrial genome as well as lipid homeostasis. However, the precise molecular function of the ERMES complex remains unclear. To solve this question, a high copy suppressor screen was performed and Mcp3 (*Mdm10 complementing protein 3)* was found to partially rescue the growth phenotype of cells lacking Mdm10. To contribute to the elucidation of the primary function of ERMES, the genetic and functional interaction of Mcp3 and ERMES was examined in the article *Mcp3 is a novel mitochondrial outer membrane protein that follows a unique IMP-dependent biogenesis pathway.* First, the involvement of Mcp3 in mitochondrial processes in general was analysed. Moreover, Mcp3 and its biogenesis was studied in this work.

8. Summary of the results

8.1 The role of Mcp3 in mitochondrial function

8.1.1 Mcp3 is a high-copy suppressor of the absence of ERMES complex

ERMES complex is involved in many mitochondrial processes, yet the molecular function of the individual subunits and the primary purpose of the complex is still unknown. Identifying novel components that genetically interact with e.g. *MDM10* may shed light on this topic. To this end, a growth phenotype rescue screen of *mdm10*Δ was performed. Among other high copy suppressors of *mdm10*Δ, *FUN14* (YAL008W) was discovered. Overexpression of Fun14 rescued the growth phenotype of *mdm10*Δ cells (Fig. 1A), the protein was therefore renamed Mcp3 for Mdm10 complementing protein 3. Mcp3 was able to complement also the growth defects resulting from deletion of other ERMES components, suggesting that the function of Mcp3 is related to the role of the entire complex rather than to the missing activity of an individual subunit (Fig. 2D-F). Furthermore, overexpression of Mcp3 led to a partial restoration of the tubular mitochondrial network in cells lacking Mdm10, as demonstrated by fluorescence microscopy (Fig. 1B), which is congruent with the partial growth rescue. Considering that the loss of Mdm10 leads to changes in the assembly of respiratory chain supercomplexes and a hampered TOM and TOB complex assembly, the rescuing ability of Mcp3 in respect to these phenotypes was assessed. Figure 2A and B demonstrate that the overexpression of Mcp3 led to minor restorations of the aforementioned defects, as shown by blue native polyacrylamide gel electrophoresis (BN-PAGE).

It has been shown that cells lacking Mdm10 exhibit an altered mitochondrial lipid composition, specifically increased amount of PS and ergosterol (ERG) were observed, whereas PE and CL levels were reduced (Kornmann *et al.*, 2009; Osman *et al.*, 2009; Yamano *et al.*, 2010; Nguyen *et al.*, 2012; Tamura *et al.*, 2012; Tan *et al.*, 2013). Since CL and PE levels play a role in the biogenesis and function of several mitochondrial membrane protein complexes (Jiang *et al.*, 2000; Schagger, 2002; Zhang *et al.*, 2002; Pfeiffer *et al.*, 2003; van den Brink-van der Laan *et al.*, 2004; Zhong *et al.*, 2004; Nury *et al.*, 2005; Zhang *et al.*, 2005; Claypool *et al.*, 2008; Kutik *et al.*, 2008), we wanted to know if the rescuing ability of Mcp3 derives from effects on the mitochondrial lipid homeostasis. To this end, the lipid profile of mitochondria lacking Mdm10 with or

without elevated Mcp3 levels was analysed by mass spectrometry (In collaboration with C. Özbalci and B. Brügger). Indeed, the overexpression of Mcp3 partially rescued PS, PE and ERG levels (Fig. 2C), consistent with the partial rescue of the growth phenotype and recovery of mitochondrial morphology and complex assembly in *mdm10*Δ cells by Mcp3.

8.1.2 Effects of altered Mcp3 levels on growth of yeast cells, mitochondrial morphology and lipid profile

To further address the role of Mcp3 in cellular function, *mcp3*Δ cells of different genetic backgrounds were tested for growth under different conditions. Cells of the BY4741 background lacking Mcp3 exhibited a slightly reduced growth on glycerol-containing medium, YPG (Fig. 3A).

Since the loss of Mdm10 or other ERMES components results in changes in mitochondrial morphology, the influence of Mcp3 on proper mitochondrial morphology and ERMES assembly was investigated by fluorescence microscopy and electron microscopy. A fraction of the cells possessed thicker, shortened and less interconnected mitochondria when *MCP3* was deleted in BY4741 cells (Fig. 3B). However, no alteration in the number and morphology of cristae, as well as the co-localization of ERMES with mitochondria in punctate structures was observed in such cells (Fig. EV1A and Fig. EV2A and B, in collaboration with X. Chelius and B. Westermann). Consistently, the loss of Mcp3 had no effect on the lipid profile of mitochondria (Fig. 3C and D).

On the other hand, wildtype cells of the W303 background overexpressing Mcp3 displayed various mitochondrial deformations such as fragmentation, condensation, or web-like structures (Fig. 3E). Nevertheless, in the same cells, formation of ERMES punctae or co-localization of the ERMES subunit Mmm1 with mitochondria was not altered compared to wildtype cells (Fig. EV2C).

Taken together, the deletion of *MCP3* in BY4741 cells did not lead to pronounced effects on the growth of yeast cells or effects on mitochondrial morphology, lipid composition, cristae formation or ERMES assembly. Yet, W303 cells overexpressing Mcp3 possessed a slightly altered mitochondrial morphology.

8.2 Biogenesis of Mcp3

8.2.1 Mcp3 is a mitochondrial outer membrane protein

Several high-throughput studies suggest that Mcp3 is a mitochondrial protein located in the MOM. Mcp3 was found in the proteome of mitochondria (Sickmann *et al.*, 2003), and the mitochondrial localization of a C-terminal GFP fusion construct of Mcp3 was described by others (Huh *et al.*, 2003). Furthermore, Mcp3 was specifically found in the MOM proteome (Zahedi *et al.*, 2006). Of note, the sequence of Mcp3 contains two putative transmembrane domains (TMDs). In contrast to a possible localization of Mcp3 in the MOM, Mcp3 displays typical features of a classical mitochondrial targeting sequence and contains a predicted cleavage site between Asn69 and Asp70 for Imp1, a subunit of the inner membrane peptidase (IMP) (Esser *et al.*, 2004) (Fig. 4A). However, the prediction of IMP processing could not be tested in the aforementioned study, because a tag at the C-terminus rendered the protein non-detectable. This observation is in line with our finding that C-terminally hemagglutinin (HA)-tagged Mcp3 was non-functional, since it could not complement the growth defect of cells lacking Mdm10 (data not shown). Nevertheless, a high-throughput study using mass spectrometry revealed that the N-terminus of endogenous Mcp3 starts with Asp70, corresponding to the predicted Imp1 processing site (Vogtle *et al.*, 2009). To study the localization and topology on a single gene level, an internally tagged version of Mcp3 was constructed, where the HA epitope was inserted 4 amino acids C-terminally to the N-terminus of the mature protein (DSLG-HA tag). The functionality of this construct was confirmed by growth rescue of cells lacking Mdm10 (Fig. 4B). Indeed, HA-Mcp3 could be detected in isolated mitochondria and, consistent with the expected size of the mature protein, migrated at 17 kDa (Fig. 4C).

To show its mitochondrial localization, cells lacking endogenous Mcp3 and overexpressing HA-Mcp3 were subjected to subcellular fractionation, where HA-Mcp3 located exclusively to mitochondria (Fig. 4D). Immunofluorescence microscopy confirmed the mitochondrial localization of Mcp3 (Fig. 4E). Of note, enriched mitochondrial fractions contained processed C-terminally HA-tagged Mcp3 (Fig. 4F) suggesting that an altered C-terminus of Mcp3 probably interferes with function rather than biogenesis or stability of the protein.

Since the protein sequence of Mcp3 implies two putative TMDs, we wanted to know whether Mcp3 actually is embedded in a mitochondrial membrane. To this end, carbonate extraction was performed wherein HA-Mcp3, like the integral membrane protein Tom20, was solely detected in the pellet fraction (Fig. 4G). Considering mitochondria harbor two membranes, it was of interest if Mcp3 is integral to the MIM or the MOM. Figure 4H demonstrates that HA-Mcp3 is digested by proteinase K in intact mitochondria, indicating that Mcp3 is located in the MOM and exposed to the cytosol. This finding was supported by a sucrose density gradient experiment, where MIM and MOM vesicles were separated. Similarly to the MOM marker protein Tom20, HA-Mcp3 was mostly found in the lighter fractions of MOM enriched vesicles (Fig. 4I).

Further, we investigated whether the function of Mcp3 is dependent on the predicted TMDs. To this end, two additional versions of Mcp3 were constructed that lacked either the first or the second TMD. Neither of the constructs was able to rescue the growth defect of cells lacking Mdm10 (Fig. 4J). Of note, loss of TMD1 or TMD2 resulted in non-detectable or lower detectable amounts of Mcp3, respectively (Fig. 4K).

Collectively, the results demonstrate that Mcp3 is a mitochondrial membrane protein integral to the MOM.

8.2.2 Mcp3 follows a unique import pathway

In order to investigate the biogenesis of Mcp3 in detail, we first established a read out for the correct import of Mcp3. When radiolabeled Mcp3 was incubated *in vitro* with isolated mitochondria, two bands at about 10 and 15 kDa emerged in a time-dependent manner, corresponding to the cleaved mitochondrial targeting sequence (MTS) and the mature form, respectively (Fig. 5A).

Figures 5B, 5C and S2A demonstrate that the import receptors Tom70/71, but not Tom20 play a role in the biogenesis of Mcp3 as shown by *in vitro* import or western blot analysis. Several studies indicate that multispan proteins can be inserted to the MOM without the involvement of the Tom40 channel (Otera *et al.*, 2007; Becker *et al.*, 2011; Papic *et al.*, 2011). However, upon employing a strain with a temperature sensitive allele of Tom40, the *in vitro* import and steady state levels of Mcp3 were highly reduced in mutant mitochondria (Fig. 5D and E). Furthermore, protease protection assay shows that non-processed precursor accumulates and does not reach the IMS in the altered organelles (Fig. EV3A). We could also show that radiolabeled Mcp3 can physically interact with the

soluble cytosolic domains of Tom70 and Tom20 GST fusion proteins, and to a minor extent also with GST-Tom22 (Fig. 6A), which is in line with the previous results. Incubating mitochondria that contain His-tagged Tom22 with radiolabeled Mcp3, we were able to substantiate these findings *in organello* by affinity pulldown or antibody shift in BN-PAGE (Fig. 6B and C). Taken together, the data strongly support the idea that Mcp3 is initially recognized by the Tom70 receptor and is then handed over to Tom22 which mediates the relay to Tom40. Eventually, Mcp3 crosses the MOM through the central pore of the TOM complex, making Mcp3 and Om45 the only known α-helical MOM proteins depending on functional Tom40 (Wenz *et al.*, 2014).

Considering that the TIM23 complex plays an additional role in the biogenesis of the MOM protein Om45, we were interested if this is also the case for Mcp3. An involvement of the TIM complex is suggested by the observation that Mcp3 contains a cleavable MTS, potentially removed by MPP and/or IMP, as processing proteases of the MOM were not reported so far. Indeed, the *in vitro* import of radiolabeled Mcp3, as well as the steady state levels of HA-Mcp3 were significantly reduced in mitochondria harboring a temperature sensitive allele of Tim23 (Fig. 7A and B, respectively). Additionally, the formation of mature Mcp3 was significantly reduced when mitochondria depolarized with either CCCP or valinomycin were used for *in vitro* import (Fig. 7C and Fig. EV4, respectively), indicating that the mitochondrial membrane potential is required for processing of Mcp3. Mcp3 contains a predicted MTS which is usually cleaved by MPP, yet mature Mcp3 emerged in *in vitro* import assay even when MPP was inhibited by chelators for bivalent cations, ortho-phenanthroline, and EDTA. Additionally, incubation of recombinant MPP with radiolabeled Mcp3 precursor did not yield mature Mcp3 (Fig. 7C). Furthermore, processing of radiolabeled Mcp3 was not influenced in mitochondria isolated from cells harboring a temperature sensitive allele of Mas1, a subunit of MPP (Fig. S3).

The previous results raise the question, by which peptidase, other than MPP, Mcp3 is processed. Figure 7D demonstrates that the mature form of Mcp3 could not be detected in cells lacking either subunit of IMP, whereas lack of other mitochondrial peptidases or degrading enzymes did not abolish Mcp3 processing. To validate this result, *in vitro* import of radiolabeled Mcp3 was conducted with mitochondria isolated from cells lacking Imp1 or Imp2. Processing of Mcp3 could not be observed in such mitochondria (Fig. 7F). Additionally, a mutation in the putative Imp1 processing site at amino acid position 70 (D70G) rendered the protein non-cleavable (Fig. 7G). Of note, C-terminally tagged Mcp3 could also be processed by IMP, reinforcing the assumption that a tag at the C-terminus interferes with the function of Mcp3, rather than biogenesis or stability (Fig. 7E).

The data show that Mcp3 is the first IMP-dependent MOM protein. In order to decipher the individual steps of Mcp3 processing, the D70G mutant was analysed in more detail. Figure 7G shows that the non-cleavable precursor of Mcp3 was resistant to externally added protease (lane 3), suggesting that Mcp3 precursor translocates at least to the level of the IMS before being processed. Indeed, also in mitochondria lacking Imp1 or Imp2 Mcp3 precursor accumulated in the IMS (Fig. 7G, lanes 11 and 12). Even in wildtype mitochondria there was a fraction of mature Mcp3 being protease protected, probably corresponding to a processed Mcp3 IMS intermediate (Fig. 7G and H, lanes 4, asterisks). This band disappeared when mitochondria were pretreated with the uncoupler CCCP, suggesting that an intact membrane potential is required for the translocation of Mcp3 through the TOM complex (Fig. 7H, lane 5).

Finally, we were interested whether, and if so which MOM complex mediates the insertion of Mcp3 from the IMS to the MOM. The β-barrel insertion machinery was ruled out by performing *in vitro* import experiments with mitochondria isolated from cells lacking the TOB subunit Mas37 (Fig. S2B). Consistently, the import chaperones Tim8/10/13 which play a role in the biogenesis of β-barrel proteins of the MOM and carrier proteins of the MIM were not required for Mcp3 biogenesis, as demonstrated by *in vitro* import into mitochondria lacking sTIMs (Fig. S2C and D). Since the insertion of some α-helical proteins to the MOM is mediated by the MIM complex, we investigated the requirement of Mim1 and Mim2 for Mcp3 biogenesis. Indeed, the *in vitro* import of radiolabeled Mcp3, as well as steady state levels of HA-Mcp3 were lessened when either of the MIM subunits was missing (Fig. 8A and B). It was shown that the assembly of the

TOM complex is hampered in *mim1*Δ and *mim2*Δ cells, therefore the import of Mcp3 might be influenced indirectly by the absence of the MIM complex. To verify that the observed effects are direct, we aimed at demonstrating the physical interaction of Mcp3 with the MIM complex subunit Mim1. Figure 8C shows that radiolabeled Mcp3 precursor co-purified with MBP-Mim1 in a considerably higher amount than with MBP alone.

Collectively, the results show that Mcp3 precursor crosses the MOM via the TOM complex and that the biogenesis of Mcp3 is dependent on the TIM23 complex, as well as the membrane potential across the MIM. Furthermore, Mcp3 is not processed by MPP, but rather by IMP. Considering that the activity of IMP requires both subunits Imp1 and Imp2, the experiments can not specify which of the subunits processes Mcp3. Regardless, the results are consistent with studies imposing Imp1 as the responsible processing subunit (Esser *et al.*, 2004; Vogtle *et al.*, 2009). The experiments suggest that the MIM complex might be directly involved in the insertion of Mcp3 to the MOM.

9. Discussion

The ERMES complex and its subunits have been a subject of extensive research within the last two decades. Its involvement in many important cellular processes, such as the biogenesis of β-barrel proteins, maintenance of mitochondrial morphology and lipid homeostasis, as well as inheritance of the mitochondrial genome, was reported (Burgess *et al.*, 1994; Sogo and Yaffe, 1994; Berger *et al.*, 1997; Boldogh *et al.*, 1998; Hanekamp *et al.*, 2002; Kornmann *et al.*, 2009; Yamano *et al.*, 2010). The most prominent feature of the ERMES complex is the ability to establish a physical connection between mitochondria and ER, thereby facilitating the lipid exchange between the two organelles (Kornmann *et al.*, 2009). It is still unclear, whether the ERMES complex simply creates a region of close proximity between mitochondria and ER or if it actively contributes in the transfer of lipids. Nevertheless, the ability of ERMES components to directly bind lipids was predicted and recently demonstrated implying an active role for the complex in lipid transport (Lee and Hong, 2006; Kopec *et al.*, 2010; AhYoung *et al.*, 2015).

Since the different cellular processes involving the ERMES complex are interdependent, it is difficult to interpret the results obtained from experiments with absent ERMES components. The observed phenotypes might be direct effects, but could as well be an indirect outcome of another defect, making it complicated to unravel the primary function of ERMES. The whole picture grows further in complexity because at least two alternative ways of mitochondria to exchange lipids with the remainder of the cell exist, namely the EMC between mitochondria and ER, and vCLAMP between mitochondria and vacuole (Elbaz-Alon *et al.*, 2014; Lahiri *et al.*, 2014).

Studying ERMES complex mutants is problematic considering the high frequency by which endogenous suppressors tend to emerge in cells deleted for ERMES genes. (Berger *et al.*, 1997; Hanekamp *et al.*, 2002). Recently, two high-copy suppressors of the *mdm10*Δ phenotype were identified, namely Mcp1 and Mcp2 (Tan *et al.*, 2013). In this study we report a third suppressor, Mcp3, which can alleviate several negative phenotypes caused by loss of ERMES. The rescuing capacity of Mcp3 might be related to one or more processes, however substantial evidence points towards a direct or indirect involvement of Mcp3 in lipid metabolism. A tempting hypothesis is that the partial restoration of the lipid profile in turn ameliorates the defects in mitochondrial morphology, thereby improving the fitness and growth of the cells. The observation that

Mcp3 can restore defects in the assembly pattern of respiratory chain supercomplexes caused by lipid imbalances supports the potential involvement of Mcp3 in mitochondrial lipid homeostasis. On the other hand, the influence of Mcp3 on the morphology apparatus of mitochondria remains to be studied. It has been shown that the biogenesis of Mgm1, a protein required for mitochondrial fusion, depends on CL. Reduced levels of CL thereby lead to fragmented mitochondria and the loss of mtDNA (DeVay *et al.*, 2009; Joshi *et al.*, 2012). It would be interesting to dissect, whether there is a functional relationship between Mcp3 and Mgm1 or another protein involved in the maintenance of tubular mitochondrial morphology. In fact, the overexpression of Mcp3 in the W303a background resulted in a slightly altered mitochondrial morphology, suggesting an involvement of the protein in processes determining mitochondrial dynamics. However, the deletion of *MCP3* in W303 cells did not result in aberrant mitochondria or reduced growth of the cells. The BY4741 cells carry a mutation in the *HAP1* transcription factor, which regulates genes that are involved in electron transfer reactions. The *HAP1* mutation thereby leads to reduced ability of the cells to respire and increased sensitivity to altered protein levels (Gaisne *et al.*, 1999; Ocampo *et al.*, 2012). Indeed cells lacking Mcp3 in the BY4741 background displayed a slight growth defect on non-fermentable medium. However, the mitochondrial morphology in this background was only marginally altered and no other tested cellular process was affected when Mcp3 was missing. It should also be of interest to study, whether the simultaneous lack of *MCP3* and *MDM10* causes any additional cellular defects, or if such a double deletion might even result in synthetic lethality.

Contacts between ER and mitochondria are mediated by the MOM, therefore the circumstance that two of the ERMES suppressors, Mcp1 and Mcp3, are MOM proteins is of no surprise, but it also shows that understanding the biogenesis and topology of a protein can contribute in comprehending the molecular processes in which the protein partakes. Many factors challenged the investigations on the biogenesis pathway of Mcp3. Even though C-terminally HA-tagged Mcp3 was detectable, it was not functional. Consistent with our results, the authors of another study could not detect at all C-terminally myc-tagged Mcp3 in protein extracts, concluding that the construct is poorly expressed or the tag renders the protein instable (Esser *et al.*, 2004). In contrast, a C-terminal GFP construct of Mcp3 used in a different study localized to mitochondria in fluorescence microscopy experiments, demonstrating that even a large C-terminal tag not necessarily interferes with mitochondrial localization or stability of Mcp3 (Huh *et al.*,

2003). However, a tag in close proximity to the C-terminal TMD might compromise membrane integration or function of Mcp3. Since tagging Mcp3 at the N-terminus would lead to removal of the tag during processing, an internally tagged version of Mcp3 had to be constructed. The result of Mcp3 being located in the MOM was puzzling, because its sequence contains a predicted MTS. This led us to study the biogenesis of Mcp3 further, revealing that in contrast to most presequence containing proteins, the biogenesis of Mcp3 is dependent on Tom70 and not Tom20 (Fig. 3). However, the involvement of Tom70 was also shown for other proteins harboring an MTS, mostly hydrophobic precursors with a tendency to aggregate (Yamamoto *et al.*, 2009). This can be explained by the chaperoning activity of Tom70, which helps to keep proteins in an unfolded and import competent state. Furthermore, Tom70 provides the platform for the cytosolic chaperone Ssa1, which delivers hydrophobic precursors to mitochondria (Young *et al.*, 2003). It is tempting to assume that Tom70 evolved as a receptor for the biogenesis of Mcp3, since Mcp3 contains two hydrophobic TMDs and a hydrophobic patch at the N-terminus.

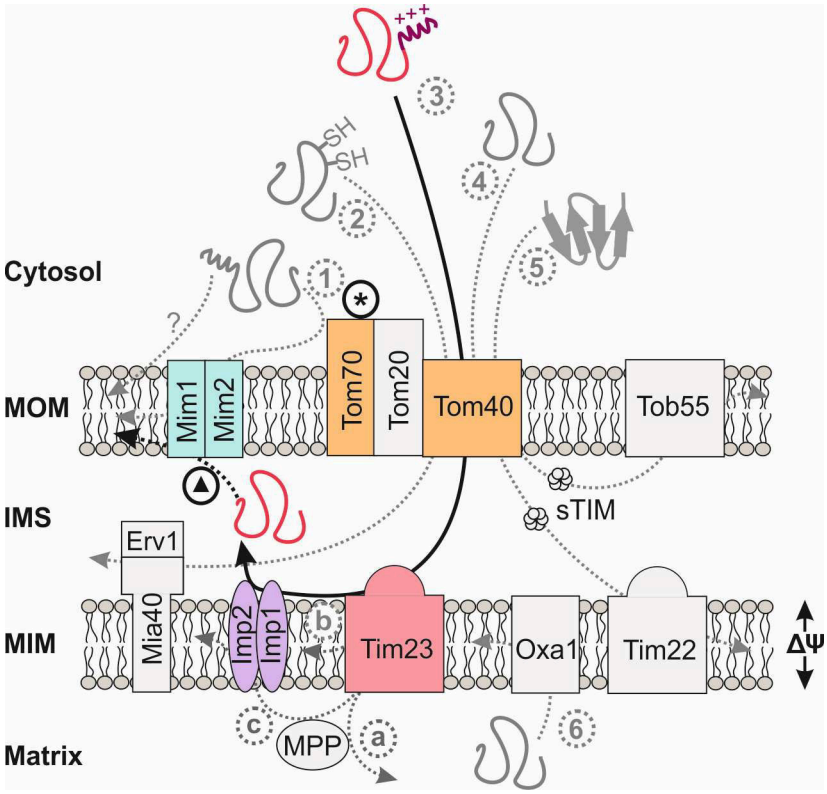

Figure 3. Mcp3 follows a unique biogenesis pathway. Mcp3 is translated in the cytosol and initially recognized by the import receptor Tom70. Mcp3 subsequently crosses the outer membrane through a pore formed by Tom40. Mcp3 is then handed over to the Tim23 complex and afterwards processed by IMP. The MIM complex might be involved in the integration of Mcp3 to the MOM. Steps diverging from the pathway of classical presequence containing proteins are marked by an asterisk or triangle.

Apart from Mcp3 there are other MOM multispan proteins whose biogenesis depend on the Tom70 receptor, such as Ugo1 and Scm4 (Becker *et al.*, 2011; Papic *et al.*, 2011). These proteins are reported to be inserted into the MOM without further involvement of the central TOM pore, whereas Mcp3 is translocated across the MOM via the channel formed by Tom40.

Next, Mcp3 is handed over to the TIM23 complex (Fig. 3). It can be speculated that the N-terminal part of Mcp3 is inserted into the MIM in a stop-transfer mechanism. The involvement of the TIM23 complex in the biogenesis of a MOM protein was also reported for Om45, with the difference that Om45 is not processed by any peptidase (Song *et al.*, 2014; Wenz *et al.*, 2014). Therefore, Mcp3 is the first MOM protein known to be processed by a peptidase of the MIM. A classical MTS is predicted for Mcp3, yet unlike the majority of presequence containing proteins it is not processed by MPP. The only known yeast protein that omits MPP processing despite containing an MTS is Hsp10. Even though the subunit responsible for Mcp3 processing could not be determined, an Imp1 consensus sequence is located at amino acid positions 67-70 (IFND), consistent with the identification of the endogenous N-terminus to start with aspartate at residue 70 (Vogtle *et al.*, 2009).

Following processing, mature Mcp3 is integrated into the MOM in a MIM complex dependent manner (Fig. 3). This observation may be due to a direct involvement of the MIM complex in the biogenesis of Mcp3, or an indirect effect since the levels of the TOM complex are reduced in cells lacking functional MIM complex (Becker *et al.*, 2008; Popov-Celeketic *et al.*, 2008). The physical interaction of Mcp3 precursor with Mim1 observed in this study favors a direct involvement of the MIM complex. It implies that the MIM complex can mediate the integration of membrane proteins from both sides of the membrane. None of the membrane insertases identified so far (e.g. Oxa1/YidC/Alb3 from mitochondria, bacteria and chloroplasts respectively, as well as the GET or SEC machinery) is reported to achieve this. Further evidence for this ability could be obtained by reconstituting the MIM complex from recombinant proteins into liposomes and testing the insertion of MIM complex substrates into these artificial membranes. It is also conceivable that the TMD of MOM proteins is directly handed over from the TOM to the MIM complex. This would demand a lateral release of the precursor protein from the central pore of the TOM complex. Whether the β-barrel protein Tom40 can laterally release precursor proteins into the MOM is a matter of debate and a recent

study argues that the separation of β-strands is energetically costly and would demand major rearrangements of other TOM subunits (Bausewein *et al.*, 2017). Yet, another article provides evidence for a lateral release of preproteins from the TOM complex (Harner *et al.*, 2011). In such a scenario, MOM proteins that do not acquire the classical signal anchored topology but rather face the IMS with the bulk of the protein might require the TIM23 complex to direct the large C-terminal part to the IMS.

The reason for requirement of the TIM23 complex and the membrane potential in the biogenesis of Mcp3 remains unsolved. It can be speculated that the physiological state of the organelle influences the membrane potential, thereby affecting the biogenesis of Mcp3 as a sensor for damaged mitochondria. The protein Pink1 in higher eukaryotes functions as such a sensor. In case of a proper membrane potential, Pink1 is targeted to the inner membrane, where it gets degraded by the protease PARL (presenilins-associated rhomboid-like protein). In case of depolarized mitochondria, Pink1 is not degraded by PARL and instead is integrated to the MOM, where it induces autophagy by the recruitment of parkin (Okatsu *et al.*, 2015).

Our results suggest a topology for Mcp3 where the N- and C-termini face the cytosol. In the reverse orientation (Fig. 4B, HA-tag blue), protease treatment should yield a fragment of about 8 kDa. Since fragments containing the HA-tag could not be detected upon protease treatment of intact mitochondria, our data support a topology where the HA-tag is exposed to the cytosol (Fig. 4A). Still, IMS orientation of the C- and N- termini cannot be excluded simply based on the absent detection of the 8 kDa fragment.

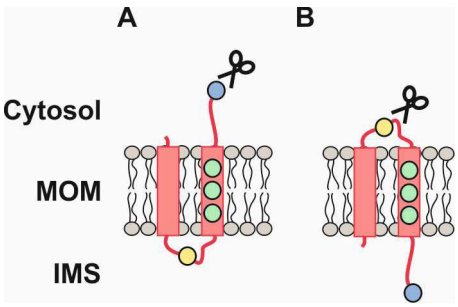

Figure 4. Putative topologies of Mcp3 and localization of specific amino acids. Mcp3 is located in the MOM probably with the N- and C- termini facing the cytosol (A). The proteolytic digestion of Mcp3 in conformation B should yield an HA-tagged (blue) fragment of about 8 kDa. Mcp3 contains three glycine residues in TMD1 (green) and a single cysteine in the loop region (yellow).

Additionally, Mcp3 contains a cysteine in the loop region (Fig. 4, yellow dot) between the two TMDs. A cysteine residue in the IMS could serve the formation of a disulfide bond with another protein, maybe even an inner membrane protein for the establishment of a contact site between the MIM and the MOM. It can be speculated that such a connection might facilitate the exchange of lipids between the MIM and the MOM, thereby alleviating defects related to the loss of ERMES complex. It was shown that such a contact site between the MIM and the MOM is mediated by mitochondrial contact site complex (MICOS), which is also involved in maintaining a correct mitochondrial lipid homeostasis (Hoppins *et al.*, 2011; Aaltonen *et al.*, 2016).

Interactions of Mcp3 with other proteins might as well be facilitated by the two connected glycine motifs GxxxGxxxG (G, glycine; x, any amino acid) in the N- terminal TMD of Mcp3 (Fig. 4, green dots). The presence of glycine motifs might assist in the formation of TMD helix dimers by enabling the close proximity of two α-helices (Ospina *et al.*, 2011). However, GxxxG motifs might not only be relevant for oligomerization, but also for protein folding (Teese and Langosch, 2015). Interestingly, this glycine motif is conserved between Mcp3 (also known as Fun14) and the mammalian protein FUNDC1 (Fun14 domain containing protein 1). FUNDC1 was reported to be a mitochondrial outer membrane protein enriched at the MAM by interacting with the ER resident protein calnexin during hypoxia. It was also shown that FUNDC1 acts as a receptor for hypoxia-induced mitophagy and drives mitochondrial fission by recruiting DRP1 (Dnm1 in yeast) to mitochondria (Liu *et al.*, 2012; Wu *et al.*, 2016). Hence, FUNDC1 integrates mitochondrial fission and mitophagy at the MAM, which is reminiscent of ERMES as an important player in mitophagy in yeast (Bockler and Westermann, 2014). These observations raise questions which should be addressed in future experiments: Does Mcp3 function as a receptor for mitophagy similar to FUNDC1? Can the overexpression of Mcp3 alleviate mitophagy defects of ERMES mutants or can increased mitophagy rates supply the remainder of the cell with mitochondrial lipids? So far, there are no indications for a role of Mcp3 in mitophagy since neither the deletion nor the overexpression of *MCP3* resulted in altered mitochondrial degradation (data not shown). Considering that mitochondrial fission is required for mitophagy, it would be interesting to study the role of Mcp3 for mitochondrial dynamics, as discussed previously in this chapter. Furthermore, identification of interaction partners involved in mitophagy, maintenance of mitochondrial morphology or other cellular processes might help to understand the molecular function of Mcp3 and in turn of the ERMES complex.

10. References

Aaltonen, M.J., J.R. Friedman, C. Osman, B. Salin, J.P. di Rago, J. Nunnari, T. Langer, and T. Tatsuta. 2016. MICOS and phospholipid transfer by Ups2-Mdm35 organize membrane lipid synthesis in mitochondria. *The Journal of Cell Biology*. 213:525-534.

AhYoung, A.P., J. Jiang, J. Zhang, X. Khoi Dang, J.A. Loo, Z.H. Zhou, and P.F. Egea. 2015. Conserved SMP domains of the ERMES complex bind phospholipids and mediate tether assembly. *Proceedings of the National Academy of Science of the United States of America*. 112:E3179-3188.

Ardail, D., F. Gasnier, F. Lerme, C. Simonot, P. Louisot, and O. Gateau-Roesch. 1993. Involvement of mitochondrial contact sites in the subcellular compartmentalization of phospholipid biosynthetic enzymes. *The Journal of Biological Chemistry.* 268:25985-25992.

Bausewein, T., D.J. Mills, J.D. Langer, B. Nitschke, S. Nussberger, and W. Kuhlbrandt. 2017. Cryo-EM Structure of the TOM Core Complex from Neurospora crassa. *Cell*. 170:693-700 e697.

Becker, T., S. Pfannschmidt, B. Guiard, D. Stojanovski, D. Milenkovic, S. Kutik, N. Pfanner, C. Meisinger, and N. Wiedemann. 2008. Biogenesis of the mitochondrial TOM complex: Mim1 promotes insertion and assembly of signal-anchored receptors. *The Journal of Biological Chemistry.* 283:120-127.

Becker, T., L.S. Wenz, V. Kruger, W. Lehmann, J.M. Muller, L. Goroncy, N. Zufall, T. Lithgow, B. Guiard, A. Chacinska, R. Wagner, C. Meisinger, and N. Pfanner. 2011. The mitochondrial import protein Mim1 promotes biogenesis of multispanning outer membrane proteins. *The Journal of Cell Biology*. 194:387-395.

Berger, K.H., L.F. Sogo, and M.P. Yaffe. 1997. Mdm12p, a component required for mitochondrial inheritance that is conserved between budding and fission yeast. *The Journal of Cell Biology.* 136:545-553.

Bockler, S., and B. Westermann. 2014. Mitochondrial ER contacts are crucial for mitophagy in yeast. *Developmental Cell*. 28:450-458.

Boldogh, I., N. Vojtov, S. Karmon, and L.A. Pon. 1998. Interaction between mitochondria and the actin cytoskeleton in budding yeast requires two integral

mitochondrial outer membrane proteins, Mmm1p and Mdm10p. *The Journal of Cell Biology*. 141:1371-1381.

Bottinger, L., S.E. Horvath, T. Kleinschroth, C. Hunte, G. Daum, N. Pfanner, and T. Becker. 2012. Phosphatidylethanolamine and cardiolipin differentially affect the stability of mitochondrial respiratory chain supercomplexes. *Journal of Molecular Biology*. 423:677-686.

Brix, J., G.A. Ziegler, K. Dietmeier, J. Schneider-Mergener, G.E. Schulz, and N. Pfanner. 2000. The mitochondrial import receptor Tom70: identification of a 25 kDa core domain with a specific binding site for preproteins. *Journal of Molecular Biology*. 303:479-488.

Burgess, S.M., M. Delannoy, and R.E. Jensen. 1994. MMM1 encodes a mitochondrial outer membrane protein essential for establishing and maintaining the structure of yeast mitochondria. *The Journal of Cell Biology*. 126:1375-1391.

Cavalier-Smith, T. 1987. The origin of eukaryotic and archaebacterial cells. *Annals of the New York Academy of Sciences*. 503:17-54.

Ceh-Pavia, E., M.P. Spiller, and H. Lu. 2013. Folding and biogenesis of mitochondrial small Tim proteins. *International Journal of Molecular Sciences*. 14:16685-16705.

Chacinska, A., C.M. Koehler, D. Milenkovic, T. Lithgow, and N. Pfanner. 2009. Importing mitochondrial proteins: machineries and mechanisms. *Cell*. 138:628-644.

Chan, D.C. 2006. Mitochondria: dynamic organelles in disease, aging, and development. *Cell*. 125:1241-1252.

Chicco, A.J., and G.C. Sparagna. 2007. Role of cardiolipin alterations in mitochondrial dysfunction and disease. *American Journal of Physiology. Cell Physiology*. 292:C33-44.

Claypool, S.M., Y. Oktay, P. Boontheung, J.A. Loo, and C.M. Koehler. 2008. Cardiolipin defines the interactome of the major ADP/ATP carrier protein of the mitochondrial inner membrane. *The Journal of Cell Biology*. 182:937-950.

Comte, J., B. Maisterrena, and D.C. Gautheron. 1976. Lipid composition and protein profiles of outer and inner membranes from pig heart mitochondria. Comparison with microsomes. *Biochimica et Biophysica Acta*. 419:271-284.

Connerth, M., T. Tatsuta, M. Haag, T. Klecker, B. Westermann, and T. Langer. 2012. Intramitochondrial transport of phosphatidic acid in yeast by a lipid transfer protein. *Science*. 338:815-818.

DeVay, R.M., L. Dominguez-Ramirez, L.L. Lackner, S. Hoppins, H. Stahlberg, and J. Nunnari. 2009. Coassembly of Mgm1 isoforms requires cardiolipin and mediates mitochondrial inner membrane fusion. *The Journal of Cell Biology.* 186:793-803.

Dimmer, K.S., D. Papic, B. Schumann, D. Sperl, K. Krumpe, D.M. Walther, and D. Rapaport. 2012. A crucial role for Mim2 in the biogenesis of mitochondrial outer membrane proteins. *Journal of Cell Science*. 125:3464-3473.

Elbaz-Alon, Y., M. Eisenberg-Bord, V. Shinder, S.B. Stiller, E. Shimoni, N. Wiedemann, T. Geiger, and M. Schuldiner. 2015. Lam6 Regulates the Extent of Contacts between Organelles. *Cell Reports*. 12:7-14.

Elbaz-Alon, Y., E. Rosenfeld-Gur, V. Shinder, A.H. Futerman, T. Geiger, and M. Schuldiner. 2014. A dynamic interface between vacuoles and mitochondria in yeast. *Developmental Cell*. 30:95-102.

Esser, K., P.S. Jan, E. Pratje, and G. Michaelis. 2004. The mitochondrial IMP peptidase of yeast: functional analysis of domains and identification of Gut2 as a new natural substrate. *Molecular Genetics and Genomics*. 271:616-626.

Fekkes, P., K.A. Shepard, and M.P. Yaffe. 2000. Gag3p, an outer membrane protein required for fission of mitochondrial tubules. *The Journal of Cell Biology.* 151:333-340.

Flinner, N., L. Ellenrieder, S.B. Stiller, T. Becker, E. Schleiff, and O. Mirus. 2013. Mdm10 is an ancient eukaryotic porin co-occurring with the ERMES complex. *Biochimica et Biophysica Acta*. 1833:3314-3325.

Flis, V.V., and G. Daum. 2013. Lipid transport between the endoplasmic reticulum and mitochondria. *Cold Spring Harbor Perspectives in Biology*. 5.

Frazier, A.E., C. Kiu, D. Stojanovski, N.J. Hoogenraad, and M.T. Ryan. 2006. Mitochondrial morphology and distribution in mammalian cells. *Biological Chemistry*. 387:1551-1558.

Frederick, R.L., J.M. McCaffery, K.W. Cunningham, K. Okamoto, and J.M. Shaw. 2004. Yeast Miro GTPase, Gem1p, regulates mitochondrial morphology via a novel pathway. *The Journal of Cell Biology.* 167:87-98.

Gaigg, B., R. Simbeni, C. Hrastnik, F. Paltauf, and G. Daum. 1995. Characterization of a microsomal subfraction associated with mitochondria of the yeast,

Saccharomyces cerevisiae. Involvement in synthesis and import of phospholipids into mitochondria. *Biochimica et Biophysica Acta*. 1234:214-220.

Gaisne, M., A.M. Becam, J. Verdiere, and C.J. Herbert. 1999. A 'natural' mutation in Saccharomyces cerevisiae strains derived from S288c affects the complex regulatory gene HAP1 (CYP1). *Current Genetics*. 36:195-200.

Gakh, O., P. Cavadini, and G. Isaya. 2002. Mitochondrial processing peptidases. *Biochimica et Biophysica Acta*. 1592:63-77.

Gatta, A.T., L.H. Wong, Y.Y. Sere, D.M. Calderon-Norena, S. Cockcroft, A.K. Menon, and T.P. Levine. 2015. A new family of StART domain proteins at membrane contact sites has a role in ER-PM sterol transport. *Elife*. 4.

Gebert, N., A. Chacinska, K. Wagner, B. Guiard, C.M. Koehler, P. Rehling, N. Pfanner, and N. Wiedemann. 2008. Assembly of the three small Tim proteins precedes docking to the mitochondrial carrier translocase. *EMBO Reports*. 9:548-554.

Gebert, N., A.S. Joshi, S. Kutik, T. Becker, M. McKenzie, X.L. Guan, V.P. Mooga, D.A. Stroud, G. Kulkarni, M.R. Wenk, P. Rehling, C. Meisinger, M.T. Ryan, N. Wiedemann, M.L. Greenberg, and N. Pfanner. 2009. Mitochondrial cardiolipin involved in outer-membrane protein biogenesis: implications for Barth syndrome. *Current Biology*. 19:2133-2139.

Glick, B.S., C. Wachter, and G. Schatz. 1992. The energetics of protein import into mitochondria. *Biochimica et Biophysica Acta*. 1101:249-251.

Gohil, V.M., M.N. Thompson, and M.L. Greenberg. 2005. Synthetic lethal interaction of the mitochondrial phosphatidylethanolamine and cardiolipin biosynthetic pathways in Saccharomyces cerevisiae. *The Journal of Biological Chemistry*. 280:35410-35416.

Graack, H.R., and B. Wittmann-Liebold. 1998. Mitochondrial ribosomal proteins (MRPs) of yeast. *Biochemical Journal*. 329 (Pt 3):433-448.

Gray, M.W., G. Burger, and B.F. Lang. 1999. Mitochondrial evolution. *Science*. 283:1476-1481.

Hahne, K., V. Haucke, L. Ramage, and G. Schatz. 1994. Incomplete arrest in the outer membrane sorts NADH-cytochrome b5 reductase to two different submitochondrial compartments. *Cell*. 79:829-839.

Hailey, D.W., A.S. Rambold, P. Satpute-Krishnan, K. Mitra, R. Sougrat, P.K. Kim, and J. Lippincott-Schwartz. 2010. Mitochondria supply membranes for autophagosome biogenesis during starvation. *Cell*. 141:656-667.

Hanekamp, T., M.K. Thorsness, I. Rebbapragada, E.M. Fisher, C. Seebart, M.R. Darland, J.A. Coxbill, D.L. Updike, and P.E. Thorsness. 2002. Maintenance of mitochondrial morphology is linked to maintenance of the mitochondrial genome in Saccharomyces cerevisiae. *Genetics*. 162:1147-1156.

Harner, M., W. Neupert, and M. Deponte. 2011. Lateral release of proteins from the TOM complex into the outer membrane of mitochondria. *The EMBO Journal*. 30:3232-3241.

Hartl, F.U., B. Schmidt, E. Wachter, H. Weiss, and W. Neupert. 1986. Transport into mitochondria and intramitochondrial sorting of the Fe/S protein of ubiquinol-cytochrome c reductase. *Cell*. 47:939-951.

Hell, K., J.M. Herrmann, E. Pratje, W. Neupert, and R.A. Stuart. 1998. Oxa1p, an essential component of the N-tail protein export machinery in mitochondria. *Proceedings of the National Academy of Science of the United States of America*. 95:2250-2255.

Hoch, F.L. 1992. Cardiolipins and biomembrane function. *Biochimica et Biophysica Acta*. 1113:71-133.

Honscher, C., M. Mari, K. Auffarth, M. Bohnert, J. Griffith, W. Geerts, M. van der Laan, M. Cabrera, F. Reggiori, and C. Ungermann. 2014. Cellular metabolism regulates contact sites between vacuoles and mitochondria. *Developmental Cell*. 30:86-94.

Hoppins, S., S.R. Collins, A. Cassidy-Stone, E. Hummel, R.M. Devay, L.L. Lackner, B. Westermann, M. Schuldiner, J.S. Weissman, and J. Nunnari. 2011. A mitochondrial-focused genetic interaction map reveals a scaffold-like complex required for inner membrane organization in mitochondria. *The Journal of Cell Biology*. 195:323-340.

Huh, W.K., J.V. Falvo, L.C. Gerke, A.S. Carroll, R.W. Howson, J.S. Weissman, and E.K. O'Shea. 2003. Global analysis of protein localization in budding yeast. *Nature*. 425:686-691.

Ieva, R., A.K. Heisswolf, M. Gebert, F.N. Vogtle, F. Wollweber, C.S. Mehnert, S. Oeljeklaus, B. Warscheid, C. Meisinger, M. van der Laan, and N. Pfanner. 2013. Mitochondrial inner membrane protease promotes assembly of presequence translocase by removing a carboxy-terminal targeting sequence. *Nature Communications*. 4:2853.

Imai, K., N. Fujita, M.M. Gromiha, and P. Horton. 2011. Eukaryote-wide sequence analysis of mitochondrial beta-barrel outer membrane proteins. *BMC Genomics*. 12:79.

Jan, P.S., K. Esser, E. Pratje, and G. Michaelis. 2000. Som1, a third component of the yeast mitochondrial inner membrane peptidase complex that contains Imp1 and Imp2. *Molecular & General Genetics*. 263:483-491.

Jiang, F., M.T. Ryan, M. Schlame, M. Zhao, Z. Gu, M. Klingenberg, N. Pfanner, and M.L. Greenberg. 2000. Absence of cardiolipin in the crd1 null mutant results in decreased mitochondrial membrane potential and reduced mitochondrial function. *The Journal of Biological Chemistry*. 275:22387-22394.

John Peter, A.T., B. Herrmann, D. Antunes, D. Rapaport, K.S. Dimmer, and B. Kornmann. 2017. Vps13-Mcp1 interact at vacuole-mitochondria interfaces and bypass ER-mitochondria contact sites. *The Journal of Cell Biology*.

Jores, T., and D. Rapaport. 2017. Early stages in the biogenesis of eukaryotic beta-barrel proteins. *FEBS Letters*. 591:2671-2681.

Joshi, A.S., M.N. Thompson, N. Fei, M. Huttemann, and M.L. Greenberg. 2012. Cardiolipin and mitochondrial phosphatidylethanolamine have overlapping functions in mitochondrial fusion in Saccharomyces cerevisiae. *The Journal of Biological Chemistry*. 287:17589-17597.

Joshi, A.S., J. Zhou, V.M. Gohil, S. Chen, and M.L. Greenberg. 2009. Cellular functions of cardiolipin in yeast. *Biochimica et Biophysica Acta*. 1793:212-218.

Kemper, C., S.J. Habib, G. Engl, P. Heckmeyer, K.S. Dimmer, and D. Rapaport. 2008. Integration of tail-anchored proteins into the mitochondrial outer membrane does not require any known import components. *Journal of Cell Science*. 121:1990-1998.

Kitakawa, M., and K. Isono. 1991. The mitochondrial ribosomes. *Biochimie*. 73:813-825.

Kopec, K.O., V. Alva, and A.N. Lupas. 2010. Homology of SMP domains to the TULIP superfamily of lipid-binding proteins provides a structural basis for lipid exchange between ER and mitochondria. *Bioinformatics*. 26:1927-1931.

Kornmann, B., E. Currie, S.R. Collins, M. Schuldiner, J. Nunnari, J.S. Weissman, and P. Walter. 2009. An ER-mitochondria tethering complex revealed by a synthetic biology screen. *Science*. 325:477-481.

Kornmann, B., C. Osman, and P. Walter. 2011. The conserved GTPase Gem1 regulates endoplasmic reticulum-mitochondria connections. *Proceedings of the National Academy of Science of the United States of America*. 108:14151-14156.

Kuroda, T., M. Tani, A. Moriguchi, S. Tokunaga, T. Higuchi, S. Kitada, and O. Kuge. 2011. FMP30 is required for the maintenance of a normal cardiolipin level and mitochondrial morphology in the absence of mitochondrial phosphatidylethanolamine synthesis. *Molecular Microbiology*. 80:248-265.

Kutik, S., M. Rissler, X.L. Guan, B. Guiard, G. Shui, N. Gebert, P.N. Heacock, P. Rehling, W. Dowhan, M.R. Wenk, N. Pfanner, and N. Wiedemann. 2008. The translocator maintenance protein Tam41 is required for mitochondrial cardiolipin biosynthesis. *The Journal of Cell Biology*. 183:1213-1221.

Lahiri, S., J.T. Chao, S. Tavassoli, A.K. Wong, V. Choudhary, B.P. Young, C.J. Loewen, and W.A. Prinz. 2014. A conserved endoplasmic reticulum membrane protein complex (EMC) facilitates phospholipid transfer from the ER to mitochondria. *PLoS Biology*. 12:e1001969.

Lang, A.B., A.T. John Peter, P. Walter, and B. Kornmann. 2015. ER-mitochondrial junctions can be bypassed by dominant mutations in the endosomal protein Vps13. *The Journal of Cell Biology*. 210:883-890.

Lange, C., J.H. Nett, B.L. Trumpower, and C. Hunte. 2001. Specific roles of protein-phospholipid interactions in the yeast cytochrome bc1 complex structure. *The EMBO Journal*. 20:6591-6600.

Lee, C.M., J. Sedman, W. Neupert, and R.A. Stuart. 1999. The DNA helicase, Hmi1p, is transported into mitochondria by a C-terminal cleavable targeting signal. *The Journal of Biological Chemistry*. 274:20937-20942.

Lee, I., and W. Hong. 2006. Diverse membrane-associated proteins contain a novel SMP domain. *FASEB Journal*. 20:202-206.

Lill, R., K. Diekert, A. Kaut, H. Lange, W. Pelzer, C. Prohl, and G. Kispal. 1999. The essential role of mitochondria in the biogenesis of cellular iron-sulfur proteins. *Biological Chemistry*. 380:1157-1166.

Liu, L., D. Feng, G. Chen, M. Chen, Q. Zheng, P. Song, Q. Ma, C. Zhu, R. Wang, W. Qi, L. Huang, P. Xue, B. Li, X. Wang, H. Jin, J. Wang, F. Yang, P. Liu, Y. Zhu, S. Sui, and Q. Chen. 2012. Mitochondrial outer-membrane protein FUNDC1 mediates hypoxia-induced mitophagy in mammalian cells. *Nature Cell Biology*. 14:177-185.

Meineke, B., G. Engl, C. Kemper, A. Vasiljev-Neumeyer, H. Paulitschke, and D. Rapaport. 2008. The outer membrane form of the mitochondrial protein Mcr1 follows a TOM-independent membrane insertion pathway. *FEBS Letters*. 582:855-860.

Meisinger, C., S. Pfannschmidt, M. Rissler, D. Milenkovic, T. Becker, D. Stojanovski, M.J. Youngman, R.E. Jensen, A. Chacinska, B. Guiard, N. Pfanner, and N. Wiedemann. 2007. The morphology proteins Mdm12/Mmm1 function in the major beta-barrel assembly pathway of mitochondria. *The EMBO Journal*. 26:2229-2239.

Meisinger, C., M. Rissler, A. Chacinska, L.K. Szklarz, D. Milenkovic, V. Kozjak, B. Schonfisch, C. Lohaus, H.E. Meyer, M.P. Yaffe, B. Guiard, N. Wiedemann, and N. Pfanner. 2004. The mitochondrial morphology protein Mdm10 functions in assembly of the preprotein translocase of the outer membrane. *Developmental Cell*. 7:61-71.

Mejia, E.M., and G.M. Hatch. 2016. Mitochondrial phospholipids: role in mitochondrial function. *Journal of Bioenergetics and Biomembranes*. 48:99-112.

Merklinger, E., Y. Gofman, A. Kedrov, A.J. Driessen, N. Ben-Tal, Y. Shai, and D. Rapaport. 2012. Membrane integration of a mitochondrial signal-anchored protein does not require additional proteinaceous factors. *Biochemical Journal*. 442:381-389.

Merz, S., M. Hammermeister, K. Altmann, M. Durr, and B. Westermann. 2007. Molecular machinery of mitochondrial dynamics in yeast. *Biological Chemistry*. 388:917-926.

Mozdy, A.D., J.M. McCaffery, and J.M. Shaw. 2000. Dnm1p GTPase-mediated mitochondrial fission is a multi-step process requiring the novel integral membrane component Fis1p. *The Journal of Cell Biology*. 151:367-380.

Murley, A., R.D. Sarsam, A. Toulmay, J. Yamada, W.A. Prinz, and J. Nunnari. 2015. Ltc1 is an ER-localized sterol transporter and a component of ER-mitochondria and ER-vacuole contacts. *The Journal of Cell Biology*. 209:539-548.

Neupert, W., and J.M. Herrmann. 2007. Translocation of proteins into mitochondria. *Annual Review of Biochemistry*. 76:723-749.

Nguyen, T.T., A. Lewandowska, J.Y. Choi, D.F. Markgraf, M. Junker, M. Bilgin, C.S. Ejsing, D.R. Voelker, T.A. Rapoport, and J.M. Shaw. 2012. Gem1 and ERMES

do not directly affect phosphatidylserine transport from ER to mitochondria or mitochondrial inheritance. *Traffic*. 13:880-890.

Nunnari, J., T.D. Fox, and P. Walter. 1993. A mitochondrial protease with two catalytic subunits of nonoverlapping specificities. *Science*. 262:1997-2004.

Nunnari, J., W.F. Marshall, A. Straight, A. Murray, J.W. Sedat, and P. Walter. 1997. Mitochondrial transmission during mating in Saccharomyces cerevisiae is determined by mitochondrial fusion and fission and the intramitochondrial segregation of mitochondrial DNA. *Molecular Biology of the Cell*. 8:1233-1242.

Nury, H., C. Dahout-Gonzalez, V. Trezeguet, G. Lauquin, G. Brandolin, and E. Pebay-Peyroula. 2005. Structural basis for lipid-mediated interactions between mitochondrial ADP/ATP carrier monomers. *FEBS Letters*. 579:6031-6036.

Ocampo, A., J. Liu, E.A. Schroeder, G.S. Shadel, and A. Barrientos. 2012. Mitochondrial respiratory thresholds regulate yeast chronological life span and its extension by caloric restriction. *Cell Metabolism*. 16:55-67.

Okamoto, K., and J.M. Shaw. 2005. Mitochondrial morphology and dynamics in yeast and multicellular eukaryotes. *Annual Review of Genetics*. 39:503-536.

Okatsu, K., M. Kimura, T. Oka, K. Tanaka, and N. Matsuda. 2015. Unconventional PINK1 localization to the outer membrane of depolarized mitochondria drives Parkin recruitment. *Journal of Cell Science*. 128:964-978.

Osman, C., M. Haag, C. Potting, J. Rodenfels, P.V. Dip, F.T. Wieland, B. Brugger, B. Westermann, and T. Langer. 2009. The genetic interactome of prohibitins: coordinated control of cardiolipin and phosphatidylethanolamine by conserved regulators in mitochondria. *The Journal of Cell Biology*. 184:583-596.

Osman, C., M. Haag, F.T. Wieland, B. Brugger, and T. Langer. 2010. A mitochondrial phosphatase required for cardiolipin biosynthesis: the PGP phosphatase Gep4. *The EMBO Journal*. 29:1976-1987.

Ospina, A., A. Lagunas-Martinez, J. Pardo, and J.A. Carrodeguas. 2011. Protein oligomerization mediated by the transmembrane carboxyl terminal domain of Bcl-XL. *FEBS Letters*. 585:2935-2942.

Otera, H., Y. Taira, C. Horie, Y. Suzuki, H. Suzuki, K. Setoguchi, H. Kato, T. Oka, and K. Mihara. 2007. A novel insertion pathway of mitochondrial outer membrane proteins with multiple transmembrane segments. *The Journal of Cell Biology*. 179:1355-1363.

Otsuga, D., B.R. Keegan, E. Brisch, J.W. Thatcher, G.J. Hermann, W. Bleazard, and J.M. Shaw. 1998. The dynamin-related GTPase, Dnm1p, controls mitochondrial morphology in yeast. *The Journal of Cell Biology*. 143:333-349.

Ou, W.J., A. Ito, M. Umeda, K. Inoue, and T. Omura. 1988. Specific binding of mitochondrial protein precursors to liposomes containing cardiolipin. *The Journal of Biochemistry*. 103:589-595.

Papic, D., K. Krumpe, J. Dukanovic, K.S. Dimmer, and D. Rapaport. 2011. Multispan mitochondrial outer membrane protein Ugo1 follows a unique Mim1-dependent import pathway. *The Journal of Cell Biology*. 194:397-405.

Paschen, S.A., W. Neupert, and D. Rapaport. 2005. Biogenesis of beta-barrel membrane proteins of mitochondria. *Trends in Biochemical Sciences*. 30:575-582.

Pfeiffer, K., V. Gohil, R.A. Stuart, C. Hunte, U. Brandt, M.L. Greenberg, and H. Schagger. 2003. Cardiolipin stabilizes respiratory chain supercomplexes. *The Journal of Biological Chemistry*. 278:52873-52880.

Pizzo, P., and T. Pozzan. 2007. Mitochondria-endoplasmic reticulum choreography: structure and signaling dynamics. *Trends in Cell Biology*. 17:511-517.

Popov-Celeketic, J., T. Waizenegger, and D. Rapaport. 2008. Mim1 functions in an oligomeric form to facilitate the integration of Tom20 into the mitochondrial outer membrane. *Journal of Molecular Biology*. 376:671-680.

Rapaport, D., M. Brunner, W. Neupert, and B. Westermann. 1998. Fzo1p is a mitochondrial outer membrane protein essential for the biogenesis of functional mitochondria in Saccharomyces cerevisiae. *The Journal of Biological Chemistry*. 273:20150-20155.

Rospert, S., T. Junne, B.S. Glick, and G. Schatz. 1993. Cloning and disruption of the gene encoding yeast mitochondrial chaperonin 10, the homolog of E. coli groES. *FEBS Letters*. 335:358-360.

Sauerwald, J., T. Jores, M. Eisenberg-Bord, S.G. Chuartzman, M. Schuldiner, and D. Rapaport. 2015. Genome-Wide Screens in Saccharomyces cerevisiae Highlight a Role for Cardiolipin in Biogenesis of Mitochondrial Outer Membrane Multispan Proteins. *Molecular and Cellular Biology*. 35:3200-3211.

Schagger, H. 2002. Respiratory chain supercomplexes of mitochondria and bacteria. *Biochimica et Biophysica Acta*. 1555:154-159.

Schug, Z.T., and E. Gottlieb. 2009. Cardiolipin acts as a mitochondrial signalling platform to launch apoptosis. *Biochimica et Biophysica Acta*. 1788:2022-2031.

Shiao, Y.J., G. Lupo, and J.E. Vance. 1995. Evidence that phosphatidylserine is imported into mitochondria via a mitochondria-associated membrane and that the majority of mitochondrial phosphatidylethanolamine is derived from decarboxylation of phosphatidylserine. *The Journal of Biological Chemistry*. 270:11190-11198.

Sickmann, A., J. Reinders, Y. Wagner, C. Joppich, R. Zahedi, H.E. Meyer, B. Schonfisch, I. Perschil, A. Chacinska, B. Guiard, P. Rehling, N. Pfanner, and C. Meisinger. 2003. The proteome of Saccharomyces cerevisiae mitochondria. *Proceedings of the National Academy of Science of the United States of America*. 100:13207-13212.

Sogo, L.F., and M.P. Yaffe. 1994. Regulation of mitochondrial morphology and inheritance by Mdm10p, a protein of the mitochondrial outer membrane. *The Journal of Cell Biology*. 126:1361-1373.

Song, J., Y. Tamura, T. Yoshihisa, and T. Endo. 2014. A novel import route for an N-anchor mitochondrial outer membrane protein aided by the TIM23 complex. *EMBO Reports*. 15:670-677.

Steger, H.F., T. Sollner, M. Kiebler, K.A. Dietmeier, R. Pfaller, K.S. Trulzsch, M. Tropschug, W. Neupert, and N. Pfanner. 1990. Import of ADP/ATP carrier into mitochondria: two receptors act in parallel. *The Journal of Cell Biology*. 111:2353-2363.

Tamura, Y., Y. Harada, S. Nishikawa, K. Yamano, M. Kamiya, T. Shiota, T. Kuroda, O. Kuge, H. Sesaki, K. Imai, K. Tomii, and T. Endo. 2013. Tam41 is a CDP-diacylglycerol synthase required for cardiolipin biosynthesis in mitochondria. *Cell Metabolism*. 17:709-718.

Tamura, Y., O. Onguka, A.E. Aiken Hobbs, R.E. Jensen, M. Iijima, S.M. Claypool, and H. Sesaki. 2012. Role for two conserved intermembrane space proteins, Ups1p and Up2p, in intra-mitochondrial phospholipid trafficking. *Journal of Biological Chemistry*.

Tan, T., C. Ozbalci, B. Brugger, D. Rapaport, and K.S. Dimmer. 2013. Mcp1 and Mcp2, two novel proteins involved in mitochondrial lipid homeostasis. *Journal of Cell Science*. 126:3563-3574.

Teese, M.G., and D. Langosch. 2015. Role of GxxxG Motifs in Transmembrane Domain Interactions. *Biochemistry*. 54:5125-5135.

Tieu, Q., V. Okreglak, K. Naylor, and J. Nunnari. 2002. The WD repeat protein, Mdv1p, functions as a molecular adaptor by interacting with Dnm1p and Fis1p during mitochondrial fission. *The Journal of Cell Biology*. 158:445-452.

Tzagoloff, A., and C.L. Dieckmann. 1990. PET genes of Saccharomyces cerevisiae. *Microbiological Reviews*. 54:211-225.

van den Brink-van der Laan, E., J.A. Killian, and B. de Kruijff. 2004. Nonbilayer lipids affect peripheral and integral membrane proteins via changes in the lateral pressure profile. *Biochimica et Biophysica Acta*. 1666:275-288.

van der Laan, M., S.E. Horvath, and N. Pfanner. 2016. Mitochondrial contact site and cristae organizing system. *Current Opinion in Cell Biology*. 41:33-42.

Vance, J.E. 1990. Phospholipid synthesis in a membrane fraction associated with mitochondria. *The Journal of Biological Chemistry*. 265:7248-7256.

Voelker, D.R. 1990. Lipid transport pathways in mammalian cells. *Experientia*. 46:569-579.

Vogtle, F.N., S. Wortelkamp, R.P. Zahedi, D. Becker, C. Leidhold, K. Gevaert, J. Kellermann, W. Voos, A. Sickmann, N. Pfanner, and C. Meisinger. 2009. Global analysis of the mitochondrial N-proteome identifies a processing peptidase critical for protein stability. *Cell*. 139:428-439.

Voss, C., S. Lahiri, B.P. Young, C.J. Loewen, and W.A. Prinz. 2012. ER-shaping proteins facilitate lipid exchange between the ER and mitochondria in S. cerevisiae. *Journal of Cell Science*. 125:4791-4799.

Wallace, D.C. 2005. A mitochondrial paradigm of metabolic and degenerative diseases, aging, and cancer: a dawn for evolutionary medicine. *Annual Review of Genetics*. 39:359-407.

Wenz, L.S., L. Opalinski, M.H. Schuler, L. Ellenrieder, R. Ieva, L. Bottinger, J. Qiu, M. van der Laan, N. Wiedemann, B. Guiard, N. Pfanner, and T. Becker. 2014. The presequence pathway is involved in protein sorting to the mitochondrial outer membrane. *EMBO Reports*. 15:678-685.

Westermann, B. 2008. Molecular machinery of mitochondrial fusion and fission. *The Journal of Biological Chemistry*. 283:13501-13505.

Westermann, B., and W. Neupert. 2003. 'Omics' of the mitochondrion. *Nature Biotechnology*. 21:239-240.

Wideman, J.G., R.M. Gawryluk, M.W. Gray, and J.B. Dacks. 2013. The ancient and widespread nature of the ER-mitochondria encounter structure. *Molecular Biology and Evolution*. 30:2044-2049.

Wu, W., W. Li, H. Chen, L. Jiang, R. Zhu, and D. Feng. 2016. FUNDC1 is a novel mitochondrial-associated-membrane (MAM) protein required for hypoxia-induced mitochondrial fission and mitophagy. *Autophagy*. 12:1675-1676.

Yamamoto, H., K. Fukui, H. Takahashi, S. Kitamura, T. Shiota, K. Terao, M. Uchida, M. Esaki, S. Nishikawa, T. Yoshihisa, K. Yamano, and T. Endo. 2009. Roles of Tom70 in import of presequence-containing mitochondrial proteins. *The Journal of Biological Chemistry*. 284:31635-31646.

Yamano, K., S. Tanaka-Yamano, and T. Endo. 2010. Mdm10 as a dynamic constituent of the TOB/SAM complex directs coordinated assembly of Tom40. *EMBO Reports*. 11:187-193.

Yamano, K., Y. Yatsukawa, M. Esaki, A.E. Hobbs, R.E. Jensen, and T. Endo. 2008. Tom20 and Tom22 share the common signal recognition pathway in mitochondrial protein import. *The Journal of Biological Chemistry*. 283:3799-3807.

Yeung, T., G.E. Gilbert, J. Shi, J. Silvius, A. Kapus, and S. Grinstein. 2008. Membrane phosphatidylserine regulates surface charge and protein localization. *Science*. 319:210-213.

Youle, R.J., and M. Karbowski. 2005. Mitochondrial fission in apoptosis. *Nature Reviews Molecular Cell Biology*. 6:657-663.

Young, J.C., N.J. Hoogenraad, and F.U. Hartl. 2003. Molecular chaperones Hsp90 and Hsp70 deliver preproteins to the mitochondrial import receptor Tom70. *Cell*. 112:41-50.

Youngman, M.J., A.E. Hobbs, S.M. Burgess, M. Srinivasan, and R.E. Jensen. 2004. Mmm2p, a mitochondrial outer membrane protein required for yeast mitochondrial shape and maintenance of mtDNA nucleoids. *The Journal of Cell Biology*. 164:677-688.

Zahedi, R.P., A. Sickmann, A.M. Boehm, C. Winkler, N. Zufall, B. Schonfisch, B. Guiard, N. Pfanner, and C. Meisinger. 2006. Proteomic analysis of the yeast mitochondrial outer membrane reveals accumulation of a subclass of preproteins. *Molecular Biology of the Cell*. 17:1436-1450.

Zhang, M., E. Mileykovskaya, and W. Dowhan. 2002. Gluing the respiratory chain together. Cardiolipin is required for supercomplex formation in the inner mitochondrial membrane. *The Journal of Biological Chemistry.* 277:43553-43556.

Zhang, M., E. Mileykovskaya, and W. Dowhan. 2005. Cardiolipin is essential for organization of complexes III and IV into a supercomplex in intact yeast mitochondria. *The Journal of Biological Chemistry.* 280:29403-29408.

Zhong, Q., V.M. Gohil, L. Ma, and M.L. Greenberg. 2004. Absence of cardiolipin results in temperature sensitivity, respiratory defects, and mitochondrial DNA instability independent of pet56. *The Journal of Biological Chemistry.* 279:32294-32300.

Zinser, E., and G. Daum. 1995. Isolation and biochemical characterization of organelles from the yeast, Saccharomyces cerevisiae. *Yeast*. 11:493-536.

11. Acknowledgements

First of all I want to thank Prof. Dr. Doron Rapaport for offering me the opportunity to do a PhD in his laboratory and to continue my work on this interesting project. I am especially thankful for his extensive supervision and outstanding scientific guidance, as well as his optimism and support in matters of work and life.

I am deeply grateful to Dr. Kai Stefan Dimmer for being a patient instructor, for sharing his immense knowledge with me and for providing interesting ideas and helpful suggestions. I very much appreciate that he always had an open ear for questions, his constant help and useful advice. I would also like to thank him for critically reading the manuscript.

Additionally, I want to thank Prof. Dr. Ralf-Peter Jansen, Prof. Dr. Gabriele Dodt and Dr. Frank Essmann for their time and effort as members of my doctoral examination committee.

Furthermore, I want to thank all present and former lab members for the friendly working atmosphere, for all the silly jokes but also meaningful conversations, be it science related or private. Thanks to Bogdan Cichocki, Caroline Schönfeld, Daniela Vitali, Diana Antunes, Dr. Dražen Papić, Fenja Odendall, Dr. Hoda Hoseini, Dr. Janani Natarajan, Jialin Zhou, Dr. Katrin Krumpe, Layla Drwesh, Dr. Ravi Singhal, Dr. Tao Tan and Dr. Thomas Ulrich for sharing not only the lab but also events like BBQ, sushi dinner, cooking together or going to the movies. Special thanks go to Tobias Jores who spends a generous amount of his time helping with all kinds of scientific or technical issues and for supplying the lab with cake and diabetes, and to Johannes Heimgärtner for always making me laugh. Additionally, I want to thank Elena Kracker for being a skillful technician and our lab fairy, as well as my present and former bachelor students and student assistants Philipp Wendling, Andreas Zeitler, and Lukas Fuhs for their contributions to my project.

I want to acknowledge everyone working in AG Jansen for the successful collaboration and for sharing materials and methods.

I also want to express my gratitude for the time and effort of all the people working in the institute, especially Dr. Klaus Möschel, Alexandra Maurer, Birgit Kiesel, Mine Cosgun, Ursula Schaal, Luis Hartmann, Hermann Liggesmeyer, Dietmar Wieland and Egon Theurer.

Further credits go to all my friends in and out of Tübingen including my brother for always being there for me.

I am especially grateful to my parents for their continuous support and sympathy during all those years.

12. Appendix

1. M. Sinzel, T. Tan, P. Wendling, H. Kalbacher, C. Özbalci, X. Chelius, B. Westermann, B. Brügger, D. Rapaport, and K.S. Dimmer. 2016. Mcp3 is a novel mitochondrial outer membrane protein that follows a unique IMP-dependent biogenesis pathway. *EMBO Reports*. 17:965-981.

   JOHN WILEY AND SONS Reprint License Number 4191820515862

2. O. Hermesh, C. Genz, I. Yofe, M. Sinzel, D. Rapaport, M. Schuldiner, and R.P. Jansen. 2014. Yeast phospholipid biosynthesis is linked to mRNA localization. *Journal of Cell Science*. 127:3373-3381.

   The Company of Biologists Ltd Reprint License Number 4191820381037

Article

TRANSPARENT PROCESS

EMBO reports

Mcp3 is a novel mitochondrial outer membrane protein that follows a unique IMP-dependent biogenesis pathway

Monika Sinzel[1], Tao Tan[1], Philipp Wendling[1], Hubert Kalbacher[1], Cagakan Özbalci[2], Xenia Chelius[3], Benedikt Westermann[3], Britta Brügger[2], Doron Rapaport[1] & Kai Stefan Dimmer[1,*]

Abstract

Mitochondria are separated from the remainder of the eukaryotic cell by the mitochondrial outer membrane (MOM). The MOM plays an important role in different transport processes like lipid trafficking and protein import. In yeast, the ER–mitochondria encounter structure (ERMES) has a central, but poorly defined role in both activities. To understand the functions of the ERMES, we searched for suppressors of the deficiency of one of its components, Mdm10, and identified a novel mitochondrial protein that we named Mdm10 complementing protein 3 (Mcp3). Mcp3 partially rescues a variety of ERMES-related phenotypes. We further demonstrate that Mcp3 is an integral protein of the MOM that follows a unique import pathway. It is recognized initially by the import receptor Tom70 and then crosses the MOM via the translocase of the outer membrane. Mcp3 is next relayed to the TIM23 translocase at the inner membrane, gets processed by the inner membrane peptidase (IMP) and finally integrates into the MOM. Hence, Mcp3 follows a novel biogenesis route where a MOM protein is processed by a peptidase of the inner membrane.

Keywords ERMES complex; IMP; Mdm10; mitochondria; outer membrane
Subject Category Membrane & Intracellular Transport
DOI 10.15252/embr.201541273 | Received 31 August 2015 | Revised 19 April 2016 | Accepted 26 April 2016 | Published online 24 May 2016
EMBO Reports (2016) 17: 965–981

Introduction

Mitochondria are involved in many metabolic pathways and serve as interface for processes like cell differentiation, growth, ageing and death. Therefore, they are of eminent importance to the eukaryotic cell. Their optimal function relies on the composition of two distinct membranes, the mitochondrial inner membrane and mitochondrial outer membrane (MIM and MOM, respectively).

Most mitochondrial and all integral MOM proteins are encoded in the nucleus, imported into mitochondria and sorted inside the organelle to their correct location. Proper positioning of proteins is achieved by the MOM complexes TOM (translocase of the outer membrane), TOB (topogenesis of outer membrane β-barrel proteins, synonymously named SAM for sorting and assembly machinery) and MIM (mitochondrial import) as well as the MIM and intermembrane space (IMS) complexes TIM23, TIM22 (translocase of the inner membrane), MIA (mitochondrial intermembrane space assembly) and OXA (derived from its subunit Oxa1) complexes (for review see [1–4]). In addition, most of the imported proteins are cleaved by processing peptidases inside mitochondria (for review, see [5]).

Several proteins destined to the MIM or IMS are first recognized by the TOM complex in the outer membrane and are then handed over to the TIM23 complex. This latter complex allows the integration of precursor proteins into the inner membrane. A subgroup of proteins is processed by the heterotrimeric protease complex inner membrane peptidase (IMP) [6]. In yeast, the IMP complex contains two catalytically active subunits Imp1 and Imp2. The cleavage by IMP results in either a soluble IMS protein like Mcr1 or a MIM anchored protein like Mgr2 [7,8]. So far only MIM or IMS proteins were found to be substrates of IMP.

Over the last decade, it became obvious that the lipid composition of mitochondria depends on contact sites with other cellular compartments. The functional importance of these contacts is still not completely understood, and the molecular mechanisms by which lipid exchange between the organelles occurs are yet to be unravelled. Several contacts of mitochondria have been described in yeast. Among them are tethers between mitochondria and the vacuole [9,10] or the plasma membrane (reviewed in [11]).

Mitochondria–ER contacts that recently attracted substantial attention are mediated by the ERMES (ER–mitochondria encounter structure) complex that is composed of the mitochondrial membrane proteins Mdm10, Mdm34, the soluble protein Mdm12 and the ER membrane protein Mmm1 [12]. Loss of one ERMES component leads to several defects in yeast cells, such as reduced insertion of β-barrel proteins (reviewed in [13]), structurally altered

1 Interfaculty Institute of Biochemistry, University of Tübingen, Tübingen, Germany
2 Heidelberg University Biochemistry Center, Heidelberg, Germany
3 Cell Biology, University of Bayreuth, Bayreuth, Germany
*Corresponding author. Tel: +49 7071 2974174; Fax: +49 7071 294016; E-mail: kai-stefan.dimmer@uni-tuebingen.de

mitochondria, loss of the mitochondrial genome and inability to grow on non-fermentable carbon sources (for an overview, see [14]). ERMES complex is furthermore involved in mitochondrial division [15], and lack of the ERMES complex leads to reduced mitophagy [16]. Moreover, deletion of ERMES subunits causes alterations in the lipid composition of mitochondria, especially reduction in the levels of phosphatidylethanolamine (PE) and cardiolipin (CL) [12,17–21], as well as elevation of the yeast sterol ergosterol [20]. Some ERMES components were predicted to harbour SMP (synaptotagmin-like, mitochondrial and lipid-binding proteins) domains that could be involved in lipid binding and transport between membranes [22]. Indeed, a recent study reported that SMP domains of Mdm12 and Mmm1 bind phospholipids [23]. Of note, several studies indicate that the ERMES-mediated contact is not the only one between ER and mitochondria [24,25]. Yet an additional player, Lct1/Lam6, coordinates the extent of ER–mitochondria and vacuole–mitochondria contacts [9,26].

Despite this progress in understanding the function of the ERMES complex, the actual molecular mechanisms that lead to all the defects described above are still not clearly defined. Recently, we identified two high-copy suppressors of the growth defect of *mdm10*Δ cells [20]. We showed that the two novel mitochondrial proteins (Mcp1/2) can complement the loss of Mdm10 by partial restoration of the mitochondrial lipid composition [20]. Here, we report a third suppressor that we named Mdm10 complementing protein 3 (Mcp3). We demonstrate that Mcp3 is a MOM protein exposed to the cytosol. Remarkably, the correct biogenesis of Mcp3 depends on the mitochondrial membrane potential and the protein is processed by the inner membrane peptidase (IMP). Thus, Mcp3 is the first MOM substrate of this peptidase and follows a unique and novel import pathway.

Results

Mcp3 is a high-copy suppressor of cells lacking Mdm10

Recently, we identified two novel mitochondrial proteins that partially rescue the loss of ERMES components, Mcp (Mdm10 complementing protein) 1 and Mcp2 [20]. Re-evaluation of all clones led to the identification of a third gDNA segment that rescued the growth defect of *mdm10*Δ cells at elevated temperatures on non-fermentable carbon sources. The segment contained a C-terminally truncated part of the open reading frame (ORF) of Mdm10 and the genes *FUN14*, *SPO7* and *ERP2*. *SPO7* encodes for a putative nuclear phosphatase involved in control of nuclear growth [27]. Erp2 is a

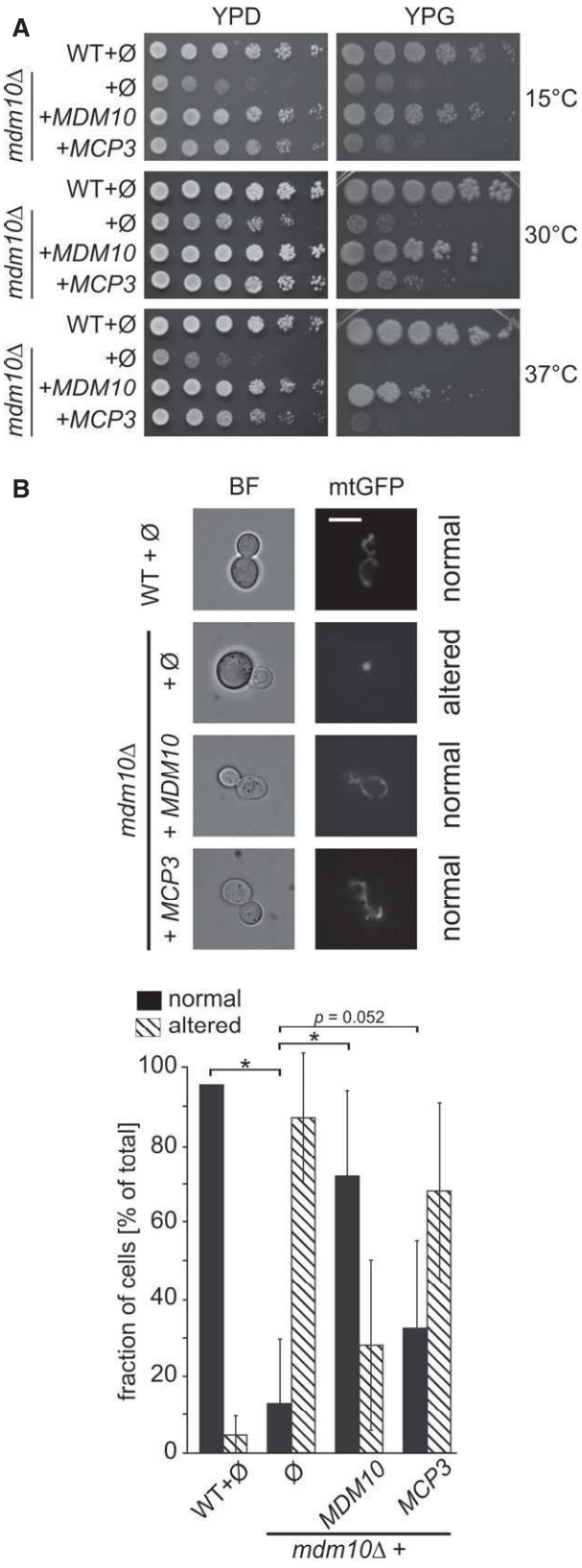

Figure 1. Mcp3 is a multicopy suppressor of *mdm10*Δ.

A Rescue of growth phenotype. Wild-type (WT) or *mdm10*Δ cells were transformed with the empty plasmid pYX142 (Ø). In addition, *mdm10*Δ cells were transformed with pYX142 encoding *MDM10* or *MCP3*. Cells were grown to an OD_{600} of 1.0 and spotted on YPD or YPG plates in a 1:5 dilution series. Plates were incubated for growth at the indicated temperatures.

B Over-expression of Mcp3 partially rescues the mitochondrial morphology defect in *mdm10*Δ cells. Cells described in (A) expressing mitochondrially targeted GFP (mtGFP) were analysed by fluorescence microscopy. Typical images (fluorescence and bright field, BF) of the four different strains are shown (scale bar = 5 μm). The quantification shows the average percentage with standard deviation bars of three independent experiments (n = 3; SD; *P < 0.05 and as indicated; two-tailed Student's t-test) with at least 100 cells per experiment.

member of the p24 family involved in ER to Golgi transport [28]. *FUN14* encodes a protein of so far unknown function (*F*unction *u*nknown *n*ow, [29]) that was found in two high-throughput studies to be a mitochondrial protein [30,31]. We cloned the *FUN14* coding sequence in an ARS/CEN plasmid containing a rather strong triose phosphate isomerase (TPI) promoter. The resulting expression of Fun14 in *mdm10*Δ cells led to a partial rescue of the growth phenotype (Fig 1A). We renamed the protein Mcp3 for *M*dm10 *c*omplementing *p*rotein 3.

Over-expression of Mcp3 partially restores mitochondrial defects of cells lacking Mdm10

Yeast cells lacking any of the ERMES subunits do not show the typical mitochondrial network but rather contain spherical mitochondria [32–35]. To test whether over-expression of Mcp3 rescues the altered mitochondrial morphology, cells were additionally transformed with a plasmid encoding a mitochondria-targeted GFP and analysed by fluorescence microscopy. Over-expression of Mcp3 in these cells resulted in a recovery in about 30% of the cells (Fig 1B). Thus, the partial rescue of the growth phenotype of *mdm10*Δ cells upon over-expression of Mcp3 is in line with the partial restoration of mitochondrial morphology.

The lipid composition of mitochondrial membranes influences the stability of different membrane protein complexes. In this context, we reported before that the loss of Mdm10 leads to alterations in the formation of respiratory chain super-complexes [20]. Another consequence of loss of Mdm10 is a change in the assembly of TOM and TOB complexes as shown by blue native PAGE (BN-PAGE) analysis. We first wanted to investigate whether the over-expression of Mcp3 in *mdm10*Δ cells has an effect on respiratory chain super-complexes assembly. To this end, we isolated mitochondria from wild-type and *mdm10*Δ cells with or without over-expression of Mcp3. As expected, mitochondria isolated from *mdm10*Δ cells showed severely reduced amounts of respiratory chain super-complexes in comparison with wild-type cells (Fig 2A). In line with the partial growth rescue, over-expression of Mcp3 led only to a minor increase of the different complex species.

Next, we asked whether the assembly of TOM and TOB complexes is influenced by over-expression of Mcp3 in *mdm10*Δ cells. The same mitochondria as above were analysed by BN-PAGE and immunodecoration with antibodies against the subunits of TOM and TOB complex, Tom40 and Tob55, respectively. As reported before, an unassembled Tom40 species emerges in organelles lacking Mdm10 ([20,36] and Fig 2B, left panel, arrowhead). This Tom40 species is nearly absent in mitochondria from *mdm10*Δ cells over-expressing Mcp3. Similar observations were obtained for the TOB complex. In control mitochondria, the main assembly form is TOB core complex with a molecular mass of around 250 kDa consisting of Tob55, Tob38 and Mas37. An additional higher molecular weight species emerges in the absence of Mdm10 (Fig 2B, right panel, asterisk). This species resembles the reported TOB-Tom5/Tom40 form [37]. Although the over-expression of Mcp3 does not fully rescue the amount of TOB core complex, the TOB-Tom5/Tom40 species is reduced to control levels (Fig 2B, right panel, third lane). We conclude that Mcp3 over-expression has partial restoring effects on the TOM and TOB complexes.

Next, we analysed the influence of Mcp3 on the mitochondrial lipid profile in cells lacking Mdm10. To this end, we extracted lipids from highly pure mitochondria and subjected them to mass spectrometric analysis. As described before, cells lacking Mdm10 show reduced amounts of the phospholipids PE and CL, an increase in PS levels and twofold increase in the ratio of ergosterol (ERG) to phospholipids (PL) (Fig 2C and [20]). Over-expression of Mcp3 leads to a partial rescue of the alteration in the levels of the non-bilayer forming phospholipids PE and CL. Of note, in contrast to the earlier reported suppressors Mcp1 and Mcp2, the effect is slightly more pronounced for CL (compare Fig 2C to [20]). The precursor of CL, PG, seems also to be affected although due to its overall very low abundance in mitochondria, the changes in PG vary strongly among the different preparations. Furthermore, the increase in both the amounts of PS and the ERG/PL ratio observed in *mdm10*Δ mitochondria is partially reduced by over-expression of Mcp3.

Taken together, the partial rescue of growth defect of *mdm10*Δ cells by over-expression of Mcp3 is in line with a partial restoration of mitochondrial morphology, protein complex assembly and lipid profile.

Over-expression of Mcp3 rescues the loss of other ERMES components

Next, we asked whether Mcp3 can rescue the deletion of any ERMES component. To address this question, we over-expressed Mcp3 in cells lacking either Mdm12, Mdm34 or Mmm1 and analysed the growth behaviour of the transformed cells. Over-expression of Mcp3 led to a similar partial rescue of the growth phenotype of cells lacking Mdm12 (Fig 2D), the ER located Mmm1 (Fig 2E) or the MOM protein Mdm34 (Fig 2F). We conclude that Mcp3 can compensate the absence of functional ERMES complex rather than the missing function of an individual subunit.

Loss of Mcp3 leads to minor effects on yeast growth and mitochondrial morphology

We wondered whether deletion of *MCP3* has an influence on viability. Loss of Mcp3 in different yeast wild-type backgrounds had no severe impact on growth of yeast cells except a moderate growth defect that was observed in the BY4741 background on non-fermentable carbon sources (Fig 3A, YPG). In addition, we investigated the mitochondrial morphology of *mcp3*Δ cells expressing a mitochondrial targeted GFP. In agreement with the hampered growth observed, loss of Mcp3 leads to measurable, but statistically insignificant alterations in the branched tubular network of the organelle to shortened, thickened and less branched tubules (Fig 3B). Accordingly, the ultrastructure of mitochondria, that is morphology and number of cristae, was as assessed by electron microscopy (EM) not altered in *mcp3*Δ cells (Fig EV1A). To investigate whether deletion of Mcp3 has a direct effect on ERMES assembly, we performed in *mcp3*Δ cells fluorescence microscopic analysis of a labelled form of the ERMES subunit Mmm1.

Employing two different wild-type backgrounds, we observed that the ERMES complex assembled similarly in both control and *mcp3*Δ cells and co-localized with mitochondria in punctate structures (Fig EV2A and B). Hence, Mcp3 is required neither for the

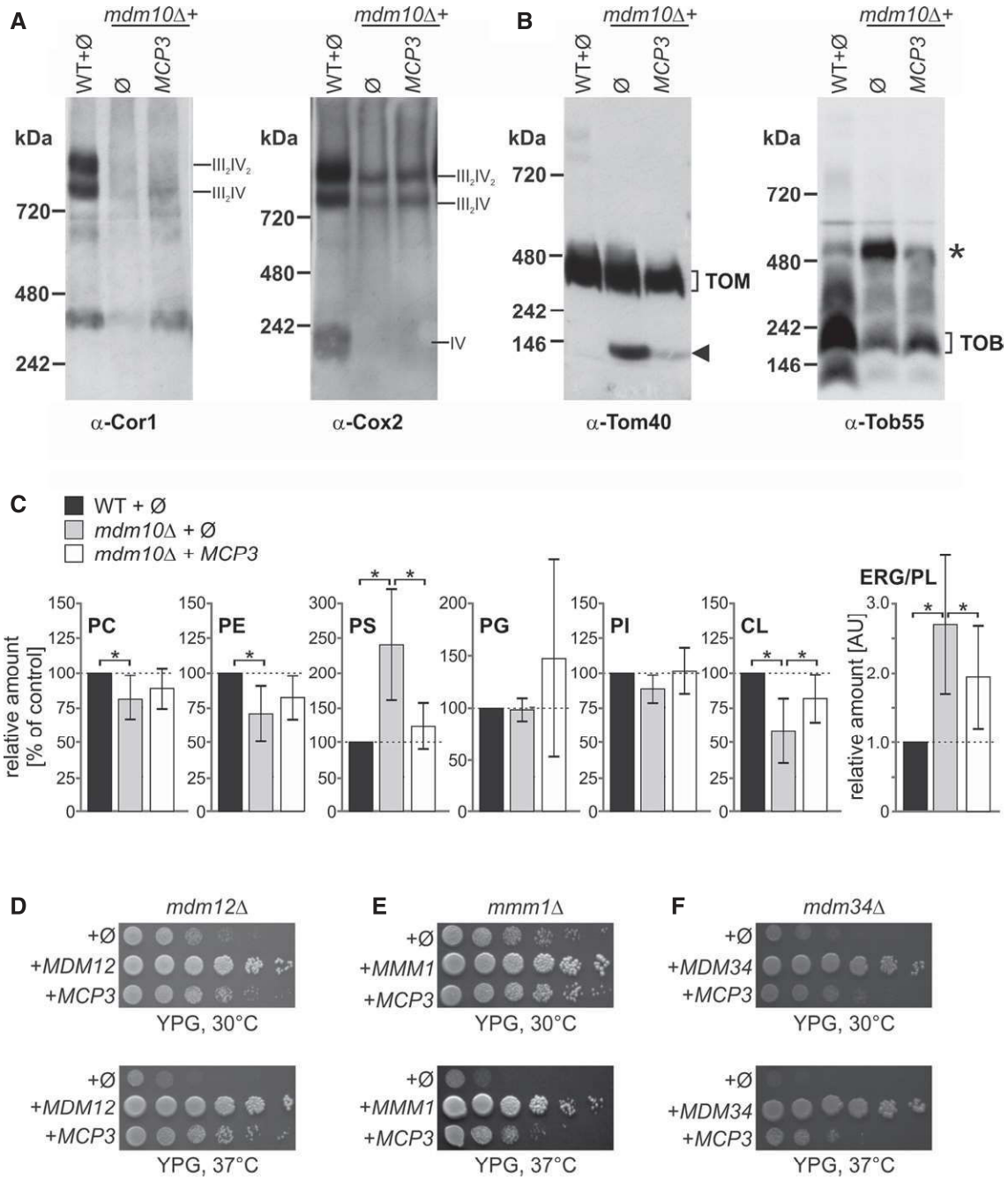

Figure 2. Mcp3 rescues assembly defects of protein complexes and lipid alterations of *mdm10*Δ cells, and restores growth of other ERMES deletion mutants.

A Respiratory chain super-complex levels are slightly restored by over-expression of Mcp3. Mitochondria isolated from the indicated strains were lysed in 1% digitonin and subjected to a 4–8% BN-PAGE. Proteins were analysed by immunodecoration with antibodies against either Cor1 of complex III or Cox2 of complex IV.

B Assembly defects in TOM and TOB complexes in *mdm10*Δ cells are partially restored by Mcp3 over-expression. Mitochondria of the indicated cells were lysed in 1% digitonin and subjected to a 6–13% BN-PAGE and immunoblotting with antibodies against Tom40 (left) or Tob55 (right). The assembled TOM complex and an unassembled Tom40 species at *c.* 100 kDa (arrowhead) are indicated as well as the TOB complex and an additional higher molecular weight species of the TOB complex (asterisk).

C Over-expression of Mcp3 partially rescues the alterations in lipid composition of cells lacking Mdm10. Lipids were extracted from highly pure mitochondria isolated from the indicated cells and then analysed by mass spectrometric analysis. The level of each phospholipid species in wild-type mitochondria was set to 100% and the ERG/PL ratio to 1. Relative changes in mitochondria from other cells are presented. The mean with standard deviations of three biological repeats with two technical repeats for each (n = 6; SD; *, $P < 0.05$; two-tailed Student's t-test) is given.

D Mcp3 rescues loss of Mdm12. Wild-type (WT) or *mdm12*Δ cells transformed with the empty plasmid pYX142 (Ø) or *mdm12*Δ cells over-expressing either Mcp3 or Mdm12 (as a control) were analysed at 30°C or 37°C by drop dilution assay on rich medium containing glycerol (YPG).

E Mcp3 rescues loss of Mmm1. WT and *mmm1*Δ cells were transformed and analysed as described in (D).

F Mcp3 rescues loss of Mdm34. WT and *mdm34*Δ cells were transformed and analysed as described in (D).

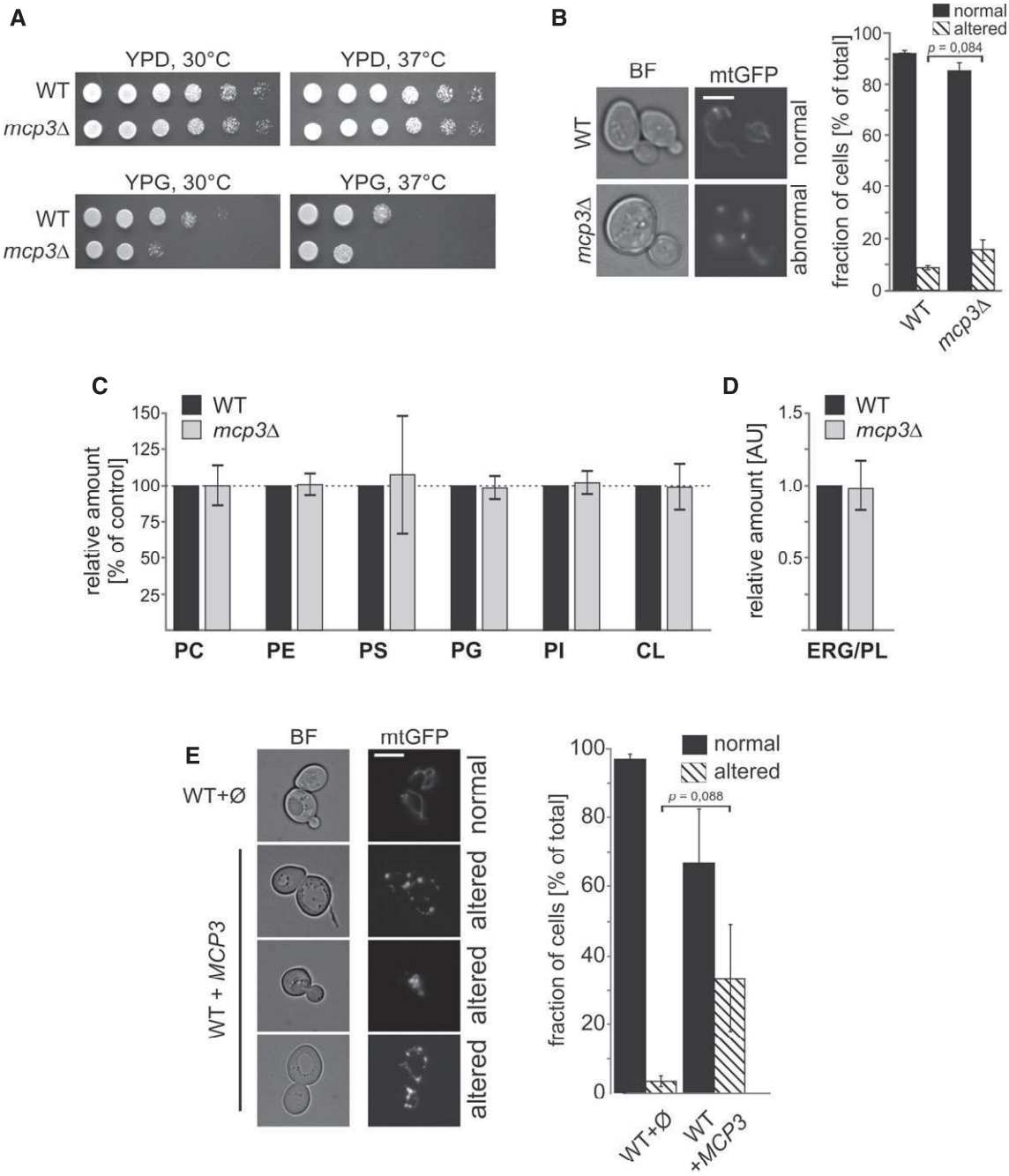

Figure 3. Elevated levels of Mcp3 influence mitochondrial morphology of yeast cells.

A Growth phenotype of *mcp3*Δ cells. WT or *mcp3*Δ cells were grown to an OD_{600} of 1.0 in YPD medium and spotted on YPD or YPG plates in a 1:5 dilution series. Plates were incubated for growth at the indicated temperatures.

B *mcp3*Δ cells have normal mitochondrial morphology. WT and *mcp3*Δ cells expressing mitochondrially targeted GFP (mtGFP) were grown to mid-logarithmic phase then analysed by fluorescence microscopy. Typical images of the two different strains are shown (scale bar = 5 μm). The quantification of the depicted strains shows the average percentage with standard deviation bars of three independent experiments with at least 100 cells per experiment (n = 3; SD; P as indicated; two-tailed Student's t-test).

C, D Loss of Mcp3 has no effect on the phospholipid composition of mitochondria. Highly pure mitochondria were isolated from the indicated yeast cells. Lipids were extracted and then analysed by mass spectrometric analysis. The level of each phospholipid species in wild-type mitochondria was set to 100% and the ERG/PL ratio to 1. Relative changes in mitochondria from *mcp3*Δ cells are presented. The mean with standard deviations of three biological repeats with two technical repeats for each (n = 6; SD) is given.

E Over-expression of Mcp3 leads to alterations in the tubular mitochondrial network. Wild-type cells expressing mitochondrially targeted GFP (mtGFP) were transformed with a plasmid over-expressing Mcp3 (*MCP3*) or an empty plasmid as control (Ø). Cells were grown to mid-logarithmic phase and then analysed by fluorescence microscopy. Typical images of the two different strains are shown (scale bar = 5 μm). The quantification shows the average percentage with standard deviation bars of three independent experiments with at least 100 cells per experiment (n = 3; SD; P as indicated; two-tailed Student's t-test).

formation of cristae structures nor for proper assembly of the ERMES complex.

Next, we asked whether the loss of Mcp3 leads to a change in the mitochondrial lipid profile. Lipids were extracted from highly pure mitochondria and analysed by mass spectrometry. Neither the phospholipid nor ergosterol levels were altered in mitochondria from *mcp3*Δ cells as compared to control organelles (Fig 3C and D, respectively).

Although over-expression of Mcp3 did not result in any growth phenotype (Appendix Fig S1), we asked whether it can cause alterations in mitochondrial morphology. Interestingly, elevated levels of Mcp3 led in some of the cells to partially fragmented mitochondria (Fig 3E), suggesting an influence of Mcp3 over-expression on mitochondrial morphology, although this trend is statistically not significant. In addition, mitochondrial ultrastructure as monitored by EM was not affected upon over-expression of Mcp3 (Fig EV1B). These findings might suggest a yet undefined role of Mcp3 in mitochondrial morphogenesis. To test whether over-expression of Mcp3 has a direct effect on ERMES complex formation, we analysed ERMES foci in cells with elevated Mcp3 levels. Over-expression of Mcp3 did not alter ERMES punctae formation or co-localization with mitochondria (Fig EV2C).

Collectively, loss of Mcp3 has no severe effect on yeast growth, cristae formation, ERMES assembly, morphology and lipid composition of mitochondria. Yet over-expression of the protein leads to slight mitochondrial morphology changes, with no obvious effects on the other tested characteristics.

Mcp3 resides in the mitochondrial outer membrane

In silico analysis of the sequence of Mcp3 predicts a canonical mitochondrial targeting sequence, followed by a hydrophobic segment and two putative transmembrane domains (TMDs, Fig 4A). A first attempt to C-terminally label Mcp3 with an HA-tag in order to analyse the protein by immunodetection resulted in a non-functional protein (see also below). A previous report predicted Mcp3 to be a putative substrate of the Imp1 subunit of the IMP peptidase and suggested the cleavage site to be between Asn69 and Asp70 [38]. In agreement with our observation that C-terminally tagged Mcp3 is non-functional, Esser *et al* were unable to test this prediction since C-terminally tagged Mcp3 was not detectable. An independent support for processing of Mcp3 by IMP is provided by high-throughput analysis of the N-terminal sequences of mitochondrial proteins [39]. This study found the N-terminus of endogenous Mcp3 to start with Asp70 (*D*SLG...) in agreement with the predicted processing site of Imp1. To further analyse Mcp3, we constructed an internal tagged version of Mcp3. The HA-tag was inserted four amino acids C-terminally to the processed N-terminus identified by mass spectrometry (DSLG-HA_{Tag}-...). Functionality of the internally tagged Mcp3 (HA-Mcp3) was shown by growth rescue of *mdm10*Δ cells (Fig 4B). To test whether this construct can be detected, we over-expressed HA-Mcp3 in cells lacking endogenous Mcp3. Using mitochondria isolated from these cells, we observed that the mature HA-Mcp3 migrates as a 17-kDa protein in line with processing of the N-terminal region (Fig 4C and see below).

Figure 4. Subcellular and submitochondrial localization of Mcp3.

A Predicted protein domains for Mcp3. Mcp3 is predicted to contain a canonical N-terminal mitochondrial targeting signal (black bar) that contains a hydrophobic stretch (hatched part). The predicted MPP and the Imp1/2 cleavage sites are indicated by a black or grey arrow head, respectively. The two predicted transmembrane domains are highlighted as grey bars.

B Internally tagged HA-Mcp3 is functional. *mdm10*Δ cells were transformed with the empty plasmid pYX142 (∅) or pYX142 encoding Mdm10, Mcp3, or an internally HA-tagged Mcp3 (*MDM10*, *MCP3*, *HA-MCP3*). Cells were grown to an OD_{600} of 1.0 and spotted on YPG plates in a 1:5 dilution series. Plates were incubated for growth at 37°C for 4 days.

C HA-Mcp3 is processed *in vivo*. Mitochondria isolated from *mdm10*Δ (Δ) cells containing the empty plasmid or expressing HA-Mcp3 were analysed by SDS–PAGE and immunodecoration with antibodies against the indicated proteins. Two different bands are detectable in case of HA-Mcp3 (p, precursor; m, mature protein). The MOM protein Tom40 serves as loading control.

D Mcp3 is a mitochondrial protein. Whole-cell lysate (WCL) and fractions corresponding to cytosol (Cyt.), light microsomal fraction (ER) and mitochondria (Mito.) of *mcp3*Δ cells either containing the empty plasmid (∅) or expressing HA-Mcp3 were analysed by SDS–PAGE and immunodecoration with antibodies against the HA-tag, the mitochondrial protein Tom70, a marker protein for the cytosol (Bmh1) and an ER marker protein (Erv2). m, mature protein.

E Mcp3 co-localizes with the mitochondrial marker protein AAC. Cells over-expressing HA-Mcp3 were fixed and analysed by fluorescence microscopy using antibodies against the HA-epitope (αHA) and the mitochondrial ADP/ATP carrier (αAAC) (scale bar = 5 μm).

F C-terminally tagged Mcp3-HA is located to mitochondria. A mitochondria-enriched fraction (Mito.) and the post-mitochondrial supernatant (PMS) of wild-type cells carrying the empty plasmid (∅) or over-expressing the C-terminally HA-tagged Mcp3 (Mcp3-HA) were analysed by SDS–PAGE and immunodecoration with antibodies against the HA-Tag, the mitochondrial protein Tom40 and a marker protein for the cytosol (Hxk1). m, mature protein.

G Mcp3 is membrane-embedded. Mitochondria isolated from *mcp3*Δ cells expressing HA-Mcp3 were left untreated (I, input) or subjected to alkaline extraction. The supernatant (SN) and pellet (P) fractions were analysed by SDS–PAGE and immunodecoration with antibodies against the indicated proteins. Tom20, an integral MOM proteins; Aco1, soluble matrix protein. m, mature protein.

H Mcp3 is a MOM protein. Mitochondria isolated from cells expressing HA-Mcp3 were treated with proteinase K (PK, 100 μg/ml) in the absence or presence of the detergent Triton X-100 (TX). Samples were precipitated with TCA and analysed by SDS–PAGE and immunodecoration with antibodies against the HA-tag or the indicated mitochondrial proteins. Tom20, a MOM protein exposed to the cytosol; Dld1, a protein located in the IMS.

I Mcp3 behaves like an outer membrane protein in density gradient centrifugation. Mitochondrial vesicles isolated from cells over-expressing HA-Mcp3 were subjected to sucrose density gradient centrifugation. Fractions of the gradient were collected and analysed by SDS–PAGE and immunodecoration with antibodies against the indicated proteins. The processed form of HA-Mcp3 is shown. Right panel: The intensities of the various bands were quantified and depicted. The sum of all intensities for each protein was set to 100%.

J Mcp3 lacking either transmembrane domain fails to rescue loss of Mdm10. Wild-type cells carrying the empty plasmid (wt + ∅) or *mdm10*Δ cells transformed with the empty plasmid (∅) or plasmid encoding Mdm10, Mcp3, or Mcp3 lacking TMD1 or TMD2 (*MDM10*, *MCP3*, Δ*TMD1*, Δ*TMD2*) were grown to an OD_{600} of 1.0 and spotted on YPG plates in a 1:5 dilution series. Plates were incubated for growth at 37°C for 4 days.

K Mcp3 lacking either of the two transmembrane domains is unstable. Crude mitochondria were obtained from wild-type cells containing an empty plasmid (∅) or *mcp3*Δ cells (Δ) transformed with plasmid encoding Mcp3 or Mcp3 lacking TMD1 or TMD2 (*MCP3*, Δ*TMD1*, Δ*TMD2*). Samples were analysed by SDS–PAGE and immunodecoration with antibodies against Mcp3 and Tom20 as loading control.

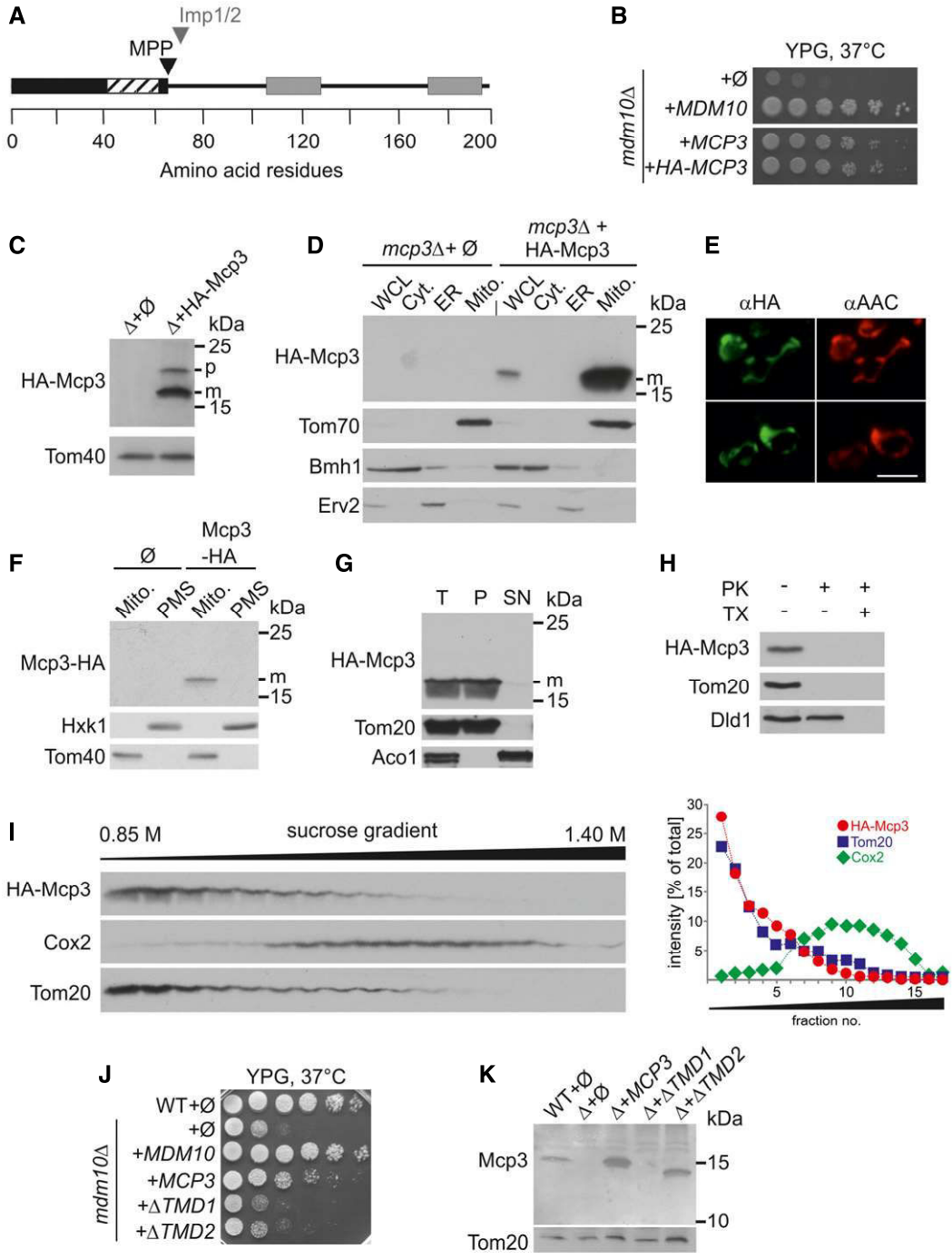

Figure 4.

Next, we wanted to confirm the predicted mitochondrial localization of Mcp3. To this end, we fractionated the aforementioned cells into various subcellular compartments. HA-Mcp3 and the mitochondrial marker Tom70 were solely detected in the mitochondrial fraction (Fig 4D). The mitochondrial localization could be confirmed by immunofluorescence microscopy. The fluorescence signal for HA-Mcp3 closely resembled the mitochondrial staining of AAC (Fig 4E). We wondered whether also non-functional C-terminally HA-tagged Mcp3 was localized to mitochondria. As shown before with the C-terminally GFP-tagged Mcp3 [30], processed Mcp3-HA was found in enriched mitochondrial fractions (Fig 4F). This suggests that an alteration of the C-terminus leads to loss of function rather than unstable or mis-targeted protein.

Several *in silico* prediction programmes suggest two TMDs for Mcp3 (Fig 4A). To investigate whether Mcp3 is indeed an integral membrane protein, mitochondria containing HA-Mcp3 were treated with an alkaline carbonate solution to extract soluble proteins and those that are peripheral attached to the membrane. Similarly to the

integral membrane protein Tom20, HA-Mcp3 was found in the pellet fraction (Fig 4G). Next, we wanted to know in which of the mitochondrial membranes Mcp3 is embedded. First, we treated isolated mitochondria containing HA-Mcp3 with proteinase K (PK). As shown in Fig 4H, HA-Mcp3 is digested in intact mitochondria similarly to the MOM protein Tom20, whereas the IMS protein Dld1 is degraded only upon lysis of the membranes with detergent. This suggests that Mcp3 is a MOM protein exposed to the cytosol. To substantiate this conclusion, we separated the two mitochondrial membranes by density gradient centrifugation. Membrane vesicles from mitochondria expressing HA-Mcp3 were obtained by hypo-osmotic swelling and sonication. These vesicles were separated by a sucrose gradient, and the different fractions were analysed for the presence of HA-Mcp3 and marker proteins for the MIM and MOM (Fig 4I). HA-Mcp3 and the MOM marker protein Tom20 are predominantly detectable in the lighter fractions corresponding to the MOM. In contrast, the MIM protein Cox2 is found, as expected, mainly in the heavier fractions (Fig 4I). Next, we wondered whether the predicted TMDs are important for the function of Mcp3. We constructed two additional versions of Mcp3 that lack either TMD1 (amino acid 106–128) or TMD2 (amino acids 172–198) and tested their rescue capacity in cells lacking Mdm10. Both constructs failed to rescue the growth defect of mdm10Δ cells (Fig 4J). We then asked whether the absence of the TMDs results in changes in protein stability. Using cells expressing these Mcp3 variants, we observed that the absence of TMD1 resulted in a non-detectable species, whereas loss of TMD2 caused lower detected amount of the protein in comparison with native Mcp3 (Fig 4K). We conclude that both TMDs are important for the stability and function of the protein.

Taken together, our results show that Mcp3 is an integral MOM protein and are in line with a high-throughput study where Mcp3 was found in the MOM proteome [40].

Mcp3 is processed *in vitro* and imported by the TOM complex

Our findings raise the unique possibility that Mcp3 is a MOM protein and also a substrate of the IMP peptidase. This led us to study the biogenesis of Mcp3. First, we asked whether Mcp3 is processed in an *in vitro* import assay. To address this question, we incubated radiolabelled Mcp3 with isolated mitochondria. Mcp3 was indeed processed into a mature form of about 15 kDa in a time-dependent manner (Fig 5A). We also noted an additional band at around 10 kDa that we assume to be the cleaved N-terminal segment of the precursor protein (Fig 5A, arrowhead). Thus, the processing of Mcp3 under both *in vivo* and *in vitro* conditions allows us to use the formation of the mature band as a read-out for correct import.

We first aimed to find out which import receptor recognizes the precursor protein on the surface of the organelles. We isolated mitochondria from strains deleted in either *TOM20* or *TOM70/71*. *In vitro* import of Mcp3 was not altered when Tom20 was absent (Appendix Fig S2A). On the other hand, the *in vitro* import of Mcp3 was strongly diminished in organelles lacking Tom70/71, whereas the *bona fide* Tom20 substrate pSu9-DHFR was not affected (Fig 5B). Accordingly, *in vivo* steady-state levels of HA-Mcp3 were strongly reduced in the absence of *TOM70/71* (Fig 5C). Taken together, Mcp3 is imported via recognition by Tom70.

Recently, an import pathway for MOM multispan proteins was described that requires Tom70 but is independent of other components of the TOM complex [41,42]. To investigate whether this is also the case for Mcp3, we tested whether its import relies on functional Tom40. To this end, we used mitochondria from cells harbouring the temperature-sensitive allele *tom40-25* [43]. Mcp3 was imported into the altered organelles with highly reduced efficiency as compared to control mitochondria. In contrast, as expected, organelles harbouring the *tom40-25* mutant showed only a slightly reduced capacity to assemble the TOM pore-independent import substrate Ugo1 (Fig 5D). In line with the *in vitro* results, the detected steady-state levels of HA-Mcp3 are strongly reduced in the *tom40-25* mutant in comparison with control cells even at the permissive temperature (Fig 5E). Of note, the non-processed precursor was degraded by addition of external protease, suggesting that Mcp3 does not reach the intermembrane space in these mitochondria (Fig EV3A). Thus, in contrast to other multispan MOM proteins, the import of Mcp3 requires functional Tom40.

We also aimed at studying physical interactions of the precursor protein with the different TOM components. First, we performed a pull-down assay with ^{35}S-Mcp3 and purified GST fusion proteins of the soluble cytosolic domains of Tom70, Tom20 and Tom22 [44]. In line with our previous results and as shown in Fig 6A, the highest amount of Mcp3 binds to GST-Tom70. Furthermore, also Tom22 binds *in vitro* Mcp3 precursor (Fig 6A). To further confirm this direct interaction *in organello*, we used mitochondria that contain His-tagged Tom22 [45]. After *in vitro* import and lysis of the organelles, proteins pulled down by Ni-NTA beads were analysed. We observed specific binding of Mcp3 to the resin only if mitochondria contained the His-tagged Tom22 (Fig 6B). Finally, we analysed the *in vitro* import reaction into the His-Tom22 mitochondria by BN-PAGE and addition of an antibody against the His-tag. Indeed, the import intermediate of radiolabelled Mcp3 associated with the TOM complex (at about 480 kDa) was shifted to higher molecular weight (Fig 6C, arrowhead). Taken together, these results strongly favour a passage of Mcp3 through the TOM complex, where Tom22 mediates the relay to Tom40 after initial binding by Tom70.

Biogenesis of Mcp3 is dependent on the TIM23 complex and the inner membrane peptidase

So far specific peptidases at the MOM were not identified. Thus, the processing of Mcp3 raised the possibility that the import pathway of the protein includes contact with a peptidase anchored to the inner membrane. Furthermore, presequence-containing proteins that are imported via the general import pathway are transferred from TOM complex to the TIM23 complex in the MIM. To test whether the Mcp3 precursor follows a similar pathway, we used a yeast strain bearing a temperature-sensitive allele of *TIM23*, *tim23ts* [46]. *In vitro* import of Mcp3 into mitochondria harbouring the altered Tim23 was strongly impaired already at permissive temperature, whereas the import of the Tim23-independent MOM protein Ugo1 was not influenced (Fig 7A). Accordingly, the steady-state levels of HA-Mcp3 were reduced in the organelles of mutant cells, whereas the levels of the MOM proteins Ugo1 and Fis1 were unaffected (Fig 7B). Hence, the presequence translocase TIM23 complex is involved in the biogenesis of Mcp3.

Establishing a requirement for the TIM23 machinery at the inner membrane, we next asked whether Mcp3 import requires the

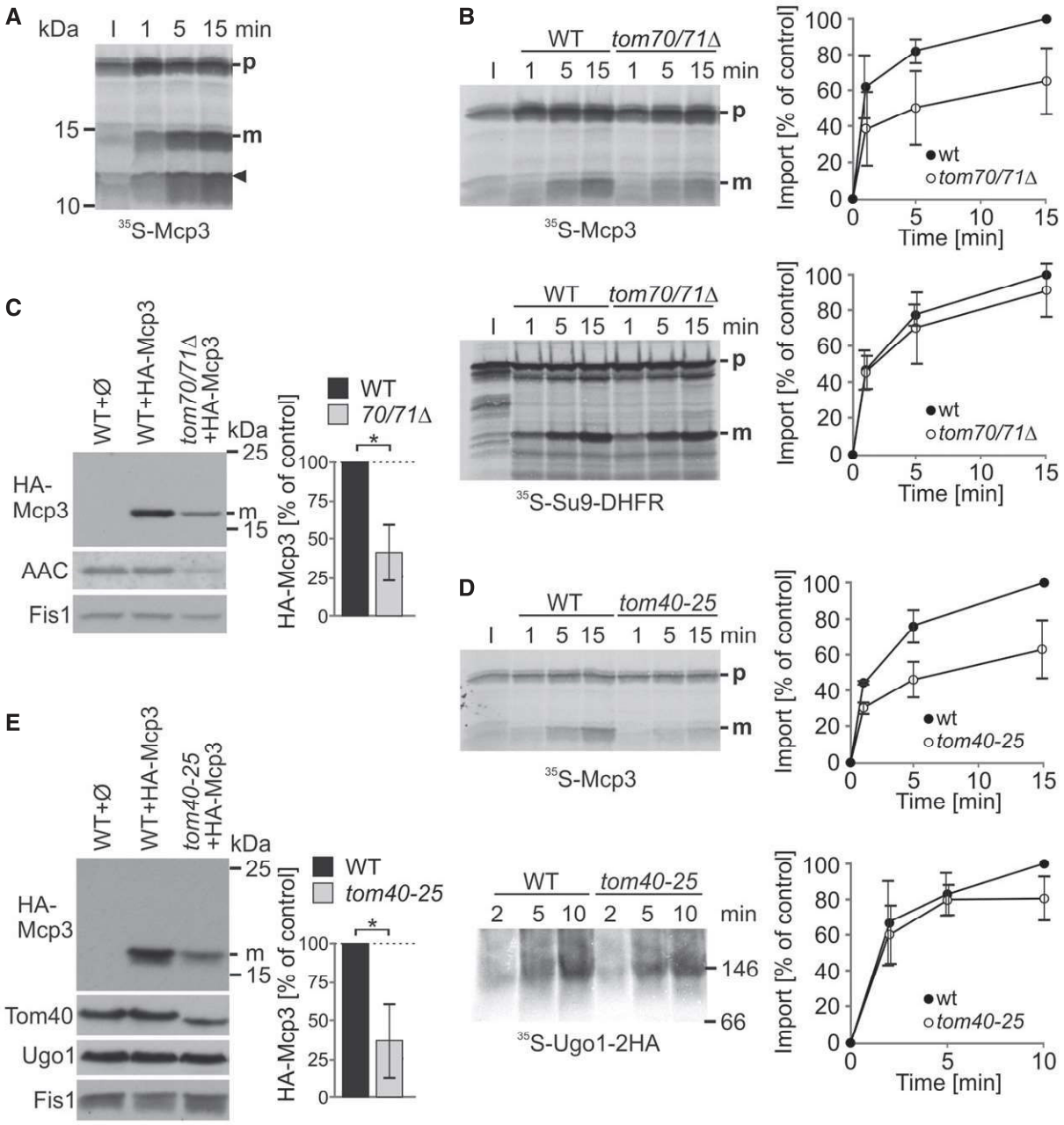

Figure 5. Mcp3 is imported by the TOM complex.

A Isolated mitochondria were incubated with radiolabelled Mcp3 precursor protein for the indicated time periods. After import, mitochondria were reisolated and analysed by SDS–PAGE and autoradiography. The arrowhead marks an additional band of the size of the cleaved N-terminus of Mcp3. p and m, precursor and mature forms, respectively.

B Import of Mcp3 is dependent on the receptor Tom70. Mitochondria isolated from wild-type or *tom70/71Δ* cells were incubated with radiolabelled Mcp3 or pSu9-DHFR (as control) for the indicated time periods. After import, mitochondria were reisolated and analysed by SDS–PAGE and autoradiography. p and m, precursor and mature forms, respectively. I, 20% of radiolabelled precursor protein used in each import reaction. Bands corresponding to the mature (m) form were quantified. Import into wild-type mitochondria after 15 min was set to 100%. The mean with standard deviations is depicted (n = 3; SD).

C Reduced steady-state levels of HA-Mcp3 in cells lacking Tom70. Crude mitochondria isolated from the indicated cells were analysed by SDS–PAGE and immunodecoration with antibodies against the HA-tag, AAC as control substrate of Tom70, and Fis1 as a loading control. HA-Mcp3 levels were quantified in relation to Fis1 levels, and the levels in WT cells were set to 100%. The bar diagram shows the mean with standard deviation (n = 3; SD; *, $P < 0.05$; two-tailed Student's t-test).

D Import of Mcp3 is dependent on Tom40. Mitochondria isolated from wild-type and *tom40-25* cells were incubated with radiolabelled Mcp3 for the indicated time periods. Next, mitochondria were reisolated and analysed by SDS–PAGE and autoradiography as described in (B). As a control, Ugo1 was imported into the same mitochondria. Organelles were reisolated and analysed by BN-PAGE and autoradiography. The band corresponding to the Ugo1 dimer at around 150 kDa was quantified. The mean with standard deviation is shown (n = 3; SD).

E Steady-state levels of HA-Mcp3 are lower in cells harbouring a mutant *TOM40* allele. Crude mitochondria from wild-type and *tom40-25* cells were obtained and analysed as described in (C). Immunodecoration was performed with antibodies against the HA-tag, Tom40, and Fis1 as loading control.

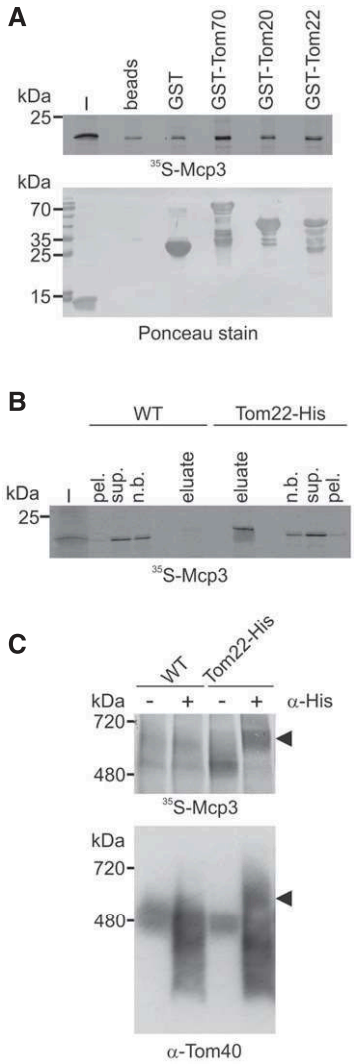

Figure 6. Mcp3 precursor physically interacts with components of the TOM complex.

A Mcp3 precursor binds *in vitro* to cytosolic domains of TOM receptors. Radiolabelled Mcp3 was incubated with recombinant GST alone or GST fused to the cytosolic domains of Tom70, Tom20 or Tom22 prebound to glutathione beads or with unloaded beads. After washing, bound material was eluted with sample buffer. Proteins were analysed by SDS–PAGE, blotting onto a membrane and autoradiography. To demonstrate equal amounts of GST fusion proteins, the membrane was stained with Ponceau S. I, input 5% of precursor used.

B Mcp3 precursor binds to Tom22 *in organello*. Radiolabelled Mcp3 was incubated with mitochondria isolated from WT His-Tom22 containing cells. Mitochondria were pre-incubated with CCCP (40 μM) to halt import. After lysis with β-dodecyl maltoside, samples were incubated with Ni-NTA beads. After washing, bound proteins were eluted with sample buffer and analysed by SDS–PAGE and autoradiography. I, 5% of ^{35}S-Mcp3 used; pel., 2% insoluble material after clarifying spin; sup., 2% of material incubated with Ni-NTA; n.b. 2% of non-bound material after binding to Ni-NTA; eluate, 100% of bound material.

C Radiolabelled Mcp3 was incubated with organelles described in (B). After import, mitochondria were solubilized in digitonin, and the lysate was cleared by centrifugation and incubated with or without an antibody against the His-tag (α-His). Samples were analysed by BN-PAGE, autoradiography and afterwards immunodecoration with an antibody against Tom40. Bands shifted by the anti-His antibody are indicated by arrowhead.

membrane potential. Hence, we tested the processing efficiency in the presence of the uncoupler CCCP and valinomycin (Fig 7C for CCCP and Fig EV4). In the presence of both substances that depolarize mitochondria, we could hardly detect a mature form. We conclude that processing of Mcp3 is dependent on the mitochondrial membrane potential. Since Mcp3 has in its N-terminal domain a predicted MTS, we wondered whether the observed processing can be mediated by the matrix processing peptidase (MPP). To that end, we added to the *in vitro* import reaction two chelators for bivalent cations, ortho-phenanthroline and EDTA, which are known to inhibit MPP. This addition had no influence on processing of Mcp3 (Fig 7C, sixth lane). Additionally, incubation of ^{35}S-Mcp3 precursor with recombinant MPP did not result in cleavage of the precursor molecules while the known MPP substrate, pSu9-DHFR, was almost completely processed (Fig 7C, L + MPP). Next, we isolated mitochondria from a temperature-sensitive mutant strain of the MPP subunit Mas1 and performed *in vitro* import assays under various conditions. Whereas the mutation had a clear effect on cleavage of the model substrate pSu9-DHFR, processing of Mcp3 was not influenced (Appendix Fig S3). Taken together, the observed mature form of Mcp3 is not a result of MPP cleavage.

To identify the peptidase that cleaves Mcp3, we over-expressed HA-Mcp3 in different yeast deletion strains each lacking one of the known enzymes involved in processing and/or degradation of mitochondrial proteins and analysed the steady-state levels of HA-Mcp3 in these cells. Only in the absence of the two subunits of the inner membrane peptidase, Imp1 and Imp2, the mature form could not be detected (Fig 7D). Interestingly, also the C-terminally tagged Mcp3 (Mcp3-HA) is processed by Imp1 (Fig 7E). This observation confirms that the C-terminal tag results in an inactive mitochondrial protein rather than mislocalization to another organelle or protein instability. To show that Mcp3 is a substrate of the IMP complex, we isolated mitochondria from *imp1*Δ or *imp2*Δ cells and performed an *in vitro* import assay. The mature form of Mcp3 was not formed in mitochondria lacking either Imp1 or Imp2 (Fig 7F). To finally confirm the predicted Imp1 cleavage site N-terminally to Asp70 [38], we performed site-directed mutagenesis of the internally HA-tagged Mcp3 variant to obtain the D70G substitution mutant. Such an Asp to Gly exchange is known to prevent cleavage of substrate proteins by IMP [6,8]. HA-tagged ^{35}S-Mcp3 was incubated *in vitro* with isolated mitochondria and was as expected processed, in an IMP-dependent manner, upon its import into a mature form (Fig 7G, m', lanes 5 and 7–9). In contrast, the D70G mutant lacking the Imp1 consensus sequence was not processed (Fig 7G, lane 3).

Next, we analysed the D70G variant. We incubated mitochondria after import with proteinase K (PK). Interestingly, the D70G precursor was resistant to PK treatment (Fig 7G, lane 3, p'), whereas the non-processed HA-tagged native Mcp3 precursor is fully degraded. Thus, it seems that the import intermediate of Mcp3-D70G, which cannot be cleaved by IMP, accumulates in the intermembrane space. This implicates that the N-terminus of Mcp3 reaches the intermembrane space before the C-terminal TMD is inserted into the outer membrane. Indeed, in the absence of the IMP peptidases also the precursor of native HA-Mcp3 accumulates in the intermembrane space (Fig 7G, lanes 10–12).

Of note, we observed a PK protected band of lower molecular weight of HA-Mcp3 in wild-type mitochondria (Fig 7G, lane 4, asterisk). This band could correspond to a processed Mcp3

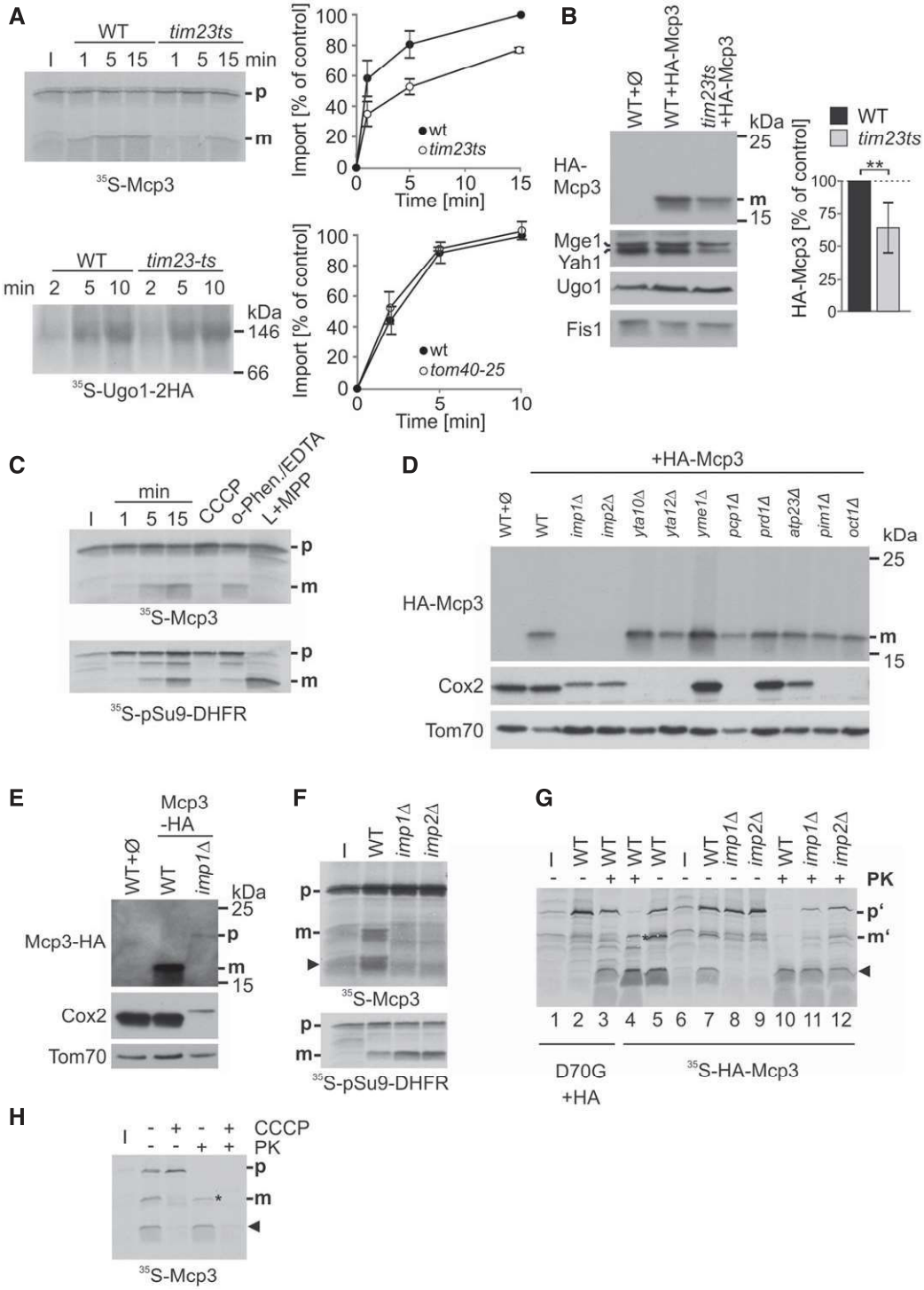

Figure 7.

intermediate in the IMS. We wanted to know whether, similarly to the overall import of Mcp3, the formation of this species is dependent on the membrane potential. Fig 7H shows that indeed, the corresponding band for Mcp3 disappears in the presence of the uncoupler CCCP. We detected this processed PK-resistant variant in many experiments, but we did not find appropriate conditions for chasing this form to a fully membrane-inserted species. Hence, we assume that it is a non-productive import intermediate of Mcp3.

Our observations confirm that the IMP complex cleaves the precursor form of Mcp3. Since Imp1 and Imp2 are only functional in a multimeric Imp1/Imp2 complex, we cannot determine which subunit is actually responsible for the processing of Mcp3. However, all results are in agreement with the *in silico* prediction of Mcp3 as substrate of Imp1 [38]. Taken together, our results demonstrate that after crossing the MOM Mcp3 is taken over by TIM23 complex and processed by IMP in the IMS.

Figure 7. Biogenesis of Mcp3 depends on the TIM23 complex and processing by IMP.

A Import of Mcp3 is dependent on the TIM23 complex. Mitochondria isolated from wild-type and *tim23ts* cells were incubated with radiolabelled Mcp3 for the indicated time periods. Further treatment and analysis (n = 3; SD) was as described for Fig 5D.

B Steady-state levels of HA-Mcp3 are lower in cells harbouring a temperature-sensitive *TIM23* allele. Crude mitochondria were obtained at the non-permissive temperature from WT or *tim23ts* cells containing a plasmid expressing HA-Mcp3. Samples were analysed by SDS–PAGE and immunodecoration with antibodies against the HA-tag, the matrix proteins Mge1 and Yah1 as typical TIM23 substrates, Ugo1 and Fis1 as TIM23-independent substrates. HA-Mcp3 levels were quantified in relation to Fis1 levels. Levels in WT cells were set to 100%. The bar diagram shows the mean with standard deviation of six independent experiments (n = 6; SD; **, $P < 0.01$; two-tailed Student's t-test).

C Import and processing of Mcp3 is dependent on the mitochondrial membrane potential. Isolated mitochondria were incubated with radiolabelled Mcp3 or pSu9-DHFR as control for the indicated time periods or for 15 min in the presence of either CCCP, or o-phenanthroline and EDTA (o-Phen./EDTA). After import, mitochondria were reisolated and analysed by SDS–PAGE and autoradiography. L + MPP: radiolabelled proteins were incubated with recombinant MPP.

D Mcp3 is processed by Imp1/2. Single-deletion strains of known mitochondrial proteases and peptidases were transformed with a plasmid expressing HA-Mcp3. Crude mitochondria were isolated and analysed by SDS–PAGE and immunodecoration with antibodies against the indicated proteins and the HA-epitope. Cox2, a known substrate of IMP; Tom70, a mitochondrial outer membrane protein.

E C-terminally tagged Mcp3-HA is processed by Imp1. WT and *imp1*Δ cells were transformed with a plasmid expressing Mcp3-HA, and further analysis was performed as described in (D).

F Mcp3 is processed by Imp1/2 after *in vitro* import into mitochondria. Mitochondria isolated from WT, *imp1*Δ or *imp2*Δ strains were incubated with radiolabelled precursor of Mcp3 or pSu9-DHFR as control. Further treatment and analysis was as described in Fig 5A.

G Full-length Mcp3 precursor accumulates during import if IMP processing is abolished. Radiolabelled internally HA-tagged Mcp3 without (HA-Mcp3) or with mutation in the Imp1 cleavage site (D70G + HA) were incubated with mitochondria as in (F). After import, samples were incubated with or without PK (20 μg/ml). Samples were analysed by SDS–PAGE and autoradiography.

H Mitochondrial membrane potential is required for efficient import of Mcp3 precursor into mitochondria. Isolated mitochondria were incubated with radiolabelled Mcp3 in the presence or absence of CCCP. After import, mitochondria were incubated with PK as in (G) and analysed by SDS–PAGE and autoradiography. I, 20% of radiolabelled precursor protein used in each import reaction; the arrowhead marks an additional band of the size of the cleaved N-terminus of Mcp3.

MIM complex is involved in the biogenesis of Mcp3

Next, we asked how Mcp3 is integrated into the MOM. Two major complexes are known to mediate insertion of proteins into the MOM, namely the TOB/SAM and MIM complexes. To test whether the β-barrel insertion machinery is involved in the membrane integration of Mcp3, we employed a yeast strain deleted for the TOB subunit Mas37/Sam37. No obvious difference in Mcp3 import was observed when mitochondria from *mas37*Δ cells were compared to wild-type organelles (Appendix Fig S2B). In addition, we did not observe any influence of the small TIM chaperones that are involved in β-barrel and carrier-type TIM22 complex substrate handling on the import of Mcp3 (Appendix Fig S2C and D). Hence, it appears that Mcp3 follows a different membrane integration pathway than β-barrel proteins.

The MIM complex, which has two known subunits Mim1 and Mim2, mediates membrane integration of various MOM helical proteins [41,42]. To investigate its role in the import of Mcp3, mitochondria from *mim1*Δ or *mim2*Δ cells were analysed. Import of Mcp3 was strongly reduced in both cases (Fig 8A). Similarly, the steady-state levels of HA-Mcp3 were highly diminished in these cells (Fig 8B). As expected, the levels of Tom20, a known substrate of MIM complex, are reduced in *mim1*Δ or *mim2*Δ cells. Since we could show that complete loss of Tom20 has no effect on import of Mcp3 (Appendix Fig S2A), this reduction should not influence Mcp3 import. Yet it is known that also the assembly of the TOM complex is affected by the absence of functional MIM complex [47–50]. Therefore, the import of most proteins is indirectly hampered in these cells as exemplified by the matrix destined model substrate pSu9-DHFR (Appendix Fig S4). To investigate whether MIM components can directly bind Mcp3 precursor, we performed an *in vitro* pull-down assay. The fusion protein MBP-Mim1 and MBP alone were expressed in *E. coli*, bound to amylose beads and further incubated with ^{35}S-Mcp3. Fig 8C shows that the amount of Mcp3 precursor pulled down with MBP-Mim1 is strongly increased in comparison with MBP alone. This result suggests a direct interaction of Mim1 and Mcp3. Taken together, we suggest that the MIM complex might play a role in the import of Mcp3 into the MOM.

Discussion

Contacts of ER and mitochondria and the presence of the ERMES tether are of great relevance for yeast cells regarding mitochondrial function. Evidence arises that ERMES does not "only" serve as a mechanical tether between the ER and mitochondria but has additional functions (for a review, see [14]). For example, several ERMES components were predicted and shown to have lipid binding capacity [22,23], and Mdm10 was reported to interact with the TOB complex in β-barrel protein import (reviewed in [13]). The whole picture is still blurry since all these processes are interdependent, and the observed phenotypes can be interpreted as an indirect outcome of a different defect.

ER–mitochondria encounter structure itself is crucial for mitochondrial function, and cells lacking this complex suffer from a severe phenotype. Its importance becomes more obvious by the fact that cells lacking one of its components easily acquire endogenous suppressors, which was already reported in the early years of the discovery of the individual components [32,51]. Furthermore, *S. cerevisiae* seems to have backup systems that can partially complement the ERMES function. We recently reported that over-expression of two mitochondrial proteins Mcp1/2 can partially rescue the defects caused by loss of ERMES function [20]. Furthermore, a close interaction of mitochondria with the vacuole was shown to contribute to mitochondrial lipid exchange and can serve as a potential backup system for ERMES-mediated interactions [9,10]. In addition, a second ER–mitochondria contact mediating complex has been described [25]. The overall picture becomes even more complex since ER–vacuole and ER–mitochondria contact sites are coordinated by the ER protein Ltc1/Lam6, which is suggested to be involved in sterol exchange between membranes [26,52].

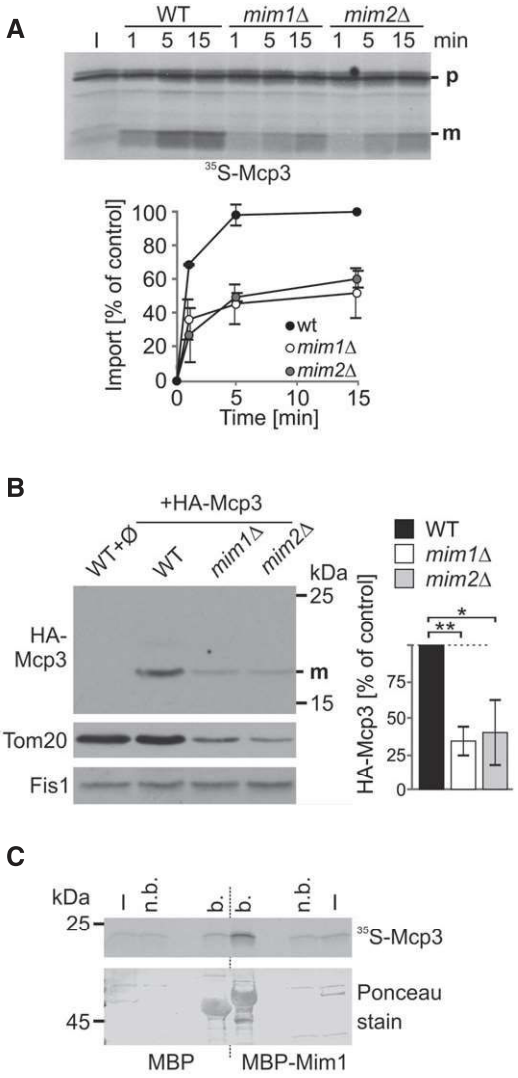

Figure 8. Insertion of Mcp3 into the MOM involves the MIM complex.

A Import of Mcp3 is mediated by the MIM complex. Mitochondria isolated from WT, *mim1*Δ, or *mim2*Δ cells were incubated with radiolabelled Mcp3 for the indicated time periods. After import, mitochondria were reisolated and analysed by SDS–PAGE and autoradiography. Bands corresponding to the mature (m) form were quantified. Import after 15 min into wild-type mitochondria was set to 100%. The mean with standard deviations is depicted (n = 3; SD). I, 20% of radiolabelled precursor protein used in each import reaction.

B Steady-state levels of over-expressed HA-Mcp3 are reduced in cells lacking MIM complex subunits. Crude mitochondria were obtained from WT cells containing an empty plasmid (Ø) and from wild-type, *mim1*Δ or *mim2*Δ cells containing a plasmid encoded HA-Mcp3. Samples were analysed by SDS–PAGE and immunodecoration with antibodies against the HA-tag, Tom20 as MIM substrate and Fis1 as a loading control. HA-Mcp3 levels were quantified in relation to Fis1 levels. Levels in wild-type cells were set to 100%. The bar diagram shows the mean with standard deviation (n = 3; SD; *, $P < 0.05$; **, $P < 0.01$; two-tailed Student's t-test).

C Mcp3 precursor binds *in vitro* to Mim1. Radiolabelled Mcp3 was incubated with amylose beads harbouring recombinant MBP or MBP fused to Mim1. After washing, proteins were eluted with sample buffer. Analysis was performed by SDS–PAGE, blotting and autoradiography. To demonstrate equal amounts of MBP fusion proteins, the membrane was stained with Ponceau S. I, input 5% of precursor used; n.b., 5% of unbound material; b, 100% of bound material.

Since contacts between mitochondria and other organelles are mediated by the MOM, it is not surprising that two of the suppressors of the ERMES identified by us (Mcp1 in [20] and Mcp3 in this work) are located in the outer membrane. Although the molecular mechanism by which these proteins ameliorate the lack of ERMES is not known, better understanding of their mode of function requires comprehensive insights into their membrane topology and biogenesis pathways.

In this respect, Mcp3 provides an example for a protein that follows a unique import pathway which was not described so far. Although it shares certain import steps with other MOM proteins, the overall import and assembly process is very unusual (Fig 9). At the surface of the organelle, Mcp3 is recognized by Tom70 (Step 1). Of note, also other presequence-containing proteins share this first recognition step by Tom70 [53]. These are proteins with a mature part that tends to aggregate and hence are protected by the chaperone-like function of Tom70. Considering the two predicted transmembrane domains and the hydrophobic stretch close to the IMP cleavage site, Tom70 might function as a receptor with a chaperone function in the import of Mcp3. This dependence on Tom70 is shared by other multispan MOM proteins but not by the single-span protein Om45 [41–43,54]. However, whereas multispan proteins like Ugo1 and Scm4 are relayed directly from Tom70 to the MIM complex, Mcp3 is translocated across the outer membrane via the Tom40 pore (Fig 9, Step 2).

Mcp3 then interacts with the TIM23 complex, and the hydrophobic patch close to its N-terminus suggests a stop-transfer mechanism followed by a lateral release (Fig 9, Step 3). An interaction of a MOM protein with the TIM23 complex was reported recently for OM45 [43,54]. Yet, while Om45 is directed from the TIM23 to the MIM complex without any processing events [43,54], Mcp3 is processed by IMP. Of note, although Mcp3 import depends on the mitochondrial membrane potential, in contrast to classical MTS

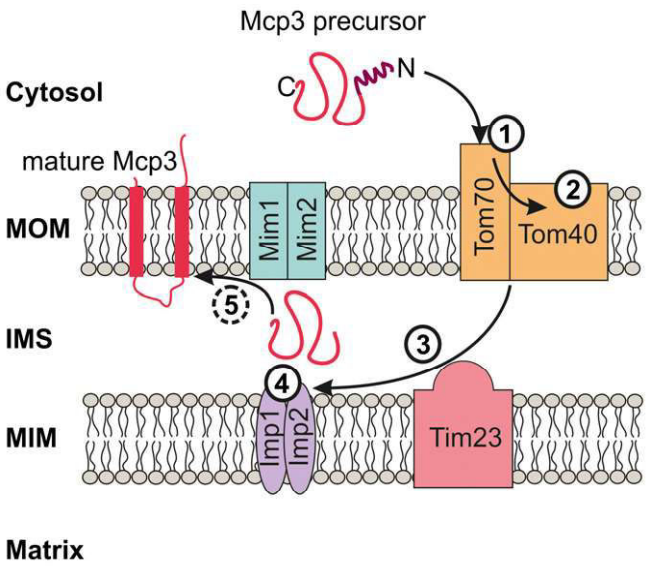

Figure 9. Biogenesis pathway of Mcp3.
Working model for the import route of Mcp3. The different steps (1–5) are described in the text.

bearing proteins it is not processed by the MPP but rather by IMP. Hence, although Mcp3 shares some import steps with the pathway taken by Om45, its recognition by Tom70 and cleavage by IMP are obvious divergences from this pathway. To our knowledge, this is the first MOM protein that is found to be processed by the peptidase of the inner membrane.

A tempting hypothesis is that after its processing, Mcp3 is relayed to the MIM machinery (Fig 9, steps 4 and 5). Indeed, Mim1 can bind Mcp3 precursor *in vitro* and Mim1 dependency was also suggested for the membrane integration of the MOM protein Om45 [43]. However, it cannot be excluded that the reduction in both *in vitro* import and steady-state levels of Mcp3 in organelles lacking Mim1 and Mim2 is due to the overall import defects of such mitochondria. Thus, to finally prove that this complex is able to mediate the membrane integration of single- and multispan MOM proteins from both sides of the membrane, further experimental evidence is needed. Such a remarkable ability would be unique and was not reported so far for other cellular membrane insertases like the YidC/Oxa/Alb3, Sec or the Get1/2 machineries.

A prominent example of a protein functioning in the mitochondrial outer membrane where the mitochondrial membrane potential plays an important role in its biogenesis is the protein kinase PINK1. Mutations in this protein, which is found in higher eukaryotes, can cause familiar Parkinson's disease. The membrane potential is crucial for the fate and the activity of PINK1. It is suggested that PINK1, as a sensor for mitochondrial dysfunction, is targeted to mitochondria similarly to Mcp3 by its canonical MTS [55]. In intact mitochondria, PINK1 is imported, reaches the MIM and is processed by the MIM protease PARL. Next, PINK1 is completely degraded and PINK/parkin signalling is suppressed [55]. The PARL processing event reminds remotely on the processing of Mcp3 by IMP. In case of mitochondrial defects, PINK1 is not completely imported into mitochondria since the driving force by the membrane potential is missing. As a result, PINK1 is inserted into the MOM in a TOM-dependent process where it initiates PINK1/parkin signalling. Although the exact function of Mcp3 is unclear, the example of PINK1 demonstrates that the physiological status of the organelle might affect the function of Mcp3 as well.

Taken together, Mcp3 follows a novel import route into mitochondria. Mcp3 is first recognized by the receptor Tom70, next channelled through the TOM complex and further imported by the TIM23 machinery. It is the first MOM protein shown to be processed by IMP.

Materials and Methods

Yeast strains and growth conditions

Yeast strains (all isogenic to W303a/α, or BY4741/2) were grown in and on standard rich or synthetic liquid and solid media, respectively [56]. For drop dilution assays, cells were cultured to an OD_{600} of 1.0 and diluted in fivefold increments followed by spotting 5 μl of each dilution on the corresponding medium. To delete complete ORFs by homologous recombination, gene-specific primers were used to amplify either the HIS3MX6 cassette from the plasmid pFA6a-HIS3MX6 [57] or the KanMX4 cassette from the plasmid pFA6a-KanMX4 [58]. All deletion strains were confirmed by PCR with gene-specific primers. Transformation of yeast cells was performed by the lithium acetate method. Yeast strains used in this study are summarized in Appendix Table 1, and primer sequences are listed in Appendix Table 2.

Recombinant DNA techniques

The ORF of the *MCP3* gene was amplified by PCR from yeast genomic DNA with specific primers and cloned into the plasmid pYX142. For expression under the control of the endogenous promoter and terminator, 500 bp upstream and downstream, respectively, of the Mcp3 ORF were amplified by PCR and together with the ORF were subcloned into the vector pRS316. Mcp3 with an internal HA-tag (HA-Mcp3) was constructed by sequential amplification of the N-terminal and C-terminal part of *MCP3* from genomic DNA and insertion into the plasmid pYX142. Primer sequences were designed in a way that the HA-tag was inserted four amino acids downstream to the anticipated Imp1 cleavage site [39]. The C-terminally HA-tagged version of Mcp3 was obtained by cloning *MCP3* without its stop codon into the plasmid pYX142. Primers for the transmembrane domain deletion constructs were designed to omit amino acids 106–128 (ΔTMD1) or 172–198 (ΔTMD2). All specific primer sequences and restriction sites used for cloning are listed in Appendix Table 2. All constructs were confirmed by DNA sequencing. Plasmids used for expression of ERMES components were described previously [20]. For synthesis of radiolabelled precursor of Mcp3, the different variants were subcloned via *EcoR*I and *Hin*dIII restriction sites into the vector pGEM4. Site-directed mutagenesis to obtain the D70G amino acid exchange mutant was performed initially with the pGEM4 construct.

Biochemical methods

Subcellular fractionation was performed according to published procedures [59]. Mitochondria were isolated by differential centrifugation as described previously [60]. Further purification of mitochondria was achieved via a self-generated Percoll gradient or a sucrose step gradient [61]. For swelling experiments, mitochondria were incubated in hypotonic buffer (20 mM Hepes, pH 7.2) for 30 min on ice. Soluble proteins were precipitated by trichloroacetic acid (TCA). Protein samples were analysed by SDS–PAGE and immunoblotting using the ECL system. Carbonate extraction to precipitate integral membrane proteins and sucrose gradient centrifugation to separate OM and IM vesicles were performed as described previously [20]. Pull-down experiments with radiolabelled precursor and GST fusion proteins or MBP fusion proteins were performed as described before [42,44]. Proteinase K accessibility of imported proteins was analysed by incubation of reisolated mitochondria with PK (20–100 μg/ml) for 30 min on ice, inhibiting the protease by 1 mM PMSF, and finally TCA precipitation of the samples.

Blue native PAGE

Mitochondria were lysed in 40 μl buffer containing digitonin (1% digitonin, 20 mM Tris–HCl, 0.1 mM EDTA, 50 mM NaCl, 10% (v/v) glycerol, 1 mM PMSF, pH 7.2). After incubation on ice for 15 min and clarifying spin (30,000 *g*, 15 min, 2°C), 5 μl of sample buffer (5% (w/v) Coomassie blue G, 500 mM 6-amino-N-caproic acid,

100 mM Bis-Tris, pH 7.0) was added, and the mixture was analysed by electrophoresis in a 6–13% or 4–8% gradient BN-PAGE [62]. Gels were blotted on polyvinylidene fluoride membranes, and proteins were further analysed by autoradiography or immunodecoration.

Fluorescence microscopy

For visualization of mitochondria, yeast cells were transformed with a vector harbouring the mitochondrial presequence of subunit 9 of F_o-ATPase of *N. crassa* fused to GFP [63]. Microscopy images were acquired with an Axioskop 20 fluorescence microscope equipped with an Axiocam MRm camera using the 43 Cy3 filter set and the AxioVision software (Carl Zeiss). For studies of ERMES foci formation and their colocalization with mitochondria, yeast cells were transformed with a plasmid expressing an ERFP tagged Mmm1 [16] and with either plasmids pYX142-mtGFP or pYX122-mtGFP expressing mitochondrially targeted GFP (mtGFP) [63]. Microscopy images were acquired with an Axioplan 2 epifluorescence microscope (Carl Zeiss) equipped with an Evolution VF Mono Cooled monochrome camera (Intas) using a Plan Neofluar 100×/1.30 Ph3 oil objective (Carl Zeiss) with QCapture Pro 6.0 software (Media Cybernetics).

Electron microscopy

Preparation of cells for electron microscopy was according to published procedures [64]. Ultrathin sections (70 nm) were cut with a diamond knife on a Leica Ultracut UCT microtome and mounted on pioloform-coated copper grids. Samples were analysed in a Zeiss CEM 902 transmission electron microscope operated at 80 kV. Micrographs were taken using a 1,350 × 1,350 pixel Erlangshen ES500W CCD camera (Gatan) and Digital Micrograph software (version 1.70.16; Gatan).

Analysis of phospholipids and ergosterol

Cells at the log phase (OD_{600} 1.0–2.0) grown on selective medium containing galactose were harvested, and mitochondria were isolated first by differential centrifugation, and then, crude organelles were purified further by a self-generated Percoll or sucrose density gradient (see above). Mass spectrometric analysis was performed as described [65]. In brief, ion mode on a triple quadrupole–linear ion trap hybrid mass spectrometer (QTRAP 5500, AB Sciex) was applied, except for analysis of cardiolipin and ergosterol, which was done in negative ion mode on a quadrupole time-of-flight mass spectrometer (QStar Elite, AB Sciex) [18]. Ergosterol quantification was performed as described before [66].

In vitro import assays and monitoring of steady-state levels of proteins

Mitochondria for import assays were isolated from yeast cells as described above. Cells were grown at 30°C in lactate containing medium to mid-logarithmic phase with the following exceptions: *tom40-25*, *mas37*Δ, *tim10-1ts* and *tim23ts* and the corresponding wild type were grown at 24°C. Radiolabelled precursor proteins were synthesized in the presence of [^{35}S]-methionine in rabbit reticulocyte lysate. The import reaction was performed by incubating the radiolabelled protein with isolated mitochondria in import buffer (250 mM sucrose, 0.25 mg/ml BSA, 80 mM KCl, 10 mM MOPS-KOH, 5 mM $MgCl_2$, 2 mM ATP and 2 mM NADH, pH 7.2). Mitochondria from *tom40-25* and *tim10-1ts* cells and from their corresponding wild-type cells were shifted *in vitro* for 15 min to the non-permissive temperature 37°C prior to the import reaction. For depletion of the membrane potential, mitochondria were preincubated for 5 min with either 40 μM CCCP or 10 μg/ml valinomycin prior to the import reaction. MPP was inhibited by the addition of 5 mM EDTA and 100 μM o-phenanthroline. The import reaction was terminated by diluting the reaction in a buffer (250 mM sucrose, 80 mM KCl, 10 mM MOPS, 2 mM PMSF, 1 mM EDTA, pH 7.2) and placing the samples on ice. In some cases, the import reactions were treated with PK as described above.

For preparation of crude mitochondria, cells were grown in minimal medium containing sucrose to mid-logarithmic phase at 30°C except cells from *tom40-25* and its corresponding wild type that were grown at 24°C. Cells from strain *tim23ts* and its corresponding wild type were grown at 24°C and shifted for 5–6 h to 37°C prior to lysis. Cells were disrupted by repeated cycles of vortexing with glass beads at 4°C. Mitochondria were enriched by differential centrifugation.

Statistical analysis

Data are presented as the mean ± sample-based standard deviation (SD). Two-tailed Student's *t*-tests were used to evaluate statistical significance of quantifications (*, $P < 0.05$; **, $P < 0.01$). Analyses were performed using Excel (Microsoft).

Expanded View for this article is available online.

Acknowledgements

We thank E. Kracker and Rita Grotjahn for technical assistance, and Drs. C. Koehler, K. Okamoto, T. Langer, D. Mokranjac, C. Meisinger, N. Pfanner, T. Becker and B. Guiard for yeast strains. This work was supported by the Deutsche Forschungsgemeinschaft (DI 1386/2-1 to K.S.D) and (DR 1028/7-1 to D.R.)

Author contributions

MS, TT, PW, HK, CÖ, XC, BW and BB performed experiments and analysed data together with DR and KSD; DR and KSD designed the study and wrote the manuscript with advice from MS, BB, BW and HK.

Conflict of interest

The authors declare that they have no conflict of interest.

References

1. Chacinska A, Koehler CM, Milenkovic D, Lithgow T, Pfanner N (2009) Importing mitochondrial proteins: machineries and mechanisms. *Cell* 138: 628 – 644
2. Endo T, Yamano K (2009) Multiple pathways for mitochondrial protein traffic. *Biol Chem* 390: 723 – 730
3. Mokranjac D, Neupert W (2009) Thirty years of protein translocation into mitochondria: unexpectedly complex and still puzzling. *Biochim Biophys Acta* 1793: 33 – 41

4. Neupert W, Herrmann JM (2007) Translocation of proteins into mitochondria. *Annu Rev Biochem* 76: 723–749
5. Teixeira PF, Glaser E (2013) Processing peptidases in mitochondria and chloroplasts. *Biochim Biophys Acta* 1833: 360–370
6. Luo W, Fang H, Green N (2006) Substrate specificity of inner membrane peptidase in yeast mitochondria. *Mole Genet Genomics* 275: 431–436
7. Hahne K, Haucke V, Ramage L, Schatz G (1994) Incomplete arrest in the outer membrane sorts NADH-cytochrome b5 reductase to two different submitochondrial compartments. *Cell* 79: 829–839
8. Ieva R, Heisswolf AK, Gebert M, Vogtle FN, Wollweber F, Mehnert CS, Oeljeklaus S, Warscheid B, Meisinger C, van der Laan M *et al* (2013) Mitochondrial inner membrane protease promotes assembly of presequence translocase by removing a carboxy-terminal targeting sequence. *Nat Commun* 4: 2853
9. Elbaz-Alon Y, Rosenfeld-Gur E, Shinder V, Futerman AH, Geiger T, Schuldiner M (2014) A dynamic interface between vacuoles and mitochondria in yeast. *Dev Cell* 30: 95–102
10. Honscher C, Mari M, Auffarth K, Bohnert M, Griffith J, Geerts W, van der Laan M, Cabrera M, Reggiori F, Ungermann C (2014) Cellular metabolism regulates contact sites between vacuoles and mitochondria. *Dev Cell* 30: 86–94
11. Westermann B (2015) The mitochondria-plasma membrane contact site. *Curr Opin Cell Biol* 35: 1–6
12. Kornmann B, Currie E, Collins SR, Schuldiner M, Nunnari J, Weissman JS, Walter P (2009) An ER-mitochondria tethering complex revealed by a synthetic biology screen. *Science* 325: 477–481
13. Hohr AI, Straub SP, Warscheid B, Becker T, Wiedemann N (2014) Assembly of beta-barrel proteins in the mitochondrial outer membrane. *Biochim Biophys Acta* 1853: 74–88
14. Klecker T, Bockler S, Westermann B (2014) Making connections: interorganelle contacts orchestrate mitochondrial behavior. *Trends Cell Biol* 24: 537–545
15. Murley A, Lackner LL, Osman C, West M, Voeltz GK, Walter P, Nunnari J (2013) ER-associated mitochondrial division links the distribution of mitochondria and mitochondrial DNA in yeast. *eLife* 2: e00422
16. Bockler S, Westermann B (2014) Mitochondrial ER contacts are crucial for mitophagy in yeast. *Dev Cell* 28: 450–458
17. Nguyen TT, Lewandowska A, Choi JY, Markgraf DF, Junker M, Bilgin M, Ejsing CS, Voelker DR, Rapoport TA, Shaw JM (2012) Gem1 and ERMES do not directly affect phosphatidylserine transport from ER to mitochondria or mitochondrial inheritance. *Traffic* 13: 880–890
18. Osman C, Haag M, Potting C, Rodenfels J, Dip PV, Wieland FT, Brugger B, Westermann B, Langer T (2009) The genetic interactome of prohibitins: coordinated control of cardiolipin and phosphatidylethanolamine by conserved regulators in mitochondria. *J Cell Biol* 184: 583–596
19. Tamura Y, Onguka O, Aiken Hobbs AE, Jensen RE, Iijima M, Claypool SM, Sesaki H (2012) Role for two conserved intermembrane space proteins, Ups1p and Up2p, in intra-mitochondrial phospholipid trafficking. *J Biol Chem* 287: 15205–15218
20. Tan T, Ozbalci C, Brugger B, Rapaport D, Dimmer KS (2013) Mcp1 and Mcp2, two novel proteins involved in mitochondrial lipid homeostasis. *J Cell Sci* 126: 3563–3574
21. Yamano K, Tanaka-Yamano S, Endo T (2010) Mdm10 as a dynamic constituent of the TOB/SAM complex directs coordinated assembly of Tom40. *EMBO Rep* 11: 187–193
22. Kopec KO, Alva V, Lupas AN (2010) Homology of SMP domains to the TULIP superfamily of lipid-binding proteins provides a structural basis for lipid exchange between ER and mitochondria. *Bioinformatics* 26: 1927–1931
23. Ah Young AP, Jiang J, Zhang J, Khoi Dang X, Loo JA, Zhou ZH, Egea PF (2015) Conserved SMP domains of the ERMES complex bind phospholipids and mediate tether assembly. *Proc Natl Acad Sci USA* 112: E3179–E3188
24. Jonikas MC, Collins SR, Denic V, Oh E, Quan EM, Schmid V, Weibezahn J, Schwappach B, Walter P, Weissman JS *et al* (2009) Comprehensive characterization of genes required for protein folding in the endoplasmic reticulum. *Science* 323: 1693–1697
25. Lahiri S, Chao JT, Tavassoli S, Wong AK, Choudhary V, Young BP, Loewen CJ, Prinz WA (2014) A conserved endoplasmic reticulum membrane protein complex (EMC) facilitates phospholipid transfer from the ER to mitochondria. *PLoS Biol* 12: e1001969
26. Murley A, Sarsam RD, Toulmay A, Yamada J, Prinz WA, Nunnari J (2015) Ltc1 is an ER-localized sterol transporter and a component of ER-mitochondria and ER-vacuole contacts. *J Cell Biol* 209: 539–548
27. Siniossoglou S, Santos-Rosa H, Rappsilber J, Mann M, Hurt E (1998) A novel complex of membrane proteins required for formation of a spherical nucleus. *EMBO J* 17: 6449–6464
28. Marzioch M, Henthorn DC, Herrmann JM, Wilson R, Thomas DY, Bergeron JJ, Solari RC, Rowley A (1999) Erp1p and Erp2p, partners for Emp24p and Erv25p in a yeast p24 complex. *Mol Biol Cell* 10: 1923–1938
29. Clark MW, Keng T, Storms RK, Zhong W, Fortin N, Zeng B, Delaney S, Ouellette BF, Barton AB, Kaback DB *et al* (1994) Sequencing of chromosome I of Saccharomyces cerevisiae: analysis of the 42 kbp SPO7-CENI-CDC15 region. *Yeast* 10: 535–541
30. Huh WK, Falvo JV, Gerke LC, Carroll AS, Howson RW, Weissman JS, O'Shea EK (2003) Global analysis of protein localization in budding yeast. *Nature* 425: 686–691
31. Sickmann A, Reinders J, Wagner Y, Joppich C, Zahedi R, Meyer HE, Schonfisch B, Perschil I, Chacinska A, Guiard B *et al* (2003) The proteome of Saccharomyces cerevisiae mitochondria. *Proc Natl Acad Sci USA* 100: 13207–13212
32. Berger KH, Sogo LF, Yaffe MP (1997) Mdm12p, a component required for mitochondrial inheritance that is conserved between budding and fission yeast. *J Cell Biol* 136: 545–553
33. Burgess SM, Delannoy M, Jensen RE (1994) MMM1 encodes a mitochondrial outer membrane protein essential for establishing and maintaining the structure of yeast mitochondria. *J Cell Biol* 126: 1375–1391
34. Dimmer KS, Fritz S, Fuchs F, Messerschmitt M, Weinbach N, Neupert W, Westermann B (2002) Genetic basis of mitochondrial function and morphology in Saccharomyces cerevisiae. *Mol Biol Cell* 13: 847–853
35. Sogo LF, Yaffe MP (1994) Regulation of mitochondrial morphology and inheritance by Mdm10p, a protein of the mitochondrial outer membrane. *J Cell Biol* 126: 1361–1373
36. Meisinger C, Rissler M, Chacinska A, Szklarz LK, Milenkovic D, Kozjak V, Schonfisch B, Lohaus C, Meyer HE, Yaffe MP *et al* (2004) The mitochondrial morphology protein Mdm10 functions in assembly of the preprotein translocase of the outer membrane. *Dev Cell* 7: 61–71
37. Thornton N, Stroud DA, Milenkovic D, Guiard B, Pfanner N, Becker T (2010) Two modular forms of the mitochondrial sorting and assembly machinery are involved in biogenesis of alpha-helical outer membrane proteins. *J Mol Biol* 396: 540–549
38. Esser K, Jan PS, Pratje E, Michaelis G (2004) The mitochondrial IMP peptidase of yeast: functional analysis of domains and identification

of Gut2 as a new natural substrate. *Mole Genet Genomics* 271: 616 – 626

39. Vogtle FN, Wortelkamp S, Zahedi RP, Becker D, Leidhold C, Gevaert K, Kellermann J, Voos W, Sickmann A, Pfanner N *et al* (2009) Global analysis of the mitochondrial N-proteome identifies a processing peptidase critical for protein stability. *Cell* 139: 428 – 439
40. Zahedi RP, Sickmann A, Boehm AM, Winkler C, Zufall N, Schonfisch B, Guiard B, Pfanner N, Meisinger C (2006) Proteomic analysis of the yeast mitochondrial outer membrane reveals accumulation of a subclass of preproteins. *Mol Biol Cell* 17: 1436 – 1450
41. Becker T, Wenz LS, Kruger V, Lehmann W, Muller JM, Goroncy L, Zufall N, Lithgow T, Guiard B, Chacinska A *et al* (2011) The mitochondrial import protein Mim1 promotes biogenesis of multispanning outer membrane proteins. *J Cell Biol* 194: 387 – 395
42. Papic D, Krumpe K, Dukanovic J, Dimmer KS, Rapaport D (2011) Multispan mitochondrial outer membrane protein Ugo1 follows a unique Mim1-dependent import pathway. *J Cell Biol* 194: 397 – 405
43. Wenz LS, Opalinski L, Schuler MH, Ellenrieder L, Ieva R, Bottinger L, Qiu J, van der Laan M, Wiedemann N, Guiard B *et al* (2014) The presequence pathway is involved in protein sorting to the mitochondrial outer membrane. *EMBO Rep* 15: 678 – 685
44. Papic D, Elbaz-Alon Y, Koerdt SN, Leopold K, Worm D, Jung M, Schuldiner M, Rapaport D (2013) The role of Djp1 in import of the mitochondrial protein Mim1 demonstrates specificity between a cochaperone and its substrate protein. *Mol Cell Biol* 33: 4083 – 4094
45. Meisinger C, Ryan MT, Hill K, Model K, Lim JH, Sickmann A, Muller H, Meyer HE, Wagner R, Pfanner N (2001) Protein import channel of the outer mitochondrial membrane: a highly stable Tom40-Tom22 core structure differentially interacts with preproteins, small tom proteins, and import receptors. *Mol Cell Biol* 21: 2337 – 2348
46. Gevorkyan-Airapetov L, Zohary K, Popov-Celeketic D, Mapa K, Hell K, Neupert W, Azem A, Mokranjac D (2009) Interaction of Tim23 with Tim50 Is essential for protein translocation by the mitochondrial TIM23 complex. *J Biol Chem* 284: 4865 – 4872
47. Waizenegger T, Schmitt S, Zivkovic J, Neupert W, Rapaport D (2005) Mim1, a protein required for the assembly of the TOM complex of mitochondria. *EMBO Rep* 6: 57 – 62
48. Ishikawa D, Yamamoto H, Tamura Y, Moritoh K, Endo T (2004) Two novel proteins in the mitochondrial outer membrane mediate beta-barrel protein assembly. *J Cell Biol* 166: 621 – 627
49. Dimmer KS, Papic D, Schumann B, Sperl D, Krumpe K, Walther DM, Rapaport D (2012) A crucial role for Mim2 in the biogenesis of mitochondrial outer membrane proteins. *J Cell Sci* 125: 3464 – 3473
50. Hulett JM, Lueder F, Chan NC, Perry AJ, Wolynec P, Likic VA, Gooley PR, Lithgow T (2008) The transmembrane segment of Tom20 is recognized by Mim1 for docking to the mitochondrial TOM complex. *J Mol Biol* 376: 694 – 704
51. Hanekamp T, Thorsness MK, Rebbapragada I, Fisher EM, Seebart C, Darland MR, Coxbill JA, Updike DL, Thorsness PE (2002) Maintenance of mitochondrial morphology is linked to maintenance of the mitochondrial genome in Saccharomyces cerevisiae. *Genetics* 162: 1147 – 1156
52. Elbaz-Alon Y, Eisenberg-Bord M, Shinder V, Stiller SB, Shimoni E, Wiedemann N, Geiger T, Schuldiner M (2015) Lam6 Regulates the Extent of Contacts between Organelles. *Cell Rep* 12: 7 – 14
53. Yamamoto H, Fukui K, Takahashi H, Kitamura S, Shiota T, Terao K, Uchida M, Esaki M, Nishikawa S, Yoshihisa T *et al* (2009) Roles of Tom70 in import of presequence-containing mitochondrial proteins. *J Biol Chem* 284: 31635 – 31646
54. Song J, Tamura Y, Yoshihisa T, Endo T (2014) A novel import route for an N-anchor mitochondrial outer membrane protein aided by the TIM23 complex. *EMBO Rep* 15: 670 – 677
55. Okatsu K, Kimura M, Oka T, Tanaka K, Matsuda N (2015) Unconventional PINK1 localization to the outer membrane of depolarized mitochondria drives Parkin recruitment. *J Cell Sci* 128: 964 – 978
56. Green SR, Moehle CM (2001) Media and culture of yeast. *Curr Protoc Cell Biol* Chapter 1: Unit 1.6
57. Wach A, Brachat A, Alberti-Segui C, Rebischung C, Philippsen P (1997) Heterologous HIS3 marker and GFP reporter modules for PCR-targeting in Saccharomyces cerevisiae. *Yeast* 13: 1065 – 1075
58. Wach A, Brachat A, Pohlmann R, Philippsen P (1994) New heterologous modules for classical or PCR-based gene disruptions in Saccharomyces cerevisiae. *Yeast* 10: 1793 – 1808
59. Walther DM, Papic D, Bos MP, Tommassen J, Rapaport D (2009) Signals in bacterial beta-barrel proteins are functional in eukaryotic cells for targeting to and assembly in mitochondria. *Proc Natl Acad Sci USA* 106: 2531 – 2536
60. Daum G, Bohni PC, Schatz G (1982) Import of proteins into mitochondria. Cytochrome b2 and cytochrome c peroxidase are located in the intermembrane space of yeast mitochondria. *J Biol Chem* 257: 13028 – 13033
61. Graham JM (2001) Purification of a crude mitochondrial fraction by density-gradient centrifugation. *Curr Protoc Cell Biol* Chapter 3: Unit 3.4
62. Schagger H (2002) Respiratory chain supercomplexes of mitochondria and bacteria. *Biochim Biophys Acta* 1555: 154 – 159
63. Westermann B, Neupert W (2000) Mitochondria-targeted green fluorescent proteins: convenient tools for the study of organelle biogenesis in Saccharomyces cerevisiae. *Yeast* 16: 1421 – 1427
64. Bauer C, Herzog V, Bauer MF (2001) Improved Technique for Electron Microscope Visualization of Yeast Membrane Structure. *Microsc Microanal* 7: 530 – 534
65. Ozbalci C, Sachsenheimer T, Brugger B (2013) Quantitative analysis of cellular lipids by nano-electrospray ionization mass spectrometry. *Methods Mol Biol* 1033: 3 – 20
66. Ejsing CS, Sampaio JL, Surendranath V, Duchoslav E, Ekroos K, Klemm RW, Simons K, Shevchenko A (2009) Global analysis of the yeast lipidome by quantitative shotgun mass spectrometry. *Proc Natl Acad Sci USA* 106: 2136 – 2141

Sinzel et al. Appendix

Table of Contents

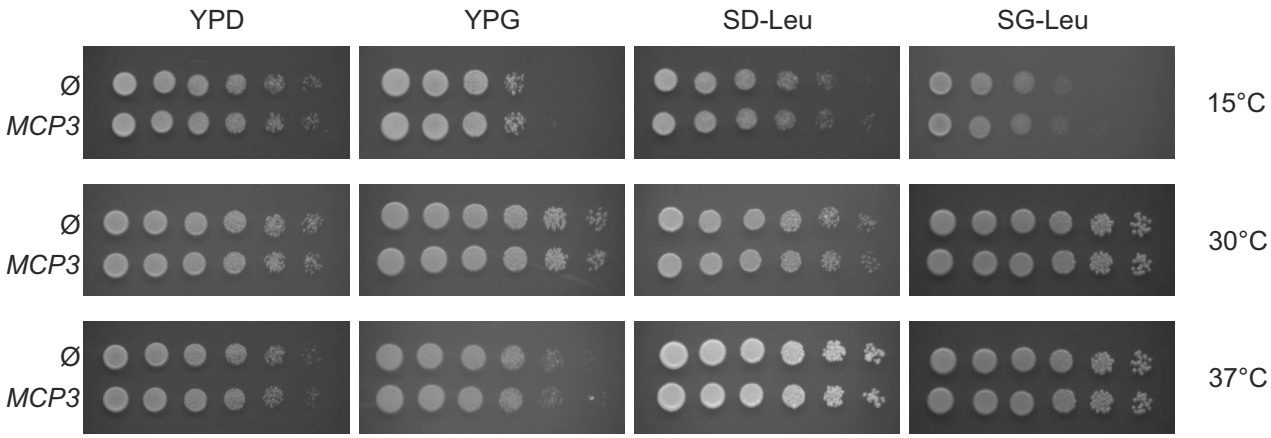

Appendix Figure S1. Over-expression of Mcp3 has no influence on the growth of yeast cells. Wild-type cells were transformed with the empty plasmid pYX142 (Ø) or pYX142 encoding Mcp3 (*MCP3*). Cells were grown to an OD_{600} of 1.0 in minimal medium lacking leucine and spotted in a 1:5 dilution series on YPD, YPG, SD-Leu or SG-Leu plates directly and in a 1:5 dilution series. Plates were incubated at the indicated temperatures.

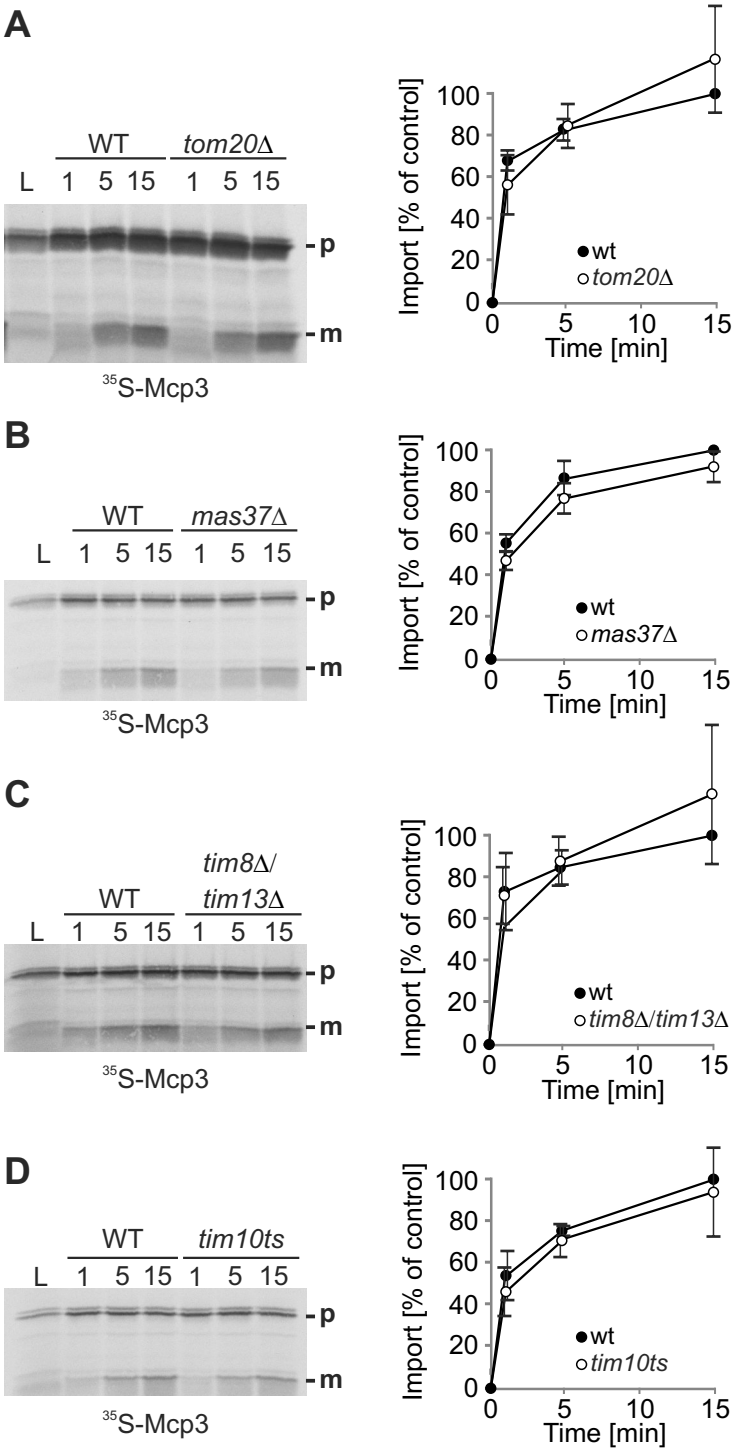

Appendix Figure S2. Import of Mcp3 is independent of receptor Tom20, TOB subunit Mas37/Sam37 and the IMS import chaperones Tim8/10/13.

(A) Mitochondria from wild-type and *tom20*Δ cells were isolated and incubated with radiolabelled Mcp3 for the indicated time periods (1, 5, 15 min). After import mitochondria were reisolated and analysed by SDS-PAGE and autoradiography. Bands corresponding to the mature (m) form were quantified. Import after 15 min into wild-type mitochondria was set to 100%. The mean with standard deviations of three independent experiments (n=3) is depicted in the graph.

(B) Mitochondria from wild-type and mas37Δ cells were isolated. Import and analysis was performed as in (A).

(C) Mitochondria from wild-type and *tim8*Δ/*tim13*Δ cells were isolated. Import and analysis was performed as in (A).

(D) Mitochondria from wild-type and the temperature sensitive mutant *tim10-1* (*tim10ts*) were isolated after growth at 24°C. Prior to import mitochondria were incubated for 15 min at the non-permissive temperature. Import and analysis were performed as in (A).

l, 20% of radiolabelled precursor protein used in each import reaction; p, precursor; m, mature form.

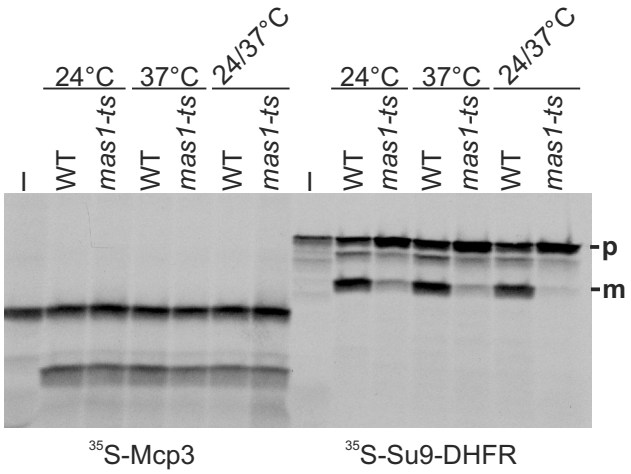

Appendix Figure S3. MPP is not responsible for processing of Mcp3. Mitochondria from wild-type (WT) and *mas1-ts* cells were isolated after growth at the permissive temperature 24°C (24°C, 24/37°C) or the non-permissive temperature 37°C (37°C). Next mitochondria were incubated with radiolabelled Mcp3 (^{35}S-Mcp3, left part) without preincubation at the non-permissive temperature (24°C, 37°C) or with in vitro shift for 15 min to 37°C prior to the import reaction (24/37°C). Radiolabelled Su9-DHFR as bona fide substrate of MPP was applied in the same way as control for impaired MPP function in mitochondria of the mutant strain (right part). After import mitochondria were reisolated and analysed by SDS-PAGE and autoradiography. I, 20% of radiolabelled precursor protein used in each import reaction; p, precursor; m, mature form.

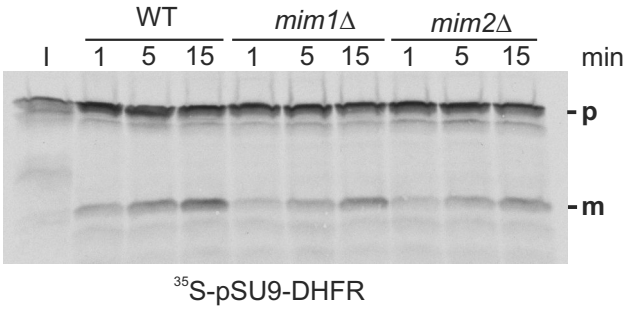

Appendix Figure S4. Mitochondria lacking Mim1 or Mim2 display an import defect for matrix destined proteins. Mitochondria from wild-type (WT), *mim1*Δ and *mim2*Δ cells were isolated and incubated with radiolabelled ^{35}S-pSu9-DHFR for the indicated time periods (1, 5, 15 min). After import mitochondria were reisolated and analysed by SDS-PAGE and autoradiography. Bands corresponding to the mature (m) and precursor (p) form are indicated.

Appendix Table 1: *S. cerevisiae* and *E. coli* strains used in this study

name	genotype	reference
S. cerevisiae		
W303a	MAT a; *ade2-1; can1-100; his3-11; leu2-3,112; trp1Δ2; ura3-52*	(Thomas and Rothstein, 1989)
W303α	MAT α; *ade2-1; can1-100; his3-11; leu2-3,112; trp1Δ2; ura3-52*	(Thomas and Rothstein, 1989)
YPH499	MAT a; *ade2-101; his3Δ200; leu2Δ1; ura3-52; trp1Δ63; lys2-801*	(Sikorski and Hieter, 1989)
BY4741	Mat a; *his3*Δ1; *leu*2Δ0; *met*15Δ0; *ura3*Δ0	Euroscarf (http://web.uni-frankfurt.de/fb15/mikro/euroscarf/
YMS018	W303a; *fun14*Δ::Kan	this study
YMS019	W303a; *fun14*Δ::His3	this study
YKD291	W303a; *mdm10*Δ::His3	(Tan *et al.*, 2013)
YKD461	W303a; *mmm1*Δ::Kan	(Tan *et al.*, 2013)
YKD227	W303a; *mmm2*Δ::Kan	(Tan *et al.*, 2013)
YKD301	W303a; *mdm12*Δ::His3	(Tan *et al.*, 2013)
YKD303	W303a; *mim2*Δ::His3	(Dimmer *et al.*, 2012)
YKD145	W303a; *mim1*Δ::Kan	(Dimmer *et al.*, 2012)
YKD132	W303α; *tom20*Δ::His3	(Muller et al., 2011)
YDR251	YPH499; *mas37*Δ::His3	(Habib et al., 2005)
2535	YPH499; *tom40*Δ::Kan; pFL39-*TOM40*	(Wenz *et al.*, 2014)
3007; tom40-2522	YPH499; *tom40*Δ::Kan; pFL39-*TOM40*-25	(Wenz *et al.*, 2014)
pTIM23t	YPH499; *tim23*Δ::Kan; pRS315-p*TIM23*t	(Gevorkyan-Airapetov et al., 2009)
pTIM23-Y70A,L71A-t	YPH499; *tim23*Δ::Kan; pRS315-p*TIM23*-Y70AL71A-t	(Gevorkyan-Airapetov et al., 2009)
YMS063	BY4741; *fun14*Δ::Kan	Euroscarf
YMS087	BY4741; *atp23*Δ::Kan	Euroscarf
YMS102	BY4741; *pcp1*Δ::Kan	Euroscarf
YMS103	BY4741; *prd1*Δ::Kan	Euroscarf
YMS106	BY4741; *yta12*Δ::Kan	Euroscarf
YMS107	BY4741; *pim1*Δ::Kan	Euroscarf
YMS108	BY4741; *yta10*Δ::Kan	Euroscarf
YMS109	BY4741; *imp1*Δ::Kan	Euroscarf
YMS110	BY4741; *imp2*Δ::Kan	Euroscarf
YMS111	BY4741; *oct1*Δ::Kan	Euroscarf
YMS116	BY4741; *yme1*Δ::Kan	Euroscarf
JSY7452	MAT α *ade2-1; can1-100; his3-11;15; leu2-3; trp1-1; ura3-1*	(Kondo-Okamoto *et al.*, 2008)
JSY8283	JSY7452; *tom70*Δ::Trp1; *tom71*Δ::His3	(Kondo-Okamoto *et al.*, 2008)
GA74-1A	MAT a *ade8*; *his3*; *leu2*; *trp1*; *ura3*	(Koehler et al., 1998)
CK14	GA74D; *tim10*Δ::His3; *tim10-1*:Trp1	(Koehler et al., 1998)
MB2	MAT a/α, ADE2/*ade2-101*^{ochre}; *his3*/*his3-Δ200*; *leu2*/*leu2-Δ1*; *lys2-801*^{amber}/*lys2-801*^{amber}; *trp1-289*/TRP1; *ura3-52*/*ura3-52*	(Maarse et al., 1992)
TU008/ YDR2628	MB2; *tim8*Δ::Ura3; *tim13*Δ::His3	(Paschen et al., 2000)
MYM104	MAT α; Ura3-52; trp1-1; leu2-3; leu2-112; his3-11; his3-15	(Witte et al., 1988)
MYM105	MYM104; mas1-ts	(Witte et al., 1988)
YTW224	YPH499; *TOM22-10His*	(Meisinger et al., 2001)
YIA30	W303a; *yme*Δ*1*::Kan	(Arnold et al., 2006)
YKD870	W303a; *yme1*Δ::Kan; *mim2*Δ::His3	this study
E. coli		
MS094	W3110; pVG18-MPPHis	(Geli, 1993)
BL21(DE3)		Thermofisher Scientific, Darmstadt, Germany
MH1		NEB biolabs, Frankfurt, Germany

References:

Arnold, I., M. Wagner-Ecker, W. Ansorge, and T. Langer. 2006. Evidence for a novel mitochondria-to-nucleus signalling pathway in respiring cells lacking i-AAA protease and the ABC-transporter Mdl1. *Gene*. 367:74-88.

Dimmer, K.S., D. Papic, B. Schumann, D. Sperl, K. Krumpe, D.M. Walther, and D. Rapaport. 2012. A crucial role for Mim2 in the biogenesis of mitochondrial outer membrane proteins. *Journal of cell science*. 125:3464-3473.

Geli, V. 1993. Functional reconstitution in Escherichia coli of the yeast mitochondrial matrix peptidase from its two inactive subunits. *Proc Natl Acad Sci U S A*. 90:6247-6251.

Gevorkyan-Airapetov, L., K. Zohary, D. Popov-Celeketic, K. Mapa, K. Hell, W. Neupert, A. Azem, and D. Mokranjac. 2009. Interaction of Tim23 with Tim50 Is essential for protein translocation by the mitochondrial TIM23 complex. *The Journal of biological chemistry*. 284:4865-4872.

Habib, S.J., T. Waizenegger, M. Lech, W. Neupert, and D. Rapaport. 2005. Assembly of the TOB complex of mitochondria. *The Journal of biological chemistry*. 280:6434-6440.

Koehler, C.M., E. Jarosch, K. Tokatlidis, K. Schmid, R.J. Schweyen, and G. Schatz. 1998. Import of mitochondrial carriers mediated by essential proteins of the intermembrane space. *Science*. 279:369-373.

Kondo-Okamoto, N., J.M. Shaw, and K. Okamoto. 2008. Tetratricopeptide repeat proteins Tom70 and Tom71 mediate yeast mitochondrial morphogenesis. *EMBO reports*. 9:63-69.

Maarse, A.C., J. Blom, L.A. Grivell, and M. Meijer. 1992. MPI1, an essential gene encoding a mitochondrial membrane protein, is possibly involved in protein import into yeast mitochondria. *The EMBO journal*. 11:3619-3628.

Meisinger, C., M.T. Ryan, K. Hill, K. Model, J.H. Lim, A. Sickmann, H. Muller, H.E. Meyer, R. Wagner, and N. Pfanner. 2001. Protein import channel of the outer mitochondrial membrane: a highly stable Tom40-Tom22 core structure differentially interacts with preproteins, small tom proteins, and import receptors. *Molecular and cellular biology*. 21:2337-2348.

Muller, J.E., D. Papic, T. Ulrich, I. Grin, M. Schutz, P. Oberhettinger, J. Tommassen, D. Linke, K.S. Dimmer, I.B. Autenrieth, and D. Rapaport. 2011. Mitochondria can recognize and assemble fragments of a beta-barrel structure. *Mol Biol Cell*. 22:1638-1647.

Paschen, S.A., U. Rothbauer, K. Kaldi, M.F. Bauer, W. Neupert, and M. Brunner. 2000. The role of the TIM8-13 complex in the import of Tim23 into mitochondria. *The EMBO journal*. 19:6392-6400.

Sikorski, R.S., and P. Hieter. 1989. A system of shuttle vectors and yeast host strains designed for efficient manipulation of DNA in Saccharomyces cerevisiae. *Genetics*. 122:19-27.

Tan, T., C. Ozbalci, B. Brugger, D. Rapaport, and K.S. Dimmer. 2013. Mcp1 and Mcp2, two novel proteins involved in mitochondrial lipid homeostasis. *Journal of cell science*. 126:3563-3574.

Thomas, B.J., and R. Rothstein. 1989. Elevated recombination rates in transcriptionally active DNA. *Cell*. 56:619-630.

Wenz, L.S., L. Opalinski, M.H. Schuler, L. Ellenrieder, R. Ieva, L. Bottinger, J. Qiu, M. van der Laan, N. Wiedemann, B. Guiard, N. Pfanner, and T. Becker. 2014. The presequence pathway is involved in protein sorting to the mitochondrial outer membrane. *EMBO reports*. 15:678-685.

Witte, C., R.E. Jensen, M.P. Yaffe, and G. Schatz. 1988. MAS1, a gene essential for yeast mitochondrial assembly, encodes a subunit of the mitochondrial processing protease. *The EMBO journal*. 7:1439-1447.

Appendix Table 2. Primers used in this study

Primers for gene-targeting		
name	sequence	remarks
PFa-For-Fun14K	5' ACG CTA GAG GGG CAA GAA GGA AGA ACT TAA AAT AAT AGG TGT AAA *CGT ACG CTG*	amplification of KanMX4 or HISMX6 cassette
PFa-Rev-Fun14K	5' AAC GAA AGA ATA TAA CCC TCG TTT ATA TCT GGT CAT TTG TCT TGC *ATC GAT GAA*	amplification of KanMX4 or HISMX6 cassette
Primers for cloning		
name	sequence	remarks
FpYX-Fun14	5' GGG GAA TTC ATG ACT TTG GCT TTT AAT ATG CA	amplification of *MCP3* ORF 5' contains *Eco*RI restriction site
RpYX-Fun14	5' GGG AAG CTT TCA TTT GTT AGC ATT TAA ACT TGC	amplification of MCP3 ORF 3' contains *Hin*dIII restriction site
FUN14intHArev	5' GGG GGA TCC *TGC GTA GTC AGG CAC ATC ATA CGG ATA* CCC TAA AGA ATC ATT GAA TAT CA	amplification of *MCP3* presequence 3' contains *BamH*I restriction site and encodes the HA tag
Fun14intHAfwd	5' GGG GGA TCC GCA GCT GTC AAA CAA CAG G	amplification of *MCP3* mature part 5' (starting 4 codons downstream of predicted Imp1 cleavage site) contains *BamH*I restriction site
D70G_Fun14fwd	5' GAT ATT CAA TGG TTC TTT AGG G	site directed mutagenesis for D70G amino acid exchange (sense)
D70G_Fun14rev	5' CTA TAA GTT ACC AAG AAA TCC C	site directed mutagenesis for D70G amino acid exchange (antisense)
F14PromFwd	5' GGG GAG CTC GTG GCT TAA AGA CGA TAA TGC	amplification of *MCP3* promoter 5' contains *Sac*I restriction site
F14PromRev	5' GGG GAA TTC TTT ACA CCT ATT ATT TTA AGT TCT T	amplification of *MCP3* promoter 3' contains *Eco*RI restriction site
F14TermFwd	5' GGG AAG CTT GCAAGA CAA ATG ACC AGA TAT A	amplification of *MCP3* terminator 5' contains *Hin*dIII restriction site
F14TermRev	5' GGG GTC GAC AGC GTT GAA AAA GGT AGA AAT TA	amplification of *MCP3* terminator 3' contains *Sal*I restriction site
delta-TMD1-Arev	5' GGG GGA TCC CTG CTT GTG ACT ACT TAT TTT G	amplification of aa 1-105 coding sequence of MCP3, contains *BamH*I restriction site
delta-TMD1-Bfwd	5' GGG GGA TCC TAT GTC GGT ATT ACA AGC ATG	amplification of aa 129-198 coding sequence of MCP3, contains *BamH*I restriction site
delta-TMD2-rev	5' GGG AAG CTT TTA ATC AAT AAG CAG TTT CTT CAA GT	amplification of aa 1-171 coding sequence of MCP3, contains *Hin*dIII restriction site
RpYX-Fun14HA	5' GGG AAG CTT TTT GTT AGC ATT TAA ACT TGC TAA	amplification of MCP3 ORF 3' contains *Hin*dIII restriction site, stop codon omitted for fusion with HA-tag

Expanded View Figures

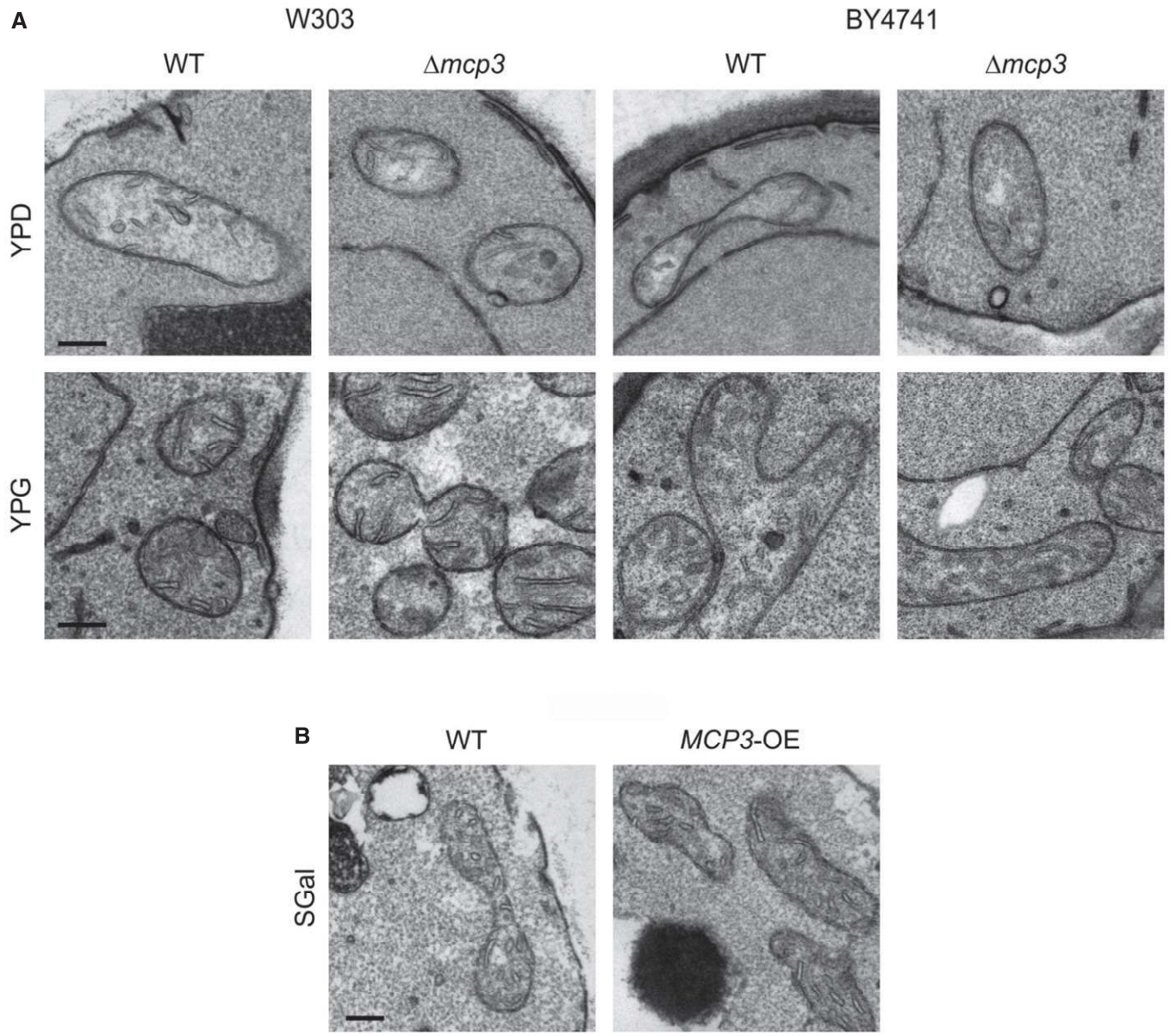

Figure EV1. Altered levels of Mcp3 have no effect on mitochondrial ultrastructure.

A WT and *mcp3*Δ cells in two different genetic backgrounds (W303 and BY4741) were grown in glucose (YPD) or glycerol (YPG) containing medium and analysed by thin-section transmission electron microscopy. Representative images of mitochondria are shown. Scale bars, 200 nm.

B WT cells carrying an empty plasmid (WT) and cells overexpressing *MCP3* from a plasmid under control of the *TPI* promoter (*MCP3*-OE) were grown in galactose-containing minimal medium (SGal) and analysed by thin-section transmission electron microscopy. Representative images of mitochondria are shown. Scale bar, 200 nm.

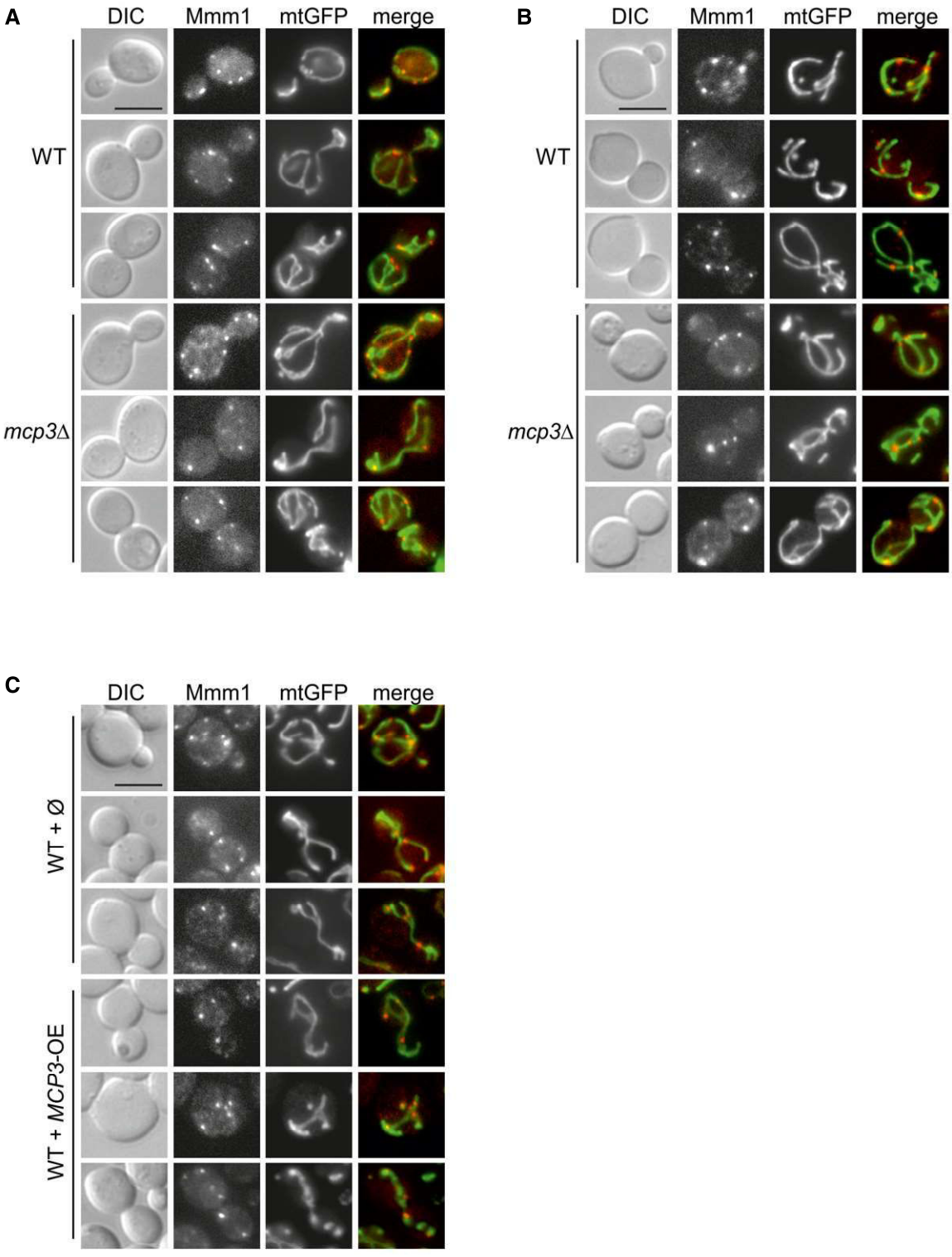

Figure EV2. Altered levels of Mcp3 have no effect on ERMES foci formation and colocalization with mitochondria.

A, B WT and *mcp3*Δ cells (from BY4741 (A) or W303 (B) background) expressing mitochondrially targeted GFP (mtGFP) and RFP-tagged Mmm1 were grown to mid-logarithmic phase and then analysed by fluorescence microscopy. Representative images are shown. Scale Bars, 5 μm.

C WT cells harbouring an empty plasmid or a plasmid overexpressing Mcp3 (BY4741 background) were transformed with plasmids encoding mitochondrially targeted GFP (mtGFP) and RFP-tagged Mmm1 and were analysed as in (A). Scale Bar, 5 μm.

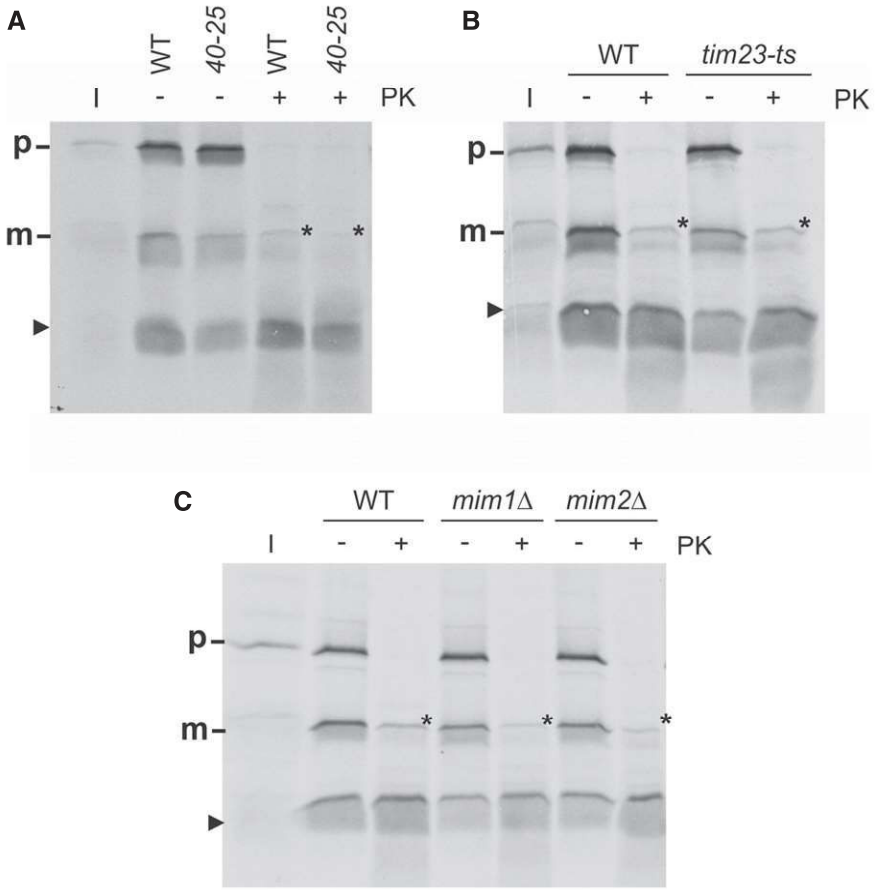

Figure EV3. Mcp3 precursor is degraded by PK *in vitro* if it does not reach the inter membrane space.

A Mitochondria from wild-type and *tom40-25* cells were isolated and incubated with radiolabelled Mcp3 for 15 min. After import, mitochondria were reisolated, left untreated or incubated with proteinase K (PK) and analysed by SDS–PAGE and autoradiography.

B Mitochondria from wild-type and *tim23ts* cells were isolated and incubated with radiolabelled Mcp3 for 15 min. Analysis was performed as in (A).

C Mitochondria from wild-type and *mim1*Δ or *mim2*Δ cells were isolated and incubated with radiolabelled Mcp3 for 15 min. Analysis was performed as in (A).

Data information: The mature (m) and precursor (p) form of Mcp3 are indicated. The arrowhead marks an additional band of the size of the cleaved N-terminus of Mcp3. The asterisk depicts a fragment of the size of mature Mcp3 that is PK protected.

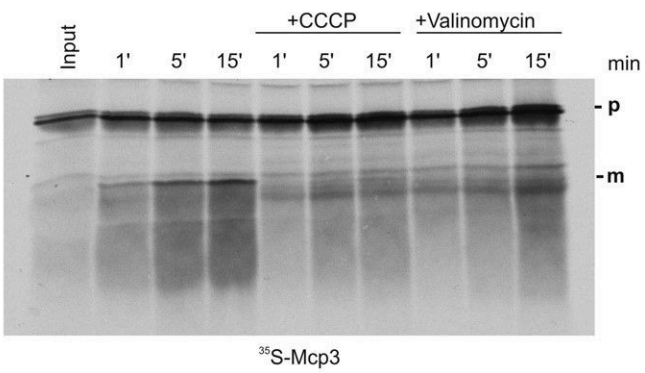

Figure EV4. Import of Mcp3 is dependent on the mitochondrial membrane potential.

Mitochondria isolated from wild-type yeast cells were incubated with radiolabelled precursor protein Mcp3 for the indicated time periods (1, 5 or 15 min) in the absence or presence of CCCP or valinomycin. After import, mitochondria were reisolated and analysed by SDS–PAGE and autoradiography. Input, 20% of radiolabeled precursor applied in the reaction.

© 2014. Published by The Company of Biologists Ltd | Journal of Cell Science (2014) 127, 3373–3381 doi:10.1242/jcs.149799

RESEARCH ARTICLE

Yeast phospholipid biosynthesis is linked to mRNA localization

Orit Hermesh[1], Christian Genz[1], Ido Yofe[2], Monika Sinzel[1], Doron Rapaport[1], Maya Schuldiner[2] and Ralf-Peter Jansen[1,*]

ABSTRACT

Regulation of the localization of mRNAs and local translation are universal features in eukaryotes and contribute to cellular asymmetry and differentiation. In *Saccharomyces cerevisiae*, localization of mRNAs that encode membrane proteins requires the She protein machinery, including the RNA-binding protein She2p, as well as movement of the cortical endoplasmic reticulum (cER) to the yeast bud. In a screen for ER-specific proteins necessary for the directional transport of *WSC2* and *EAR1* mRNAs, we have identified enzymes that are involved in phospholipid metabolism. Loss of the phospholipid methyltransferase Cho2p, which showed the strongest impact on mRNA localization, disturbs mRNA localization, as well as ER morphology and segregation, owing to an increase in the amount of cellular phosphatidylethanolamine (PtdEtn). Mislocalized mRNPs containing She2p colocalize with aggregated cER structures, suggestive of the entrapment of mRNA and She2p by the elevated PtdEtn level. This was confirmed by the elevated binding of She2p to PtdEtn-containing liposomes. These findings underscore the importance of ER membrane integrity in mRNA transport.

KEY WORDS: mRNA localization, phospholipids, *CHO2*, *SHE2*, *Saccharomyces cerevisiae*

INTRODUCTION

Control of the localization of mRNA allows spatial control of gene expression and contributes to the generation of cellular asymmetry or synaptic plasticity (Holt and Bullock, 2009; Martin and Ephrussi, 2009). Localized mRNAs are generally transported as RNA–protein complexes (RNPs) to their destination sites, where they become translationally active, allowing site-specific protein synthesis (Besse and Ephrussi, 2008; Martin and Ephrussi, 2009).

In budding yeast, >50 transcripts are selectively transported to the bud (Aronov et al., 2007; Oeffinger et al., 2007; Shepard et al., 2003), among them *ASH1* mRNA, which encodes a daughter-cell-specific transcriptional repressor of the *HO* endonuclease gene (Long et al., 1997). Localization of *ASH1* and the other mRNAs requires a set of proteins that includes the RNA-binding proteins She2p (Böhl et al., 2000; Niessing et al., 2004) and She3p (Böhl et al., 2000; Müller et al., 2011), as well as the myosin-V motor Myo4p (Böhl et al., 2000; Krementsova et al., 2011).

Many bud-localized mRNAs encode membrane or membrane-associated proteins (Aronov et al., 2007; Shepard et al., 2003) that are translated at the cytoplasmic face of the ER. Yeast contains two major types of ER – the perinuclear ER, which is continuous with the nuclear envelope, and the cortical ER (cER, also called plasma-membrane-attached ER), which is a meshwork of tubular ER structures underlying the plasma membrane (Du et al., 2004). During budding, tubules migrate from the mother cell into the bud, followed by the spreading of cER along the bud cortex (Du et al., 2004; West et al., 2011). Several observations indicate that the localization of a subset of mRNAs to the bud is coordinated with cER segregation. Firstly, mutations in several genes affect both processes. Mutations in Myo4p and She3p affect both ER inheritance by the daughter cell and mRNA localization (Estrada et al., 2003; Long et al., 1997). Similar observations have been made for genes that are essential for the early steps of ER inheritance, for cER docking at the bud tip (Aronov et al., 2007; Fundakowski et al., 2012) or for the formation of ER tubules (Fundakowski et al., 2012). Furthermore, the RNA-binding protein She2p co-fractionates with ER membranes and can bind to protein-free liposomes with a membrane curvature similar to that of ER tubules, suggesting that this protein connects localized mRNAs to ER (Genz et al., 2013). These findings led to the idea that localized mRNAs encoding membrane or ER proteins travel to the bud by associating with cER tubules. Similar coordinated distribution of ER and mRNAs have also been reported in other biological systems. For example, in ascidians, macho1 and HrPEM mRNAs tightly colocalize with the cER at different stages of redistribution from egg to zygote (Sardet et al., 2005). In the claw frog *Xenopus laevis*, Vg1 mRNA localization patterns highly overlap with those of ER markers at different stages of the oocyte development (Kloc and Etkin, 1995).

In order to gain more insight specifically into the mechanism and the determinants of ER-dependent mRNA localization to the yeast bud, we aimed to identify novel factors required for this type of mRNA localization. We designed a visual screen to allow us to analyze the localization pattern of two early-expressed mRNAs, *WSC2* and *EAR1*, in a collection of ER mutant strains. Here, we report the identification of several novel genes whose deletion affects the localization of *WSC2* and *EAR1*, and we show how defects in lipid biosynthesis lead to 'road blocks' in mRNA transport to the bud on ER tubules.

RESULTS

Identification of novel genes required for mRNA localization in yeast

Genetic screens to uncover proteins required for mRNA localization have previously been performed using *ASH1* mRNA as a substrate (Jansen et al., 1996; Sil and Herskowitz, 1996). However, several proteins needed for proper ER morphology and segregation that did not affect *ASH1* did affect the localization of mRNAs encoding membrane-bound proteins, including *WSC2*, *IST2* and *EAR1*. The differential requirements suggest that genetic

[1]Interfaculty Institute of Biochemistry, Universität Tübingen, 72076 Tübingen, Germany. [2]Department of Molecular Genetics, Weizmann Institute of Science, Rehovot 7610001, Israel.

*Author for correspondence (ralf.jansen@uni-tuebingen.de)

Received 15 January 2014; Accepted 20 May 2014

Journal of Cell Science (2014) 127, 3373–3381 doi:10.1242/jcs.149799

screens for mutants affecting *ASH1* localization (Jansen et al., 1996; Sil and Herskowitz, 1996) might have missed genes required for regulating the localization of mRNAs encoding membrane proteins. We therefore performed a visual screen for mutants that mislocalize *WSC2* or *EAR1* mRNAs, which are expressed at early cell cycle stages when ER segregation occurs. To mark the mRNAs, we integrated bacteriophage MS2 loops into their 3′UTRs (producing *WSC2-MS2L* and *EAR1-MS2L*). These mRNAs were coexpressed with MS2-binding protein (MS2CP) fused to 3×GFP, leading to specific labeling of the RNP granules that include these mRNAs. We limited the screen to a collection of deletion and hypomorphic mutants of essential and non-essential genes with the gene ontology term 'endoplasmic reticulum', i.e. genes that code for proteins that localize to the ER or have a function related to the ER (Fig. 1). A list of the genes that were analyzed (489 in total) is provided (supplementary material Tables S1 and S2). Two parallel screens were performed, which allowed us to validate our results in two different systems and to check the feasibility of a large-scale screen. In the first screen, plasmids carrying either *WSC2-MS2L* or *EAR1-MS2L* were co-transformed with a plasmid expressing MS2CP–3×GFP into deletion mutants, followed by manual screening for RNA localization defects (Fig. 1A). In the parallel automated screen, MS2CP–3×GFP under the control of a *MET25* promoter was integrated into the yeast genome at the *HO* locus. After transformation with *WSC2-MS2L* or *EAR1-MS2L* plasmids, the yeast were crossed with mutants carrying deletions of ER-related genes, and haploid cells were selected that carried the deletion mutation, the *MS2CP-3×GFP* gene and the corresponding plasmid (Giaever et al., 2002) (Fig. 1B). These cells were analyzed by automated fluorescence microscopy as described in Materials and Methods. The manual and automated screens revealed 45 and 24 mutants with a potential localization defect. These mutants were subjected to a second manual screen to assess the effect on localization in ≥100 cells per mutant. We observed that several mutants displayed a different mRNP mislocalization phenotype than that of the *she* mutants. Whereas the latter display an exclusive accumulation of mRNPs in the mother cell (Fig. 2A), the new mutants contained mRNPs in both the mother and the daughter cell. In neither case did we observe an exclusive localization to the bud as seen in wild-type cells. Such symmetric distribution of mRNPs (subsequently referred to as 'mislocalization') was observed following the deletion of 13 non-essential genes (Table 1). In order to obtain quantitative data, we divided cells into two classes, cells with exclusively bud-localized mRNPs and cells with symmetric distribution of mRNPs. Throughout this work we display the percentage of cells showing the mislocalization phenotype as defined above. The genes identified in this screen included genes coding for proteins required for vesicle coat formation, like *CHC1* (Gurunathan et al., 2002) and *SFB3* (Miller et al., 2002), genes affecting lipid metabolism, including phosphatidylethanolamine methyltransferase (*CHO2*, also known as *PEM1*; Kodaki and Yamashita, 1989), phospholipase C (*PLC1*; Flick and Thorner, 1993), phosphatidylinositol 3-kinase (*VPS34*; Auger et al., 1989), the transcriptional repressor of phospholipid synthesis genes *OPI1* (Wagner et al., 1999), the long-chain base-1-phosphate phosphatase (*LCB3*; Mandala et al., 1998) and an activator of serine palmitoyltransferase, *TSC3* (Gable et al., 2000). Furthermore, we found that deletion of *ICE2*, which is involved in cER inheritance and morphology (Estrada de Martin et al., 2005; Estrada et al., 2003), and of an uncharacterized open reading frame (ORF) (*YGL007C-A*) also influenced the localization of *WSC2-MS2L* and *EAR1-MS2L*. In contrast to cells of the *she2Δ* strain, of which 83.3% showed *WSC2-MS2L* mRNP mislocalization and 96.6% showed *EAR1-MS2L* mRNP mislocalization, the mislocalization was less pronounced in the mutant strains identified in this screen. Because we observed the strongest mislocalization of *WSC2* and *EAR1* in cells lacking *CHO2* (56% and 61% of cells showed mislocalization, respectively) we focused on this gene for further analysis.

Loss of Cho2p disrupts RNA localization and cER morphology

CHO2 encodes phosphatidylethanolamine N-methyltransferase (Enzyme Commission number 2.1.1.17), a key enzyme in phosphatidylcholine biosynthesis (Kodaki and Yamashita, 1989; Summers et al., 1988). *Δcho2* cells have *WSC2-MS2L* or *EAR1-MS2L* mRNPs in the mother cell and bud, indicating that only a fraction of the corresponding mRNA pool is correctly localized (Fig. 2A). By contrast, wild-type cells exclusively accumulate MS2L-tagged mRNP particles in the bud, whereas cells lacking She2p (Fig. 2A), She3p or Myo4p (Bertrand et al., 1998; Fundakowski et al., 2012) accumulate mRNPs only in the mother cell. In order to rule out the possibility that mRNA

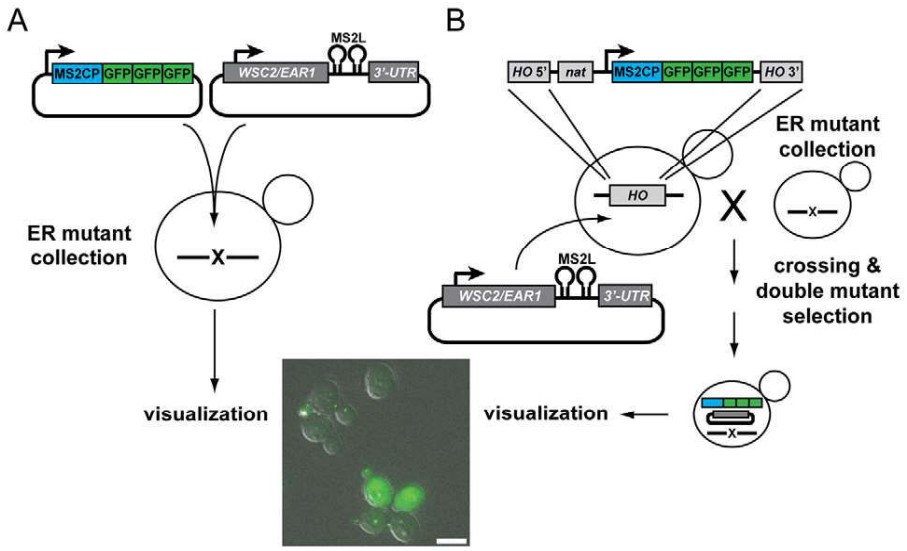

Fig. 1. Overview of microscopic screens for systematic detection of mRNA localization mutants. (A) A collection of mutants with deletions in ER-related genes was transformed with constructs allowing *in vivo* detection of *MS2L*-tagged *WSC2* or *EAR1* mRNA before subjecting them to microscopic analysis. (B) In parallel, the collection was crossed to a strain carrying an integrated expression construct for a fusion of MS2 coat protein (MS2CP) with three GFPs and plasmids containing *WSC2-MS2L* or *EAR1-MS2L*. Selection of haploid cells carrying the deletion and the expression constructs was followed by automated microscopic analysis. Scale bar: 5 µm.

Journal of Cell Science (2014) 127, 3373–3381 doi:10.1242/jcs.149799

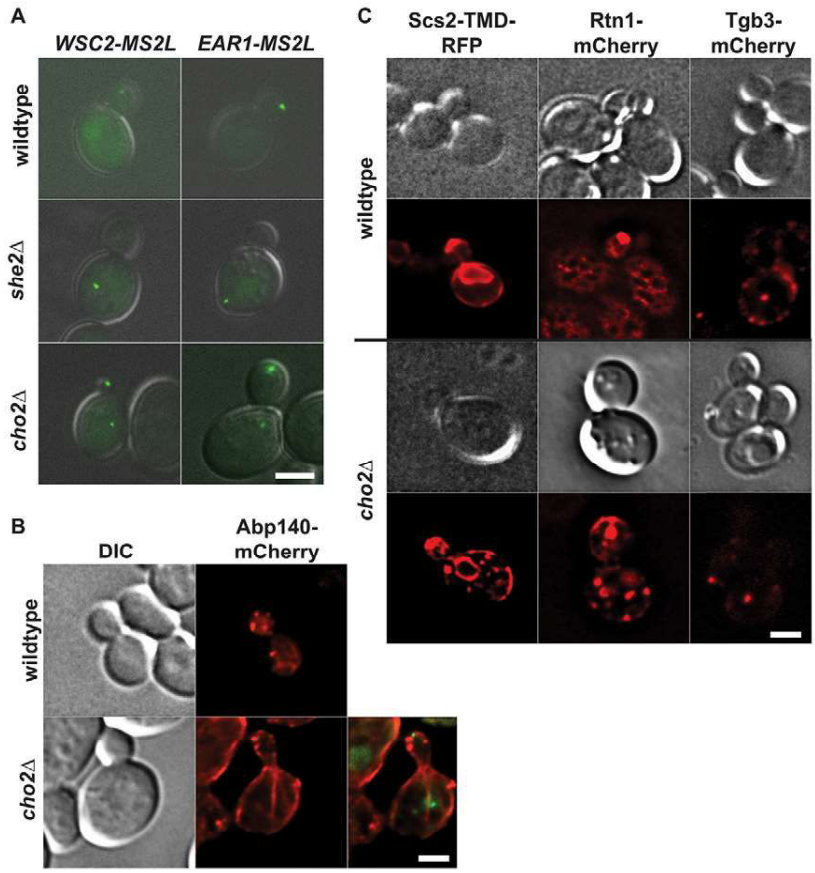

Fig. 2. Deletion of *CHO2* affects mRNA localization and cER morphology but not the actin cytoskeleton. (A) Representative images of cells expressing MS2-tagged *WSC2* and *EAR1* mRNAs in wild-type, *she2Δ* and *cho2Δ* strains. Images are an overlay of differential interference contrast (DIC) and GFP channels. (B) The actin cytoskeleton is indistinguishable between wild-type and *cho2Δ* cells. Microfilaments were visualized by the use of an Abp140–mCherry fusion protein (red). In addition to Abp140–mCherry, MS2-tagged *WSC2* and MS2-CP–GFP (green) were co-expressed in the *cho2Δ* strain to demonstrate that *WSC2* mislocalization in *cho2Δ* is not due to the disturbance of the actin cytoskeleton (lower-right image). (C) cER structure in wild-type and *cho2Δ* cells was analyzed by using three different ER markers: Scs2-TMD–RFP, Rtn1–mCherry and Tgb3–mCherry. All markers show aberrant distribution compared with that of the wild-type strain. Scale bars: 2 μm.

mislocalization is due to defective actin cytoskeleton cables stretching from mother cells to the bud, we expressed an actin-binding protein, Abp140–mCherry (Yang and Pon, 2002) in *cho2Δ* cells (Fig. 2B). No difference in Abp140–mCherry distribution between *cho2Δ* and wild-type cells could be observed.

Because we have previously found a correlation between the loss of ER segregation or altered ER morphology and RNA mislocalization (Fundakowski et al., 2012; Schmid et al., 2006), we tested whether deletion of *CHO2* results in changes in ER structure. A previous analysis suggests that this is not the case (Thibault et al., 2012). However, in this study a general luminal

Table 1. Genes required for localization of mRNAs encoding membrane proteins

ORF name	Gene name	Description	*WSC2* mislocalization (%)	*EAR1* mislocalization (%)
		wild-type	6±7.1	0
YKL130C	*SHE2*	RNA-binding protein	83.33±16.7	96.67±3.3
YGR157W	*CHO2*	phosphatidylethanolamine methyltransferase	56±14.1	61±0.6
YGL206C	*CHC1*	clathrin heavy chain	39±9.1	66±7.0
YMR123W	*PKR1*	v-ATPase assembly factor	37±3.2	35±4.3
YLR338W	*OPI9*	unknown function	34±13.2	39±1.0
YHR098C	*SFB3*	component of the Sec23p-Sfb3p heterodimer (COPII vesicle coat)	33±2.5	36.7±3.8
YGL007C-A		unknown function	31±8.9	35.2±15.8
YLR240W	*VPS34*	phosphatidylinositol 3-kinase	29±8.9	n.d.
YGL020C	*GET1*	subunit of the GET complex	25±13.3	26±2.8
YIL090W	*ICE2*	required for maintenance of ER zinc homeostasis	25±17.5	51±1.4
YJL134W	*LCB3*	long-chain base-1-phosphate phosphatase	22.7±15.0	45±1.5
YHL020C	*OPI1*	transcriptional regulator of lipid biosynthesis genes	20	60±24.0
YBR058C-A	*TSC3*	associated with serine palmitoyltransferase	22.5±0.3	46±2.9
YPL268W	*PLC1*	phospholipase C	6±2.6	30.3±9.7

Results from a visual screen for RNA localization of MS2L-tagged *WSC2* and *EAR1* mRNAs that was performed on a sub-library of a yeast deletion collection. Deletion of *SHE2* served as a control for cells that mislocalize mRNAs. 11 out of 13 newly identified genes are involved in the correct localization of *WSC2* and *EAR1*. *PLC1* deletion exclusively affects *EAR1* localization. A total of 30–400 cells were counted for each mutant. n.d., not determined. Data are shown as the mean±s.d.

Journal of Cell Science (2014) 127, 3373–3381 doi:10.1242/jcs.149799

ER protein (Kar2p) was used as an ER marker that stains mainly the perinuclear ER. In order to specifically assess potential morphological changes in the cortical ER we analyzed the distribution of three ER marker proteins, Scs2-TMD–RFP, Rtn1–mCherry and Tgb3–mCherry, all of which are membrane proteins and constituents of cER (Fig. 2C). Scs2p is a tail-anchored integral ER protein that connects cER to the plasma membrane, and its transmembrane domain (TMD) is sufficient for targeting red fluorescent protein (RFP) to ER (Loewen et al., 2007). Rtn1p belongs to the reticulon family of proteins and is involved in shaping ER tubules that are preferentially found in cortical ER (Voeltz et al., 2006). Tgb3 is a movement protein of plant potexvirus that was found to specifically bind to highly curved cER tubules in yeast (Lee et al., 2010). All three cER marker proteins were mislocalized in *cho2Δ* cells (Fig. 2C). Scs2-TMD–RFP was present in cER and perinuclear ER in wild-type cells, and a strong accumulation of Scs2-TMD–RFP could be seen at the tip of the bud, indicating the presence of cER in the bud. The cER localization of Scs2-TMD–RFP in *cho2Δ* cells was visible as several large aggregate-like structures in the cytoplasm and at the cell periphery, whereas perinuclear ER localization remained unchanged. A similar cER redistribution was seen for Rtn1–mCherry. Tgb3–mCherry was detected in patches at the cortex of wild-type mother cells and buds, but the peripheral patches disappeared in *Δcho2* cells. We conclude that loss of Cho2p results in the redistribution of cortical ER markers, severe changes to ER morphology and partial loss of mRNA localization.

Association of mislocalized mRNPs with aberrant ER structures and She2p in *cho2Δ* cells

Several localized mRNAs, including *WSC2*, require proper cER formation and segregation into the bud for their proper localization (Fundakowski et al., 2012). We therefore investigated whether mislocalization of *WSC2-MS2L* is due to the release of the mRNA from ER or whether it is caused by association of the mRNA with ER aggregates that cannot move into the bud. For colocalization studies, MS2L-tagged *WSC2* mRNA was expressed in cells carrying Rtn1–mCherry as the ER marker. Wild-type cells showed a colocalization of *WSC2-MS2L* mRNPs and cortical ER at the bud tip, indicating that both are transported to the bud (Fig. 3A, top row). In *cho2Δ* cells, *WSC2-MS2L* mRNPs still colocalized with the Rtn1–mCherry ER marker; however, colocalization was also seen within the intracellular aggregates in the mother cell (Fig. 3A, bottom row).

The RNA-binding protein She2p can associate with membranes *in vitro* and co-purifies with ER from cell extracts (Aronov et al., 2007; Genz et al., 2013; Schmid et al., 2006). In order to test whether the ER-localized *WSC2-MS2L* mRNPs in the mother cell are still associated with She2p, we co-expressed a GFP-tagged She2p with *WSC2-MS2L* and detected the mRNA by means of a fusion of the MS2 coat protein to five mCherry molecules (see Materials and Methods). The majority of *WSC2-MS2L* mRNPs in the buds of wild-type cells (100%, $n=12$), as well as those in the mother cells of *cho2Δ* mutants (83%, $n=29$), contained She2p (Fig. 3B). We therefore conclude that the intracellular cER structures observed in *cho2Δ* cells bind to *WSC2-MS2L* mRNPs that still contain She2p and that this capturing prevents the movement of both ER and localized mRNPs into the bud.

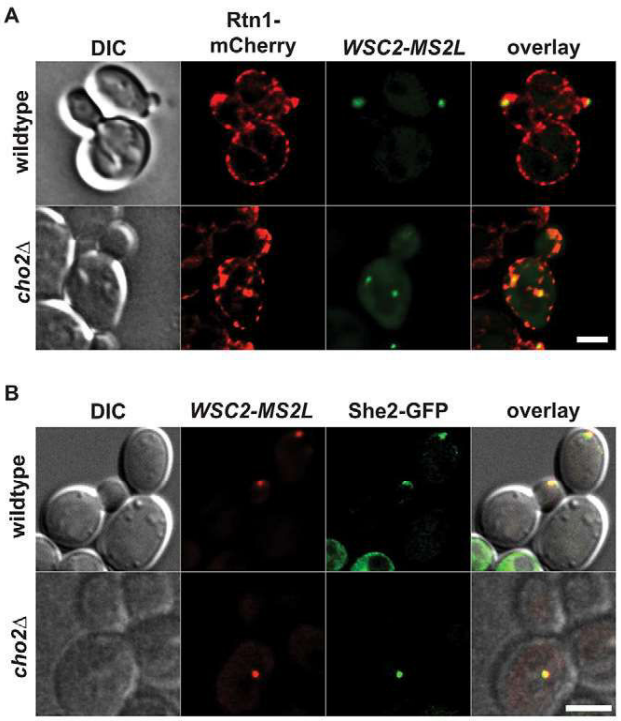

Fig. 3. Mislocalized *WSC2* colocalizes with the ER and She2p. (A) Representative images of wild-type and *cho2Δ* cells expressing Rtn1–mCherry to visualize cER and plasmids encoding MS2-tagged *WSC2* and MS2-CP–GFP. In wild-type cells, *WSC2* colocalizes with cER in the bud, whereas colocalization in *cho2Δ* cells is seen with aberrant cER structure in the mother cell. (B) Representative images of wild-type and *cho2Δ* cells expressing a She2–GFP fusion protein, MS2-tagged *WSC2* and MS2-CP–mCherry. *WSC2* mRNP colocalizes with She2p in the bud of wild-type cells and in the mother cell of *cho2Δ* cells. DIC, differential interference contrast. Scale bars: 2 μm.

Imbalance of PtdEtn and PtdCho levels causes mRNA mislocalization

Cho2p catalyzes the first step during the conversion of phosphatidyl-N-ethanolamine (PtdEtn) to phosphatidylcholine (PtdCho) in the cytidine diphosphate-diacylglycerol (CDP-DAG) methylation pathway (Fig. 4A), the primary route for the synthesis of PtdCho in the absence of exogenous choline (Kodaki and Yamashita, 1989; Summers et al., 1988). Loss of Cho2p results in a severe imbalance of PtdEtn and PtdCho levels, with PtdEtn levels increasing from 15–20% to 40–50%, whereas PtdCho levels can drop from 40–45% to 10% of total cellular lipids (Fig. 4B; Summers et al., 1988). Reduction in the amount of PtdCho is also seen in mutants lacking Opi3p, the yeast phosphatidyl-N-methylethanolamine N-methyltransferase (Kodaki and Yamashita, 1989; McGraw and Henry, 1989), which converts the product of Cho2p, phosphatidyl-N-monomethylethanolamine (PMME), to PtdCho (Fig. 4A,B; Carman and Henry, 1989). Consequently, we tested whether *opi3Δ* mutants affect mRNA localization as well. Surprisingly, although we observed the reported strong decrease in the amount of PtdCho and an increase in PMME (Fig. 4B), deletion of *OPI3* had little impact on the localization of *WSC2-MS2L* mRNA (14.7±7% of cells displayed mislocalization, compared with 56±14.1% and 83±16.6% of cells displaying mislocalization in *cho2Δ* and *she2Δ* cells, respectively; ±s.d.) (Fig. 4C; Table 1). PtdCho levels in mutants that are defective in Cho2p or Opi3p can

Journal of Cell Science (2014) 127, 3373–3381 doi:10.1242/jcs.149799

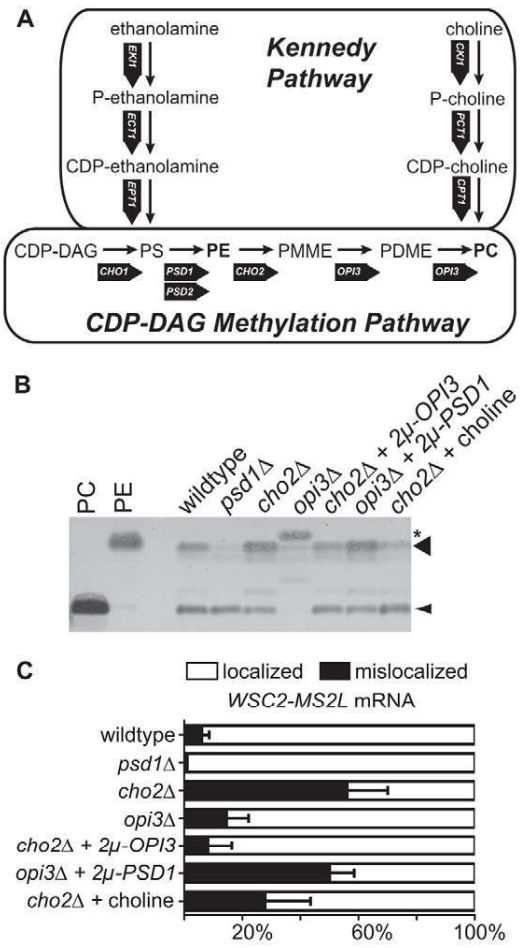

Fig. 4. PtdEtn levels influence *WSC2* mRNA localization. (A) An overview of phospholipid synthesis pathways in yeast (showing the steps relevant to this study). The triple methylation of PtdEtn (PE), catalyzed by the methyltransferases Cho2p and Opi3p, is the primary route for the synthesis of PtdCho (PC) in the absence of exogenous choline. P, phosphorylated; PS, PtdSer; PDME, phosphatidyldimethylethanolamine. (B) Phospholipid analysis. Phospholipids were extracted from a membrane fraction of the indicated yeast strains and subjected to thin layer chromatography together with PtdCho and PtdEtn standards (left). The large arrowhead indicates PtdEtn; the small arrowhead indicates PtdCho; the asterisk marks a new phospholipid species appearing in the *opi3Δ* mutant. Note the increase in the amount of PtdEtn in *cho2Δ* and the subsequent decrease in the amount of PtdEtn in *cho2Δ* cells overexpressing *OPI3*. Addition of choline to *cho2Δ* cells decreases the amount of PtdEtn and increases PtdCho. (C) Localization of *WSC2* in deletion mutants of various phospholipid biosynthesis genes. Dark bars represent the percentage of cells with mislocalized *WSC2-MS2L* particles. In each case, ≥100 cells were analyzed in three independent experiments. Data show the mean±s.d.

be increased by the addition of choline to the medium, which is metabolized to PtdCho in the Kennedy pathway (Fig. 4A; Carman and Henry, 1989). Addition of 1 mM choline to the growth medium of *cho2Δ* cells partially improved *WSC2-MS2L* localization (27.7±15.7% of cells displayed mislocalization; Fig. 4C). This partial improvement can be explained by the reduced activity of *PSD1* in the presence of choline. This gene encodes the major phosphatidylserine (PtdSer) decarboxylase that converts PtdSer into PtdEtn (Carson et al., 1984). Our results indicate that a general reduction in the amount of PtdCho is not the main cause of mRNA mislocalization and suggest a specific defect due to the accumulation of the Cho2p substrate PtdEtn. To test this idea, we overexpressed Opi3p in *cho2Δ* cells, because overexpression of Opi3p can suppress the PtdEtn methylation defect of *cho2* mutants by substituting for Cho2p in the conversion of PtdEtn to PMME (Preitschopf et al., 1993). Overexpression of Opi3p in *cho2Δ* cells reduces PtdEtn levels (Fig. 4B) and rescues *WSC2* localization (Fig. 4C; 8.3±8.2% mislocalization), indicating that the Cho2p-mediated conversion of PtdEtn to PMME is required for correct mRNA localization. Finally, in order to create a similar PtdEtn and PtdCho imbalance to that observed in *cho2Δ* cells, we tested mRNA localization in a strain lacking Opi3p (leading to a reduced PtdCho level) and overexpressing Psd1p (leading to an increased PtdEtn level). In this strain, *WSC2* localization is severely impaired (49±6.9% of cells display mislocalization). In summary, our analysis of mutants of phospholipid biosynthesis suggests that the observed mRNA mislocalization in *cho2Δ* cells is due to a failure to convert PtdEtn to PtdCho, thereby creating an imbalance of these lipids. This analysis reveals a prominent role for PtdEtn levels in regulating mRNA localization.

She2p binding to membranes increases with PtdEtn levels

The previous analysis demonstrates how an increase in the amount of PtdEtn provokes mRNA mislocalization. We have previously shown that the mRNA localization factor She2p can directly bind to protein-free liposomes (Genz et al., 2013). In order to test whether PtdEtn influences She2p binding, we generated 80-nm diameter liposomes with increasing PtdEtn contents ranging from 0% to 50% (see Materials and Methods), incubated them with recombinant She2p and performed a flotation analysis to determine the amount of She2p that fractionated with (and thus bound to) liposomes (Genz et al., 2013). We observed an increase in the amount of She2p binding as PtdEtn levels increased from 0% to 40%. At higher PtdEtn contents She2p binding decreased again, although only by 20% of its maximum level (Fig. 5A). This decrease correlated with a major collapse in the liposomes from vesicles to large clumps, as revealed by dynamic light scattering (Fig. 5B). PtdEtn belongs to the class of so-called type II lipids that have an overall conical molecular shape resulting from the comparatively small cross-sectional area of the polar head group and, thus, preferentially accumulate in curved structures. Therefore the large structures that appear with high PtdEtn levels likely represent aggregates or abnormal membrane structures, because negative curvature stress due to high PtdEtn levels can lead to malformed biological membranes (Gruner, 1985). These larger lipid-containing aggregates might be an *in vitro* counterpart of the intracellular clusters seen with cER marker proteins (Fig. 2). Previous studies have shown that an increase in membrane curvature of liposomes results in better binding of She2p, consistent with the model that She2p links localized mRNAs to tubular ER, which has a highly curved structure. The increase in She2p binding to liposomes with increasing PtdEtn contents can therefore be explained by the preference of She2p for curved membranes, which are likely to contain high PtdEtn levels.

In order to test whether She2p is required for the association of *WSC2* mRNP with ER aggregates, we determined the degree of *WSC2-MS2L* mRNP colocalization with the ER (represented by Rtn1–mCherry) in the presence and absence of She2p. In *cho2Δ she2Δ* mutants, only 12±7.3% (±s.d.) of cells displayed colocalization of *WSC2-MSL2* mRNPs with ER clusters, in

Journal of Cell Science (2014) 127, 3373–3381 doi:10.1242/jcs.149799

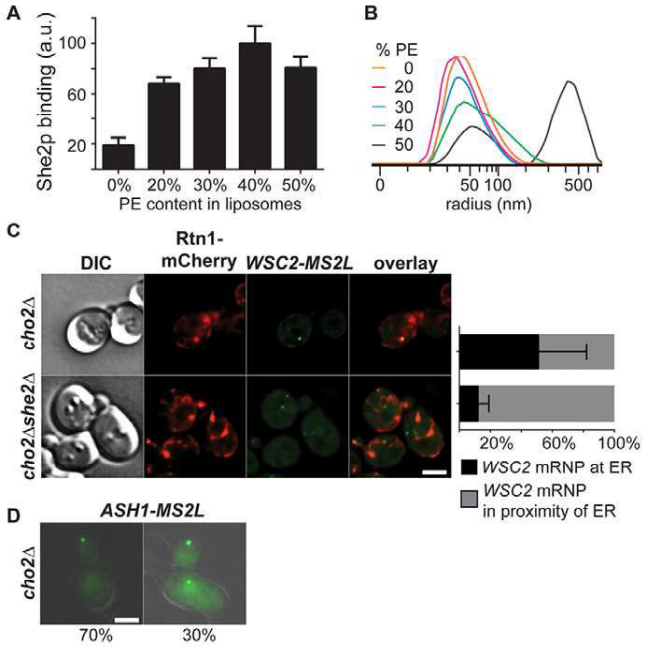

Fig. 5. She2p binding to liposomes increases with rising PtdEtn levels. (A) Co-flotation of recombinant She2p with 80-nm diameter liposomes is augmented with increasing PtdEtn (PE) content, showing a maximum at 40% PtdEtn. Percentage indicates the amount of PtdEtn as a percentage of total lipid content. Co-flotation was performed as described in Materials and Methods. Data show the mean ratio (±s.d.) of floated protein versus input, displayed as artificial units (a.u.). The amount of binding of She2p to 40% PtdEtn liposomes is set to 100 a.u. Three independent flotation experiments were performed. (B) The size distribution of liposomes generated with increasing PtdEtn levels as measured by dynamic light scattering. At high PtdEtn levels, a peak indicating structures with a diameter >1000 nm appears in addition to the 80-nm peak. (C) *WSC2* colocalization with cER in the mother cell depends on She2p. Left, representative images of *cho2Δ* and *cho2Δ she2Δ* cells expressing Rtn1–mCherry and MS2-tagged *WSC2*. Colocalization of *WSC2* with cER in the mother cell is lost in *cho2Δ she2Δ* cells. DIC, differential interference contrast. Right, quantification of the microscopy data. Data show the mean±s.d. (D) Asymmetric *ASH1-MS2L* distribution is disturbed in *cho2Δ*. Representative images of cells with correctly localized *ASH1* (left) and symmetrically distributed *ASH1* (right) are shown. The percentage of cells with the indicated phenotype is shown below the images. Scale bars: 2 μm.

contrast to 52±31% of *cho2Δ* cells (Fig. 5C). We frequently observed mRNPs in the proximity of the ER but not colocalizing with it. These experiments suggest that She2p mediates the association of *WSC2-MS2L* mRNPs with the intracellular ER aggregates. If the high content of PtdEtn in *cho2Δ* mutants led to a reduction in the overall functional amounts of She2p due to the capturing of the latter on the ER surface, one would also expect a reduction in the correct localization of *ASH1* mRNA in cells with high concentrations of PtdEtn. This is indeed the case (Fig. 5D). Whereas *ASH1-MS2L* mRNPs are localized exclusively to the bud in >90% of wild-type cells (Fundakowski et al., 2012), in 30% (n=83) of *cho2Δ* cells these mRNPs are detectable in the mother cell.

DISCUSSION

In a screen for new proteins involved in regulating the mRNA localization of membrane protein transcripts in budding yeast, we revealed the dominant role of phospholipids, especially PtdEtn, in enabling the correct localization of such mRNAs. Of the mutants that we identified in our screen, 7 out of 13 are deleted for genes encoding enzymes (*CHO2*, *LCB3*, *PLC1*, *TSC3*, *ICE2* and *VPS34*) or a transcription factor (*OPI1*) involved in phospholipid or sphingolipid metabolism. A closer analysis of the phenotype of *cho2Δ* cells showed that an imbalance of the PtdEtn:PtdCho levels results in a malformed cortical ER network and mislocalization of the two tested mRNAs, *WSC2* and *EAR1*. Other genes identified in our screen might also influence mRNA localization through effects on the levels of PtdEtn versus PtdCho. Because *OPI1* controls the expression of several phospholipid synthesis genes, including *CHO2*, its downregulation could lead to similar defects to those observed for *cho2Δ* (Carman and Han, 2011). Furthermore, the phospholipid biosynthesis phenotype observed in *cho2Δ* mutants is aggravated by deletion of *ICE2* (Tavassoli et al., 2013).

How could an increase in PtdEtn relate to inhibition of mRNA localization? To compensate for an imbalance in the PtdEtn:PtdCho ratio, cells alter their proteome and increase the synthesis of proteins involved in stress-response pathways, including the unfolded protein response, the ER-associated degradation pathway and the induction of heat-shock proteins (Thibault et al., 2012). However, we do not believe that these proteome changes are directly related to mRNA mislocalization, as loss of Opi3p, the second methyltransferase required for PtdCho biosynthesis, leads to very similar proteome changes (Thibault et al., 2012) but not to a defect in *WSC2* localization, indicating a specific role of Cho2p and of its substrate, PtdEtn. The stronger binding of She2p to liposomes with an increasing PtdEtn content supports a more specific role of PtdEtn. Previous experiments have not indicated a role for specific lipids in She2p binding (Genz et al., 2013); however, this conclusion was based on the fact that the omission of phospholipids with negative net charge, like PtdSer and phosphatidylinositol, did not alter She2p binding. However, PtdEtn was not tested in this system. The variations in She2p binding to liposomes of different PtdEtn contents as recorded in our *in vitro* assays suggest that the membrane association of She2p and associated mRNAs requires a regulated content of the curvature-supporting lipid PtdEtn, which fits with previous observations of She2p binding to highly curved membranes (Genz et al., 2013). Although we have not been able to determine whether the cER aggregates seen in *cho2Δ* cells are enriched in PtdEtn, it is likely that they are, because the total cellular PtdEtn level in *cho2Δ* mutants can reach to up to 50%, a level at which aggregation of liposomes was detectable by dynamic light scattering (DLS) (Fig. 5). Thus, the intracellular structures detected with cER markers could represent membrane aggregates that have collapsed owing to their high PtdEtn content (Gruner, 1985). These membrane structures could entrap She2p and associated localized mRNAs. In addition, extensive She2p capturing could also result from proliferation of the ER. Such proliferation is, for example, seen in conditional *sec24-11* mutants with a non-functional COPII coatomer complex (Peng et al., 2000). The *sec24-11* allele genetically interacts with *SFB3*, another gene that we have identified in our screen (Table 1). Other coatomer components have also been implicated in mRNA localization, including the COPII factors Sec21p, Sec23p and the small GTPase Arf1p (Trautwein et al., 2004). However, in contrast to the phenotype that we have observed in *cho2Δ*, where a fraction of mRNPs remain in the mother cell, mutations in these genes have been reported to disrupt late stages of mRNA localization, such as anchoring or association with the cell cortex. Nevertheless, these results underscore a direct link between

Journal of Cell Science (2014) 127, 3373–3381 doi:10.1242/jcs.149799

membrane trafficking or membrane composition and mRNA localization.

Because two additional genes whose loss reduces mRNA localization (*LCB3* and *TCB3*; Gable et al., 2000; Mandala et al., 1998) encode enzymes that are involved in sphingolipid metabolism, it remains to be determined in the future how other lipids, including sphingolipids, can influence the membrane interaction of She2p and mRNA localization. More generally, our results indicate how dynamic the process of mRNA granule targeting to the bud is; the correct localization of mRNAs requires that ER tubules acting as transport vehicles are kept unclogged and in pristine structural condition.

MATERIALS AND METHODS

Yeast strains and plasmids

All yeast strains in this study were derived from a BY4741 background. Deletion mutants in various ER-related genes were obtained from the EUROSCARF yeast deletion collection. Gene tagging or deletion of genes in specific backgrounds (e.g. to create double mutants) was performed by standard PCR-based transformation methods (Janke et al., 2004). All plasmids used in this study are listed in supplementary material Table S3. Oligonucleotides for tagging, gene disruption or cloning are listed in supplementary material Table S4, and yeast strains are listed in supplementary material Table S5.

The synthetic gene array (SGA) query strain RJY3864 was created as follows. In order to visualize the mRNP on the background of the yeast deletion collection, the MS2 coat protein (MS2CP), fused to GFP and in conjugation with the NatMX4 cassette, was genomically integrated into the *HO* locus of strain RJY3863. This was achieved by fusion PCR: MS2-CP-GFP was amplified from RJP1486 with primers RJO3992 and RJO3993. The NatMX4 cassette was amplified from plasmid RJP1873 with primers RJO3990 and RJO3991. Primers 3991 and 3992 contain overlapping sequence. The two PCR products were fused by PCR using primers 3990 and 3993, which contain overhangs homologous to the *HO* gene. The fused PCR product was transformed into strain RJY3863 and integrated into the *HO* locus. The resulting strain, RJY3864, was further transformed with RJP1773 or RJP1815, containing *WSC2-MS2L* or *EAR1-MS2L*. Plasmids used in this work are listed in supplementary material Table S3. Plasmids expressing MS2-tagged *WSC2* and *EAR1* were created as follows. *WSC2-MS2L* was amplified by PCR from the genome of strain RJY3626 using primers RJO3761 and RJO3762 and ligated into YCplac33 or YEplac195 (Gietz and Sugino, 1988). The resulting plasmids were named RJP1767 and RJP1773, respectively. EAR1-MS2 was amplified by PCR from the genome of strain RJY3624 using primers RJO3988 and RJO3989 and was ligated into Yeplac195. The resulting plasmid was named RJP1815. RJP1817 and RJP1888 were created by amplifying *OPI3* and *PSD1* from yeast genomic DNA with primers RJO4187, RJO4188, RJO4556 and RJO4557, and cloning the products by the sequence- and ligation-independent cloning (SLIC) method into plasmid YEplac181 (Li and Elledge, 2007). RJP1890 was created by digestion of ABP140-2×mCherry (first 17 amino acids of ABP140; Kilchert and Spang, 2011) with *Kpn*I and *Sac*I from plasmid 1841 and ligating into plasmid YEplac181. Plasmid RJP1889-pMS2-CP-5×mCherry was created as follows. MS2-CP, including the *MET25* promoter, was amplified from plasmid 1486 using primers RJO4577 and RJO4578 and was cloned by the SLIC method into plasmid pRS313. A single mCherry sequence was amplified using primers RJO4581 and RJO4582 from plasmid RJP1423, digested with *BamH*I and *Bgl*II and ligated into the *BamH*I site downstream of the MS2-CP. An additional mCherry unit was inserted the same way. Single mCherry and a transcriptional terminator was amplified using primers RJO4581 and RJO4595 from plasmid 1423 and was ligated into the *BamH*I site downstream of the 2×mCherry. The destroyed *Bgl*II site was converted to a *BamH*I site by site-directed mutagenesis, using primers RJO4598 and RJO4599. The 3×mCherry was then released with *BamH*I and cloned into a plasmid with 2×mCherry, thereby creating 5×mCherry.

Library screen and microscopy

A sub-library was created from the yeast deletion mutant collection (Giaever et al., 2002) by picking 318 non-essential genes that, according to the *S. cerevisiae* Genome Database (SGD), code for an ER component or are involved in lipid biosynthesis (see supplementary material Tables S1 and S2). In addition, we added a selection of ORFs coding for proteins with unknown function and additional ORFs with unrelated function for negative control. This collection was transformed with plasmids expressing either *WSC2*-MS2L or *EAR1*-MS2L together with a plasmid expressing the MS2 coat protein fused to GFP. Yeast cells from a fresh selective plate were scraped, resuspended in 2 ml of synthetic complete (SC) medium, grown for 3–4 h at 30℃ and dropped onto a thin agarose layer of SC medium with reduced methionine concentration (44 mg/l) for induction of the *MET25* promoter controlling MS2-CP–GFP expression. The agarose layer was covered with a coverslip and cells were incubated at 30℃ for 30 min before images were captured on a Zeiss CellObserver Z1 fluorescence microscope operated by Axiovision 4.8 software (Zeiss). For cER structure visualization, 40 *Z*-stack images spaced at 0.25 µm were captured and deconvolved using a theoretical point spread function, autolinear normalization and automatic *z*-correction provided by the Axiovision 4.8 software package.

The construction of the SGA query strain is described above. The SGA strain containing the mRNA visualization system was crossed against two sub-libraries using SGA methodology (Cohen and Schuldiner, 2011; Tong et al., 2001). The first sub-library was created from the yeast deletion collection (Giaever et al., 2002) and consisted of 379 non-essential genes. The second sub-library was created from a decreased abundance by mRNA perturbation (DAmP) library and consisted of 323 hypomorphic alleles of essential genes (Breslow et al., 2008; Schuldiner et al., 2005). The genes were selected according to the SGD description as related to ER or their GFP-tagged protein was reported to localize to the ER.

The cellular localization of *WSC2-MS2L* and *EAR1-MS2L* was then visualized in these mutant strains using a high-throughput microscopy setup (Cohen and Schuldiner, 2011). Briefly, cells were moved from agar plates into liquid 384-well polystyrene growth plates using the RoTor arrayer. Liquid cultures were grown overnight in SD-URA medium in a shaking incubator (LiCONiC Instruments) at 30℃. A JANUS liquid handler (Perkin Elmer) connected to the incubator was used to back-dilute the strains into plates containing the same medium, after which plates were transferred back to the incubator and were allowed to grow for 4 h at 30℃ to reach logarithmic growth. The liquid handler was then used to transfer 50 µl of strains into glass-bottomed 384-well microscope plates (Matrical Bioscience) containing 10 µl of Calcofluor White (final concentration of 10 µg/ml) and coated with concanavalin A (Sigma-Aldrich) to allow formation of a cell monolayer. Wells were washed twice with medium to remove unconnected cells, and plates were transferred into an automated inverted fluorescent microscopic ScanR system (Olympus) using a swap robot (Hamilton). The ScanR system is designed to allow autofocus and imaging of plates in 384-well format using a 60× air lens and is equipped with a cooled CCD camera. Images were acquired at an excitation time of 10 ms for the DAPI channel (Calcofluor White stain) and 1500 ms for the GFP channel. After acquisition, images were imported to the Axiovision software, processed and manually reviewed. Deletion strains that were found to show mislocalization of either *WSC2* or *EAR1* were rescreened using the manual method described. In total, ≥50 cells were counted to assess mRNP localization.

Purification of recombinant She2p and flotation assay

Purification of recombinant She2p was performed as described previously (Müller et al., 2009). Wild-type She2p was expressed as a GST fusion protein in *Escherichia coli* BL21(DE3)/pRIL (Invitrogen). Purification to >95% homogeneity was achieved by using standard protein purification techniques. The GST tag was removed by cleavage with tobacco etch virus (TEV) protease (Invitrogen). For storage, glycerol was added to final concentration of 20%. She2p was quickly cooled in liquid nitrogen and stored at −80℃.

Artificial liposomes were prepared as described previously (Genz et al., 2013). Briefly, egg yolk L α phosphatidylcholine (PtdCho) and L α phosphatidylethanolamine (PtdEtn) from Sigma were dissolved in chloroform and mixed at an appropriate ratio to obtain phospholipid mixes containing 0%, 20%, 30%, 40% and 50% PtdEtn. A lipid film was prepared by rotation and evaporation of the organic solvent under N_2 atmosphere. Membranes were dissolved to a final total lipid concentration of 10 mg/ml in degassed liposome buffer (20 mM HEPES pH 7.4, 100 mM NaCl). To create unilamellar liposomes, the emulsion was passed 21 times through a polycarbonate filter membrane with 80-nm pore size mounted in a mini extruder (Avanti Polar Lipids). Liposome size distribution was verified by dynamic light scattering in a Zetasizer Nano ZS (Malvern Instruments, Herrenberg, Germany).

For the flotation assay, 100 µl of liposome solution was mixed with 50 pmol of She2p in 190 µl of binding buffer (50 mM HEPES-KOH, 150 mM potassium acetate, 1 mM magnesium acetate, 1 mM EDTA, 1 mM DTT) and incubated for 15 min on ice. A total of 40 µl of the sample was kept as an input control, and 200 µl was mixed with 3 ml of binding buffer containing 70% sucrose and added to the bottom of an SW40 polycarbonate tube. The sample was covered with three cushions of 3 ml of binding buffer containing 50%, 40% and 0% sucrose. After centrifugation to equilibrium (70,000 ***g*** for 4 h at 4℃) the liposome-containing interface between the 40% and 0% sucrose cushions was harvested, precipitated by using trichloroacetic acid (TCA) and dissolved in 45 µl of SDS sample buffer. Flotation samples and input controls were analyzed as described above. She2p signals were analyzed densitometrically using ImageJ.

Phospholipid analysis

Yeast cell lysates were prepared by enzymatic disruption of yeast cell walls as described previously (Daum et al., 1982). A membrane fraction containing mitochondria and microsomes was isolated by centrifugation (200,000 ***g***, 4℃, 1 h) and resuspended in SEM buffer using a glass Dounce homogenizer. For thin layer chromatography of lipids, phospholipids were extracted from membranes and analyzed according to a published procedure (Vaden et al., 2005). Thin layer chromatography was performed using HPTLC silica gel 60 F254 plates. Phospholipids were stained by spraying the plate with Molybdenum Blue.

Acknowledgements

We would like to thank Chao-Wen Wang (Academia Sinica, Taipei, Taiwan) for the TGB3-mCherry expression plasmid and Anne Spang (Biozentrum, Basel, Switzerland) for ABP140-mCherry. We are grateful to Ulrike Thiess (Interfaculty Institute of Biochemistry, Tübingen, Germany) for performing secretion assays.

Competing interests

The authors declare no competing interests.

Author contributions

O. H., M. Schuldiner, D.R. and R.-P. J. conceived of the experiments. O. H., C.G., M. Sinzel and I.Y. performed the experiments and data analysis. O.H., M. Schuldiner and R.-P. J. wrote the manuscript.

Funding

O.H. and R.P.J. were funded by the Deutsche Forschungsgemeinschaft [grant number JA696 7-1]. M. Schuldiner and I.Y. are supported by a European Research Council grant [grant number StG 260395].

Supplementary material

Supplementary material available online at
http://jcs.biologists.org/lookup/suppl/doi:10.1242/jcs.149799/-/DC1

References

Aronov, S., Gelin-Licht, R., Zipor, G., Haim, L., Safran, E. and Gerst, J. E. (2007). mRNAs encoding polarity and exocytosis factors are cotransported with the cortical endoplasmic reticulum to the incipient bud in Saccharomyces cerevisiae. *Mol. Cell. Biol.* **27**, 3441-3455.

Auger, K. R., Carpenter, C. L., Cantley, L. C. and Varticovski, L. (1989). Phosphatidylinositol 3-kinase and its novel product, phosphatidylinositol 3-phosphate, are present in Saccharomyces cerevisiae. *J. Biol. Chem.* **264**, 20181-20184.

Bertrand, E., Chartrand, P., Schaefer, M., Shenoy, S. M., Singer, R. H. and Long, R. M. (1998). Localization of ASH1 mRNA particles in living yeast. *Mol. Cell* **2**, 437-445.

Besse, F. and Ephrussi, A. (2008). Translational control of localized mRNAs: restricting protein synthesis in space and time. *Nat. Rev. Mol. Cell Biol.* **9**, 971-980.

Böhl, F., Kruse, C., Frank, A., Ferring, D. and Jansen, R. P. (2000). She2p, a novel RNA-binding protein tethers ASH1 mRNA to the Myo4p myosin motor via She3p. *EMBO J.* **19**, 5514-5524.

Breslow, D. K., Cameron, D. M., Collins, S. R., Schuldiner, M., Stewart-Ornstein, J., Newman, H. W., Braun, S., Madhani, H. D., Krogan, N. J. and Weissman, J. S. (2008). A comprehensive strategy enabling high-resolution functional analysis of the yeast genome. *Nat. Methods* **5**, 711-718.

Carman, G. M. and Han, G.-S. (2011). Regulation of phospholipid synthesis in the yeast Saccharomyces cerevisiae. *Annu. Rev. Biochem.* **80**, 859-883.

Carman, G. M. and Henry, S. A. (1989). Phospholipid biosynthesis in yeast. *Annu. Rev. Biochem.* **58**, 635-667.

Carson, M. A. M., Emala, M., Hogsten, P. and Waechter, C. J. C. (1984). Coordinate regulation of phosphatidylserine decarboxylase activity and phospholipid N-methylation in yeast. *J. Biol. Chem.* **259**, 6267-6273.

Cohen, Y. and Schuldiner, M. (2011). Advanced methods for high-throughput microscopy screening of genetically modified yeast libraries. *Methods Mol. Biol.* **781**, 127-159.

Daum, G., Gasser, S. M. and Schatz, G. (1982). Import of proteins into mitochondria. Energy-dependent, two-step processing of the intermembrane space enzyme cytochrome b2 by isolated yeast mitochondria. *J. Biol. Chem.* **257**, 13075-13080.

Du, Y., Ferro-Novick, S. and Novick, P. (2004). Dynamics and inheritance of the endoplasmic reticulum. *J. Cell Sci.* **117**, 2871-2878.

Estrada, P., Kim, J., Coleman, J., Walker, L., Dunn, B., Takizawa, P., Novick, P. and Ferro-Novick, S. (2003). Myo4p and She3p are required for cortical ER inheritance in Saccharomyces cerevisiae. *J. Cell Biol.* **163**, 1255-1266.

Estrada de Martin, P., Du, Y., Novick, P. and Ferro-Novick, S. (2005). Ice2p is important for the distribution and structure of the cortical ER network in Saccharomyces cerevisiae. *J. Cell Sci.* **118**, 65-77.

Flick, J. S. and Thorner, J. (1993). Genetic and biochemical characterization of a phosphatidylinositol-specific phospholipase C in Saccharomyces cerevisiae. *Mol. Cell. Biol.* **13**, 5861-5876.

Fundakowski, J., Hermesh, O. and Jansen, R.-P. (2012). Localization of a subset of yeast mRNAs depends on inheritance of endoplasmic reticulum. *Traffic* **13**, 1642-1652.

Gable, K., Slife, H., Bacikova, D., Monaghan, E. and Dunn, T. M. (2000). Tsc3p is an 80-amino acid protein associated with serine palmitoyltransferase and required for optimal enzyme activity. *J. Biol. Chem.* **275**, 7597-7603.

Genz, C., Fundakowski, J., Hermesh, O., Schmid, M. and Jansen, R.-P. (2013). Association of the yeast RNA-binding protein She2p with the tubular endoplasmic reticulum depends on membrane curvature. *J. Biol. Chem.* **288**, 32384-32393.

Giaever, G., Chu, A. M., Ni, L., Connelly, C., Riles, L., Véronneau, S., Dow, S., Lucau-Danila, A., Anderson, K., André, B. et al. (2002). Functional profiling of the Saccharomyces cerevisiae genome. *Nature* **418**, 387-391.

Gietz, R. D. and Sugino, A. (1988). New yeast-Escherichia coli shuttle vectors constructed with in vitro mutagenized yeast genes lacking six-base pair restriction sites. *Gene* **74**, 527-534.

Gruner, S. M. (1985). Intrinsic curvature hypothesis for biomembrane lipid composition: a role for nonbilayer lipids. *Proc. Natl. Acad. Sci. USA* **82**, 3665-3669.

Gurunathan, S., David, D. and Gerst, J. E. (2002). Dynamin and clathrin are required for the biogenesis of a distinct class of secretory vesicles in yeast. *EMBO J.* **21**, 602-614.

Holt, C. E. and Bullock, S. L. (2009). Subcellular mRNA localization in animal cells and why it matters. *Science* **326**, 1212-1216.

Janke, C., Magiera, M. M., Rathfelder, N., Taxis, C., Reber, S., Maekawa, H., Moreno-Borchart, A., Doenges, G., Schwob, E., Schiebel, E. et al. (2004). A versatile toolbox for PCR-based tagging of yeast genes: new fluorescent proteins, more markers and promoter substitution cassettes. *Yeast* **21**, 947-962.

Jansen, R. P., Dowzer, C., Michaelis, C., Galova, M. and Nasmyth, K. (1996). Mother cell-specific HO expression in budding yeast depends on the unconventional myosin myo4p and other cytoplasmic proteins. *Cell* **84**, 687-697.

Kilchert, C. and Spang, A. (2011). Cotranslational transport of ABP140 mRNA to the distal pole of S. cerevisiae. *EMBO J.* **30**, 3567-3580.

Kloc, M. and Etkin, L. D. (1995). Two distinct pathways for the localization of RNAs at the vegetal cortex in Xenopus oocytes. *Development* **121**, 287-297.

Kodaki, T. and Yamashita, S. (1989). Characterization of the methyltransferases in the yeast phosphatidylethanolamine methylation pathway by selective gene disruption. *Eur. J. Biochem.* **185**, 243-251.

Krementsova, E. B., Hodges, A. R., Bookwalter, C. S., Sladewski, T. E., Travaglia, M., Sweeney, H. L. and Trybus, K. M. (2011). Two single-headed myosin V motors bound to a tetrameric adapter protein form a processive complex. *J. Cell Biol.* **195**, 631-641.

Lee, S.-C., Wu, C.-H. and Wang, C.-W. (2010). Traffic of a viral movement protein complex to the highly curved tubules of the cortical endoplasmic reticulum. *Traffic* **11**, 912-930.

Li, M. Z. and Elledge, S. J. (2007). Harnessing homologous recombination in vitro to generate recombinant DNA via SLIC. *Nat. Methods* **4**, 251-256.

Loewen, C. J. R., Young, B. P., Tavassoli, S. and Levine, T. P. (2007). Inheritance of cortical ER in yeast is required for normal septin organization. *J. Cell Biol.* **179**, 467-483.
Long, R. M., Singer, R. H., Meng, X., Gonzalez, I., Nasmyth, K. and Jansen, R. P. (1997). Mating type switching in yeast controlled by asymmetric localization of ASH1 mRNA. *Science* **277**, 383-387.
Mandala, S. M., Thornton, R., Tu, Z., Kurtz, M. B., Nickels, J., Broach, J., Menzeleev, R. and Spiegel, S. (1998). Sphingoid base 1-phosphate phosphatase: a key regulator of sphingolipid metabolism and stress response. *Proc. Natl. Acad. Sci. USA* **95**, 150-155.
Martin, K. C. and Ephrussi, A. (2009). mRNA localization: gene expression in the spatial dimension. *Cell* **136**, 719-730.
McGraw, P. and Henry, S. A. (1989). Mutations in the Saccharomyces cerevisiae opi3 gene: effects on phospholipid methylation, growth and cross-pathway regulation of inositol synthesis. *Genetics* **122**, 317-330.
Miller, E., Antonny, B., Hamamoto, S. and Schekman, R. (2002). Cargo selection into COPII vesicles is driven by the Sec24p subunit. *EMBO J.* **21**, 6105-6113.
Müller, M., Richter, K., Heuck, A., Kremmer, E., Buchner, J., Jansen, R.-P. and Niessing, D. (2009). Formation of She2p tetramers is required for mRNA binding, mRNP assembly, and localization. *RNA* **15**, 2002-2012.
Müller, M., Heym, R. G., Mayer, A., Kramer, K., Schmid, M., Cramer, P., Urlaub, H., Jansen, R.-P. and Niessing, D. (2011). A cytoplasmic complex mediates specific mRNA recognition and localization in yeast. *PLoS Biol.* **9**, e1000611.
Niessing, D., Hüttelmaier, S., Zenklusen, D., Singer, R. H. and Burley, S. K. (2004). She2p is a novel RNA binding protein with a basic helical hairpin motif. *Cell* **119**, 491-502.
Oeffinger, M., Wei, K. E., Rogers, R., DeGrasse, J. A., Chait, B. T., Aitchison, J. D. and Rout, M. P. (2007). Comprehensive analysis of diverse ribonucleoprotein complexes. *Nat. Methods* **4**, 951-956.
Peng, R., De Antoni, A. and Gallwitz, D. (2000). Evidence for overlapping and distinct functions in protein transport of coat protein Sec24p family members. *J. Biol. Chem.* **275**, 11521-11528.
Preitschopf, W., Lückl, H., Summers, E., Henry, S. A., Paltauf, F. and Kohlwein, S. D. (1993). Molecular cloning of the yeast OPI3 gene as a high copy number suppressor of the cho2 mutation. *Curr. Genet.* **23**, 95-101.
Sardet, C., Dru, P. and Prodon, F. (2005). Maternal determinants and mRNAs in the cortex of ascidian oocytes, zygotes and embryos. *Biol. Cell* **97**, 35-49.
Schmid, M., Jaedicke, A., Du, T.-G. and Jansen, R.-P. (2006). Coordination of endoplasmic reticulum and mRNA localization to the yeast bud. *Curr. Biol.* **16**, 1538-1543.
Schuldiner, M., Collins, S. R., Thompson, N. J., Denic, V., Bhamidipati, A., Punna, T., Ihmels, J., Andrews, B., Boone, C., Greenblatt, J. F. et al. (2005). Exploration of the function and organization of the yeast early secretory pathway through an epistatic miniarray profile. *Cell* **123**, 507-519.
Shepard, K. A., Gerber, A. P., Jambhekar, A., Takizawa, P. A., Brown, P. O., Herschlag, D., DeRisi, J. L. and Vale, R. D. (2003). Widespread cytoplasmic mRNA transport in yeast: identification of 22 bud-localized transcripts using DNA microarray analysis. *Proc. Natl. Acad. Sci. USA* **100**, 11429-11434.
Sil, A. and Herskowitz, I. (1996). Identification of asymmetrically localized determinant, Ash1p, required for lineage-specific transcription of the yeast HO gene. *Cell* **84**, 711-722.
Summers, E. F., Letts, V. A., McGraw, P. and Henry, S. A. (1988). Saccharomyces cerevisiae cho2 mutants are deficient in phospholipid methylation and cross-pathway regulation of inositol synthesis. *Genetics* **120**, 909-922.
Tavassoli, S., Chao, J. T., Young, B. P., Cox, R. C., Prinz, W. A., de Kroon, A. I. P. M. and Loewen, C. J. R. (2013). Plasma membrane – endoplasmic reticulum contact sites regulate phosphatidylcholine synthesis. *EMBO Rep.* **14**, 434-440.
Thibault, G., Shui, G., Kim, W., McAlister, G. C., Ismail, N., Gygi, S. P., Wenk, M. R. and Ng, D. T. W. (2012). The membrane stress response buffers lethal effects of lipid disequilibrium by reprogramming the protein homeostasis network. *Mol. Cell* **48**, 16-27.
Tong, A. H. Y., Evangelista, M., Parsons, A. B., Xu, H., Bader, G. D., Pagé, N., Robinson, M., Raghibizadeh, S., Hogue, C. W. V., Bussey, H. et al. (2001). Systematic genetic analysis with ordered arrays of yeast deletion mutants. *Science* **294**, 2364-2368.
Trautwein, M., Dengjel, J., Schirle, M. and Spang, A. (2004). Arf1p provides an unexpected link between COPI vesicles and mRNA in Saccharomyces cerevisiae. *Mol. Biol. Cell* **15**, 5021-5037.
Vaden, D. L., Gohil, V. M., Gu, Z. and Greenberg, M. L. (2005). Separation of yeast phospholipids using one-dimensional thin-layer chromatography. *Anal. Biochem.* **338**, 162-164.
Voeltz, G. K., Prinz, W. A., Shibata, Y., Rist, J. M. and Rapoport, T. A. (2006). A class of membrane proteins shaping the tubular endoplasmic reticulum. *Cell* **124**, 573-586.
Wagner, C., Blank, M., Strohmann, B. and Schüller, H. J. (1999). Overproduction of the Opi1 repressor inhibits transcriptional activation of structural genes required for phospholipid biosynthesis in the yeast Saccharomyces cerevisiae. *Yeast* **15**, 843-854.
West, M., Zurek, N., Hoenger, A. and Voeltz, G. K. (2011). A 3D analysis of yeast ER structure reveals how ER domains are organized by membrane curvature. *J. Cell Biol.* **193**, 333-346.
Yang, H.-C. and Pon, L. A. (2002). Actin cable dynamics in budding yeast. *Proc. Natl. Acad. Sci. USA* **99**, 751-756.

Table S1. Yeast open reading frames (ORFs) included in the manual screen for mRNA mislocalization. Multiwell plate number, row, and column display position of ORF deletion mutant in the yeast deletion collection (Life Technologies, Carlsbad, USA). If known, the common gene name and a short summary of the genes function are included.

Download Table S1

Table S2. Yeast open reading frames (ORFs) included in the automated screen for mRNA mislocalization. Multiwell plate number, row, and column display position of ORF deletion mutant in the yeast deletion collection (Life Technologies, Carlsbad, USA). If known, the common gene name and a short summary of the genes function are included.

Download Table S2

Supplementary Table S3 (Hermesh et al., 2014)- Plasmids

Plasmid name	Description	Source
RJP919	She2-GFP	(Du et al., 2008)
RJP1212	pFA6-hphNT1	(Janke et al., 2004)
RJP1423	pFA6a-mCherry-natMX6	(Snaith and Sawin, 2003)
RJP1486	pCP-MS2-GFPx3	(Haim et al., 2007)
RJP1686	SCS2-TMD-2xRFP -YCp50	(Loewen et al., 2007)
RJP1767	WSC2x12MS2-YCplac33	This study
RJP1773	WSC2x12MS2-YEplac195	This study
RJP1815	EAR1x12MS2-Yeplac195	This study
RJP1817	OPI3-Yeplac181	This study
RJP1841	ABP140x2mCherry-p414-ADH1	(Kilchert and Spang, 2011)
RJP1847	TGB3-mCherry	(Wu et al., 2011)
RJP1873	pFA6a-TEF2Pr-eGFP-ADH1term -NATMX4	(Breslow et al., 2008)
RJP1888	PSD1-YEplac181	This study
RJP1889	pMS2-CP-5xmCherry	This study
RJP1890	ABP140x2mCherry-YEplac181	This study

Supplementary Table S4- Oligonucleotides

Oligo name	Name	Sequence	Purpose
RJO3761	WSC2 F sphI	TACTGCATGCTCCAGCGACTGCTTTATACC	Cloning
RJO3762	WSC2 R sbfI	AGTACCTGCAGGGGTAAACATGCCTGATGGTG	Cloning
RJO3988	EAR1 SLIC F	GCCTGCAGGTCGACTCTAGAGGATCCCGGAACGGTGCGCTATAAAG	Cloning
RJO3989	EAR1 SLIC R	AAACGACGGCCAGTGAATTCGAGCTCGACACATTAAGAGGTAGCACGG	Cloning
RJO3990	HO TEF F	AAATCCATATCCTCATAAGCAGCAATCAATTCTATCTATATGAAGCTTCGTACGCTGCA	SGA screen
RJO3991	Z1 TEF R	CAGTGAAGCACTAGTAAGGGGATCCACGGCCCCATATATGAGCT	SGA screen
RJO3992	Z2 METP F	GGATCCCCTTACTAGTGCTTCACTGACAAAAGCTGGAGCTCCG	SGA screen
RJO3993	HO CYC1T R	AAATTTTACTTTTATTACATACAACTTTTTAAACTAATATCGACTCACTATAGGGCGAATTG	SGA screen
RJO4283	Rtn1 mCherry F	AAAAGTACAAAAAACTTGCAAAATGAATTGGAAAAAAACAACGCTCGGATCCCCGGGTTAATTAA	Tagging
RJO4284	Rtn1 mCherry R	AAAAGTTAGCTATTCTTGTTTGAAATGAAAAAAAAAAAGCACTCAGAATTCGAGCTCGTTTAAAC	Tagging
RJO4577	MET-MS2-CP-SLIC R	AGCCCGGGGGATCCACTAGTTCTAGATCCGTAGATGCCGGAGTTT	Cloning
RJO4578	MET-MS2-CP-SLIC F	TCCACCGCGGTGGCGGCCGCTCTAGACGGATGCAAGGGTTCGAATC	Cloning
RJO4581	mCherry BglII F	TGCAAGATCTATGGTGAGCAAGGGCGAG	Cloning
RJO4582	mCherry BglII R	TGCAGGATCCCTCGAGCTTGTACAGCTCGT	Cloning
RJO4595	mCherry Term BamHI R	TGCAGGATCCTGCCGGTAGAGGTGTGGT	Cloning
RJO4598	mCherry_BglII STM F	GCCCGGGGGATCCATGGTGAGCAAG	Site directed mutagenesis
RJO4599	mCherry_BglII STM R	CTTGCTCACCATGGATCCCCCGGGC	Site directed mutagenesis
RJO4439	Cho2 S1	CGAGTGATTTTCTTAGTGACAAAGCTTTTTCTTCATCTGTAGATGCGTACGCTGCAGGTCGAC	Gene deletion
RJO4440	Cho2 S2	ATCCTAGTACTTTTTAAATATATATACTCAAAAAAAAAAAACTCAATCGATGAATTCGAGCTCG	Gene deletion
RJO4187	OPI3 SLIC F	GCCTGCAGGTCGACTCTAGAGGATCCGTGTCAATGAGAGTGCATGTGG	Cloning
RJO4188	OPI3 SLIC R	AAACGACGGCCAGTGAATTCGAGCTCGCTGAGACTCATTCTTGCTGTG	Cloning
RJO4556	PSD1 SLIC F	GCCTGCAGGTCGACTCTAGAGGATCCGTTAAAGCCTGGTGACCGTGT	Cloning
RJO4557	PSD1 SLIC R	AAACGACGGCCAGTGAATTCGAGCTCGGAAATACCACCTCTTCGCAACTG	Cloning

Supplementary Table S5- Yeast strains

Name	Relevant genotype	Source
RJY3624	EAR1-12xMS2	(Fundakowski et al., 2012)
RJY3626	WSC2-12xMS2	(Fundakowski et al., 2012)
RJY3863	S288C MATα his3Δ1 leu2Δ0 met15Δ0 ura3Δ0 can1Δ::STE2pr-spHIS5 lyp1Δ::STE3pr-LEU2	(Breslow et al., 2008)
RJY3864	S288C MATα his3Δ1 leu2Δ0 met15Δ0 ura3Δ0 can1Δ::STE2pr-spHIS5 lyp1Δ::STE3pr-LEU2 hoΔ::NatMX4-MS2-CP-GFP	This study
RJY4508	cho2Δ::KanMX4	EUROSCARF collection
RJY2053	she2Δ::KanMX4	EUROSCARF collection
RJY4507	RJP1767 RJP1486	This study
RJY4509	RJP1815 RJP1486	This study
RJY4510	she2Δ::KanMX4 RJP1767,RJP1486	This study
RJY4511	she2Δ::KanMX4 RJP1815 RJP1486	This study
RJY4512	cho2Δ::KanMX4 RJP1767 RJP1486	This study
RJY4513	cho2Δ::KanMX4 RJP1815 RJP1486	This study
RJY4514	RJP1686	This study
RJY4515	cho2Δ::KanMX4 RJP1686	This study
RJY4036	RTN1-mCherry::ClonNAT	This study
RJY4067	cho2Δ::KanMX4 Rtn1-mCherry::ClonNAT	This study
RJY4516	RJP1847	This study
RJY4517	cho2Δ::KanMX4 RJP1847	This study
RJY4518	RTN1-mCherry::ClonNAT RJP1767 RJP1486	This study
RJY4519	cho2Δ::KanMX4 Rtn1-mCherry::ClonNAT RJP1767 RJP1486	This study
RJY4520	RJP1773 RJP919 RJP1889	This study
RJY4521	cho2Δ::KanMX4 RJP1773 RJP919 RJP1889	This study
RJY4522	psd1Δ::KanMX4	EUROSCARF collection
RJY4523	psd1Δ::KanMX4 RJP1767 RJP1486	This study
RJP4362	psd1Δ::KanMX4 cho2Δ::hphNTI	This study
RJY4524	psd1Δ::KanMX4 cho2Δ::hphNTI RJP1767 RJP1486	This study
RJY4525	opi3Δ::KanMX4	EUROSCARF collection
RJY4526	opi3Δ::KanMX4 RJP1767 RJP1486	This study
RJY4527	cho2Δ::KanMX4 RJP1767 RJP1486 RJP1817	This study
RJY4528	cho2Δ::KanMX4 RJP1767 RJP1486 RJP1888	This study
RJY4529	opi3Δ::KanMX4 RJP1767 RJP1486 RJP1888	This study

Strains RJY3624 and RJY3626 are derived from W303a background which has the genotype *MAT a ade2-1 trp1-1 can1-100 leu2-3,112 his3-11,15 ura3*. All the rest of the strains (except for strains RJY3683 and RJY3684) are derived from BY4741 background, which has the genotype *MAT a his3Δ1 leu2Δ0 met15Δ0 ura3Δ0*.